

UNIVERSIDAD POLITÉCNICA DE MADRID

E.T.S. de Ingenieros Aeronáuticos

New avenues in computational fluid dynamics

Esteban Ferrer

esteban.ferrer@upm.es

<http://sites.google.com/site/eferrerdg>

<https://numath.dmae.upm.es/>



@FerrerCfd



Esteban Ferrer

UPM Collaborators: E Valero, G Rubio, S Le Clainche, L Gonzalez, J Garicano...

Ext. Collaborators: DA Kopriva (San Diego), C Hirsch (Numeca), Paniagua (Purdue), P García (Zaragoza), R Vinuesa (KTH), S Sherwin (IC), R Willden (Oxford), H Blackburn (Monash)

Industrial collaborators: Numeca-Cadence, Airbus, McLaren F1, Dassault Syst., Siemens-Gamesa...



Students / Postdocs



L Botaro



E Jané



G Ntoukas



O Marino



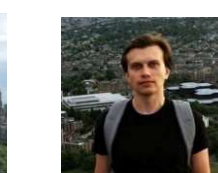
S Joshi



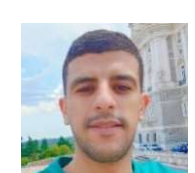
J Kou



A Hurtado-Mendoza



W Laskowski



K Otmani

F Manrique
de Lara

A Ballout



M de Frutos



S Colombo



D Huergo



A Portillo



J Manzanero



A Rueda



M Chavez



Y Wang



M Kompenhan



O Browne

Funding

Financiado por la Unión Europea
NextGenerationEU

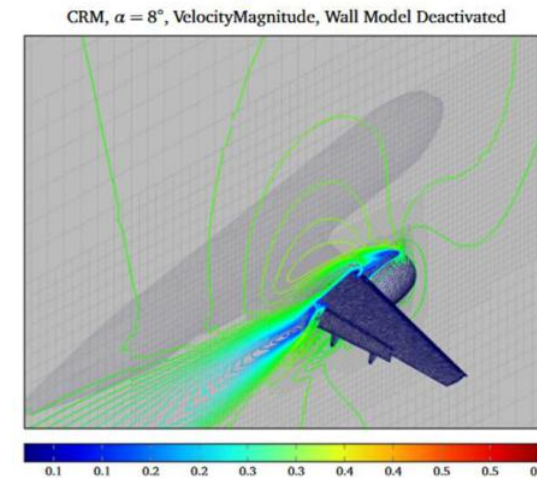
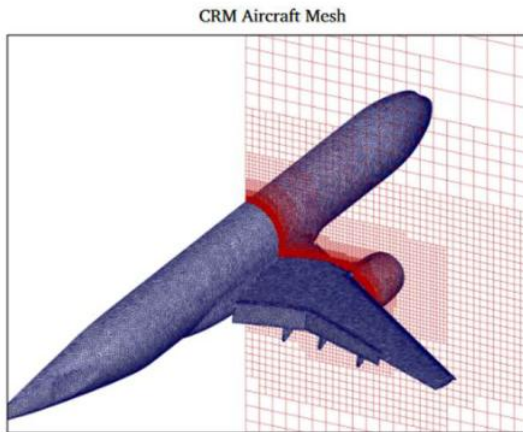
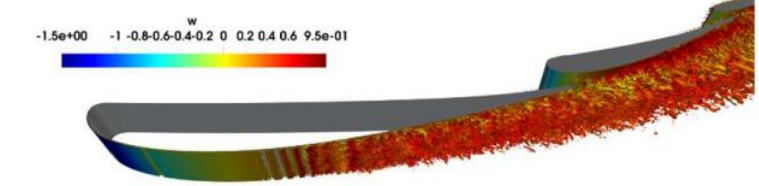
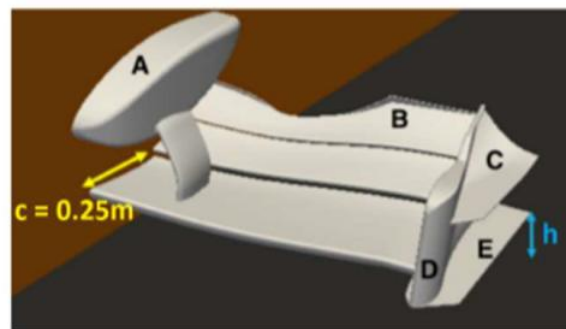
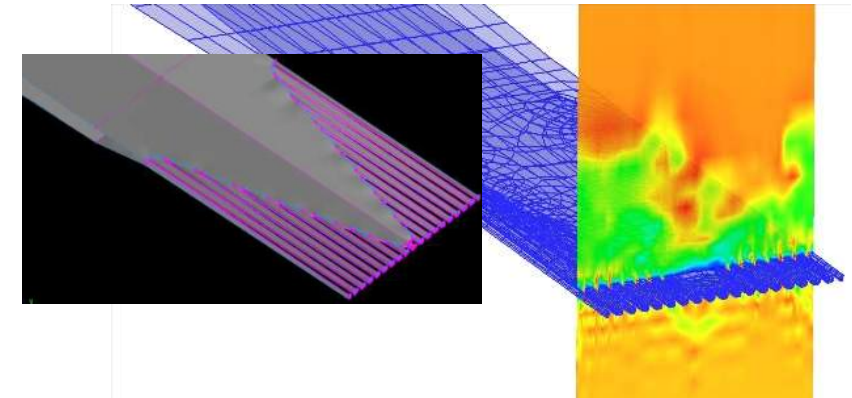
We acknowledge the funding received by the Grant DeepCFD (Project No. PID2022-137899OB-I00) funded by MICIU/AEI/10.13039/501100011033 and by ERDF, EU.

We thank the support of Agencia Estatal de Investigación for the grant "Europa Excelencia" for the project EUR2022-134041 funded by MCIN/AEI/10.13039/501100011033) y the European Union NextGenerationEU/PRTR

Funded by
the European UnionEuropean Research Council
Established by the European Commission

This research has been cofunded by the European Union (ERC, Off-coustics, project number 101086075). Views and opinions expressed are, however, those of the author(s) only and do not necessarily reflect those of the European Union or the European Research Council. Neither the European Union nor the granting authority can be held responsible for them

Collaborations with Industry

AIRBUS **MCLaren**
F O R M U L A 1 T E A M **SIEMENS Gamesa**
R E N E W A B L E E N E R G Y

Summary

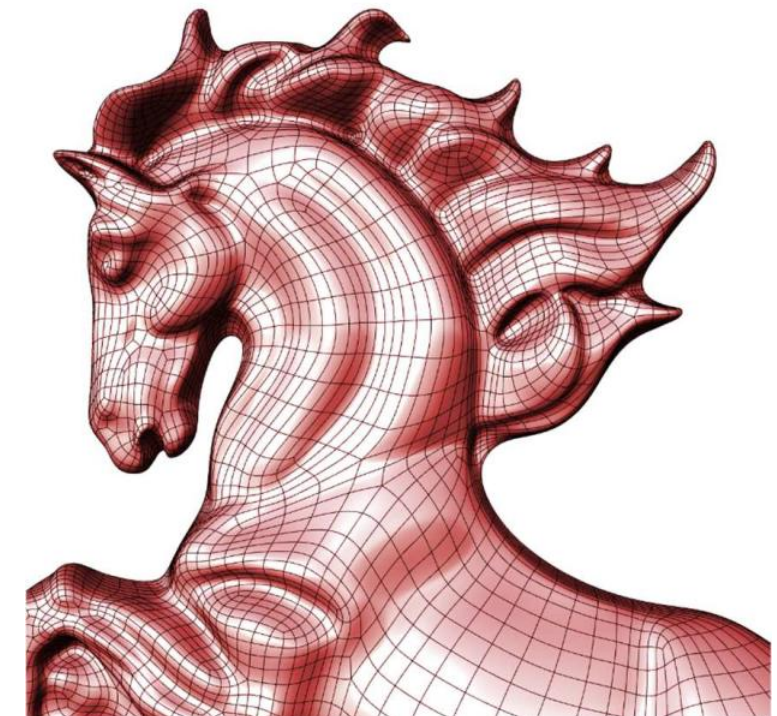
1- Introduction to DG & Horses3d

2- Multiphysics

- Wind turbines
- Turbulence

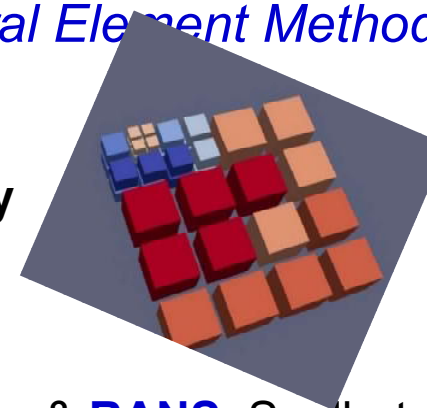
3. Machine Learning + CFD

- Mesh adaption
- NN acceleration
- RL for automation



DGSEM: nodal Discontinuous Galerkin Spectral Element Methods

- Compressible & Incompressible
- Entropy / Energy conserving schemes for stability
- Local p-adaption / h-adaption (hanging nodes)
- Explicit / implicit time stepping
- Turbulence models: **LES**: SVV-Smag., Wale, Vreman & **RANS**: Spallart-Almaras
- Multi-physics: Multiphase, Immersed Boundaries, Shock etc..



HORSES3D <https://github.com/loganoz/horses3d>

Computer Physics Communications 287 (2023) 108700



Contents lists available at ScienceDirect

Computer Physics Communications

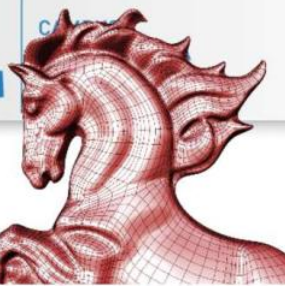
journal homepage: www.elsevier.com/locate/cpc



HORSES3D: A high-order discontinuous Galerkin solver for flow simulations and multi-physics applications

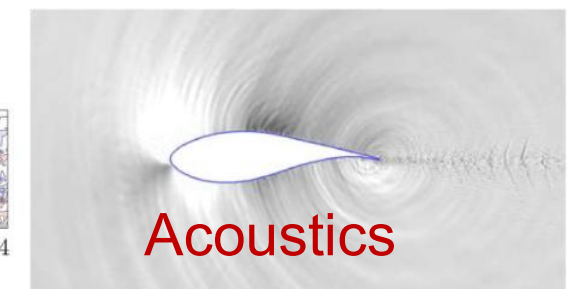
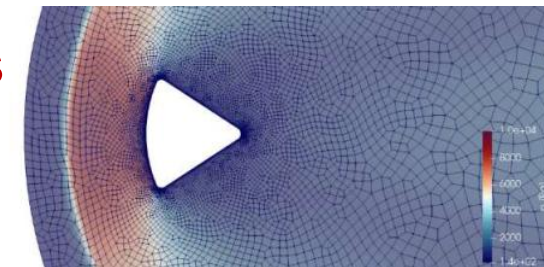
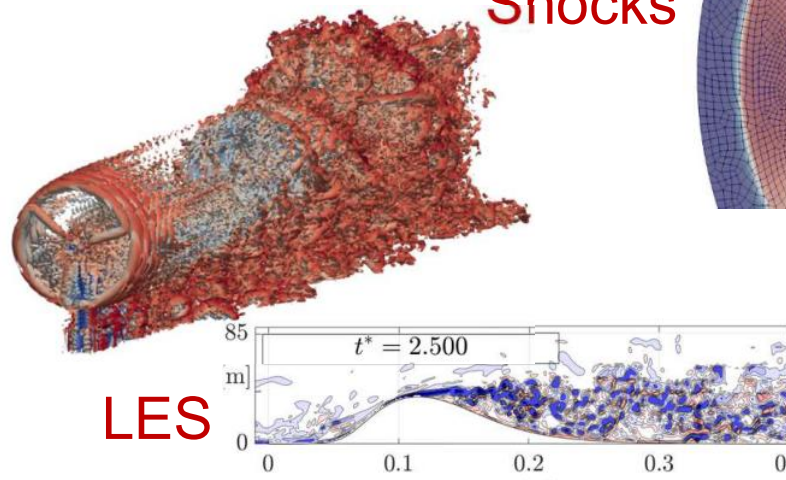
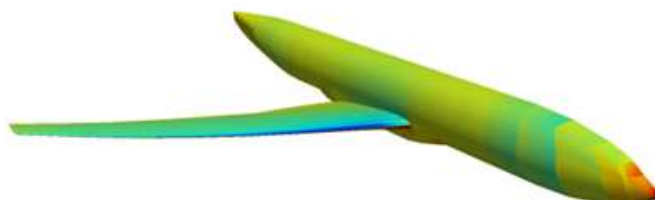
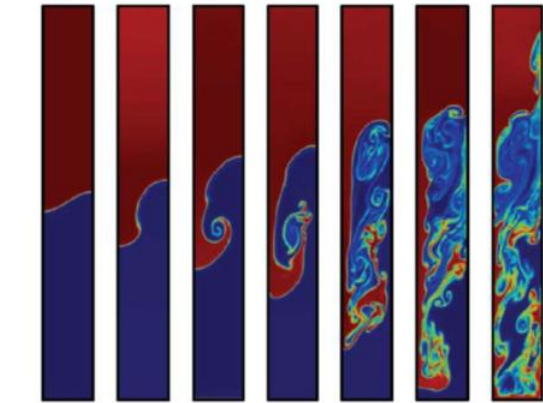
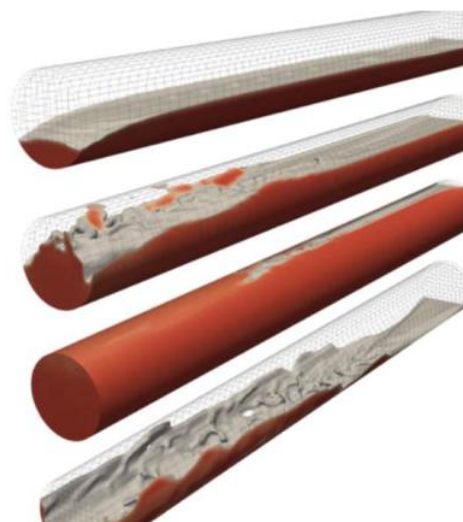
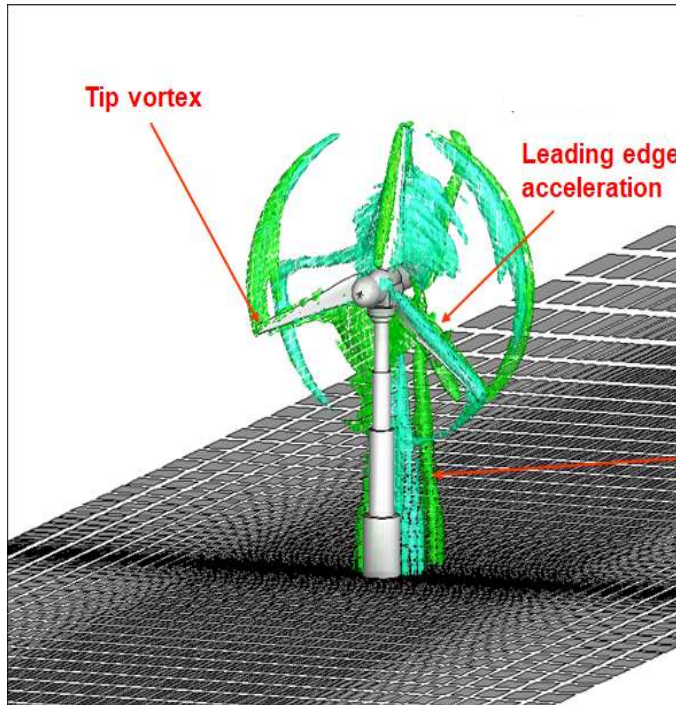


E. Ferrer ^{a,b}, G. Rubio ^{a,b,*}, G. Ntoukas ^a, W. Laskowski ^a, O.A. Mariño ^a, S. Colombo ^a,
A. Mateo-Gabín ^a, H. Marbona ^a, F. Manrique de Lara ^a, D. Huergo ^a, J. Manzanero ^e,
A.M. Rueda-Ramírez ^c, D.A. Kopriva ^d, E. Valero ^{a,b}



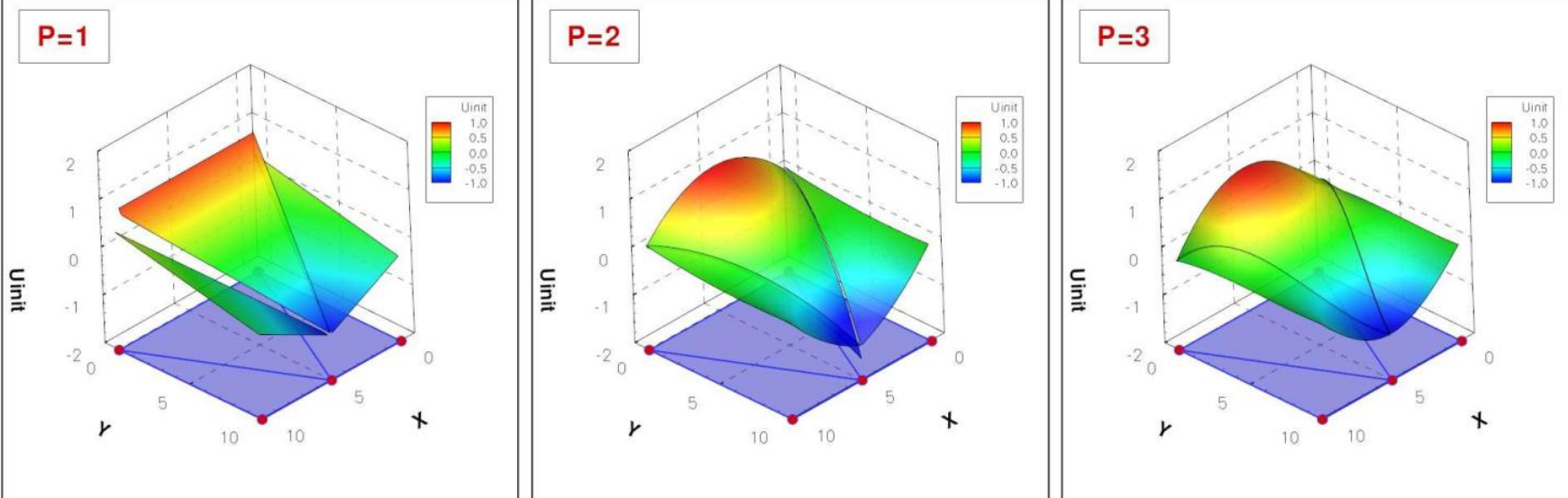
HORSES3D

<http://github.com/loganoz/horses3d>



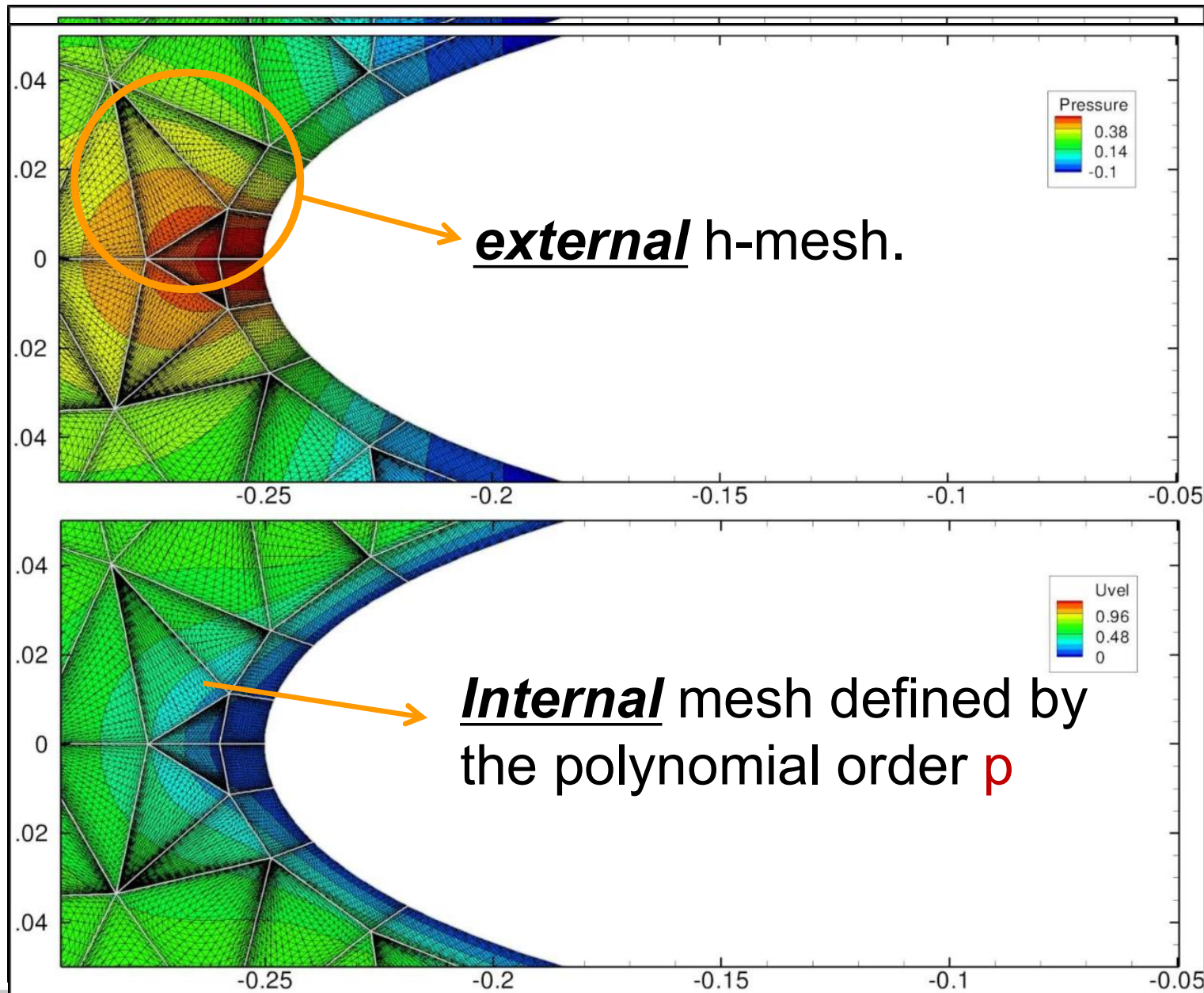
High order methods

2D Discontinuous Galerkin Projection on triangular elements for various polynomial order

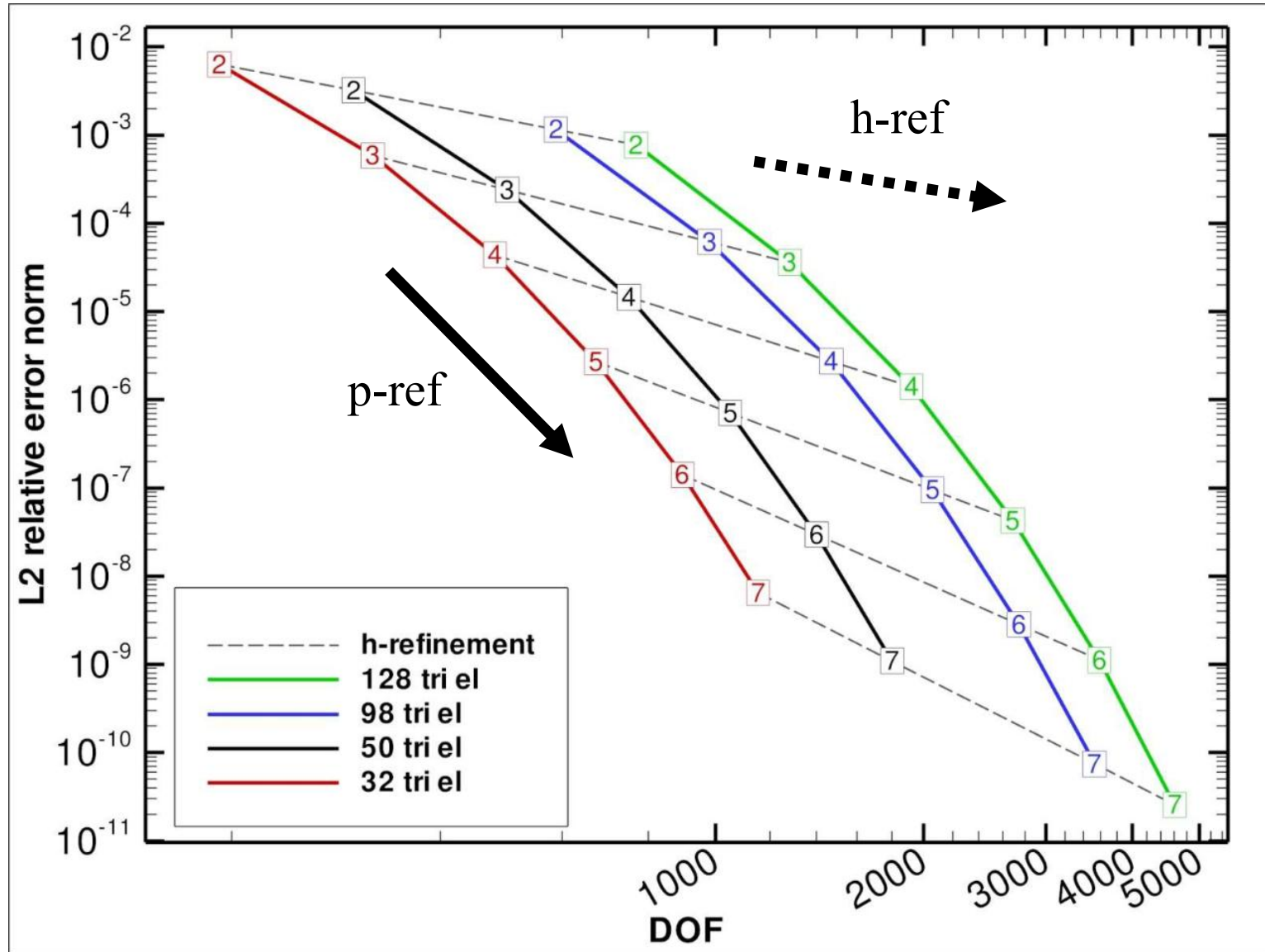


- High order is generally defined for $P \geq 2$
- High order allows h/p refinement
 - h -refinement offers constant decay of the error
 - p -refinement offers exponential decay of the error

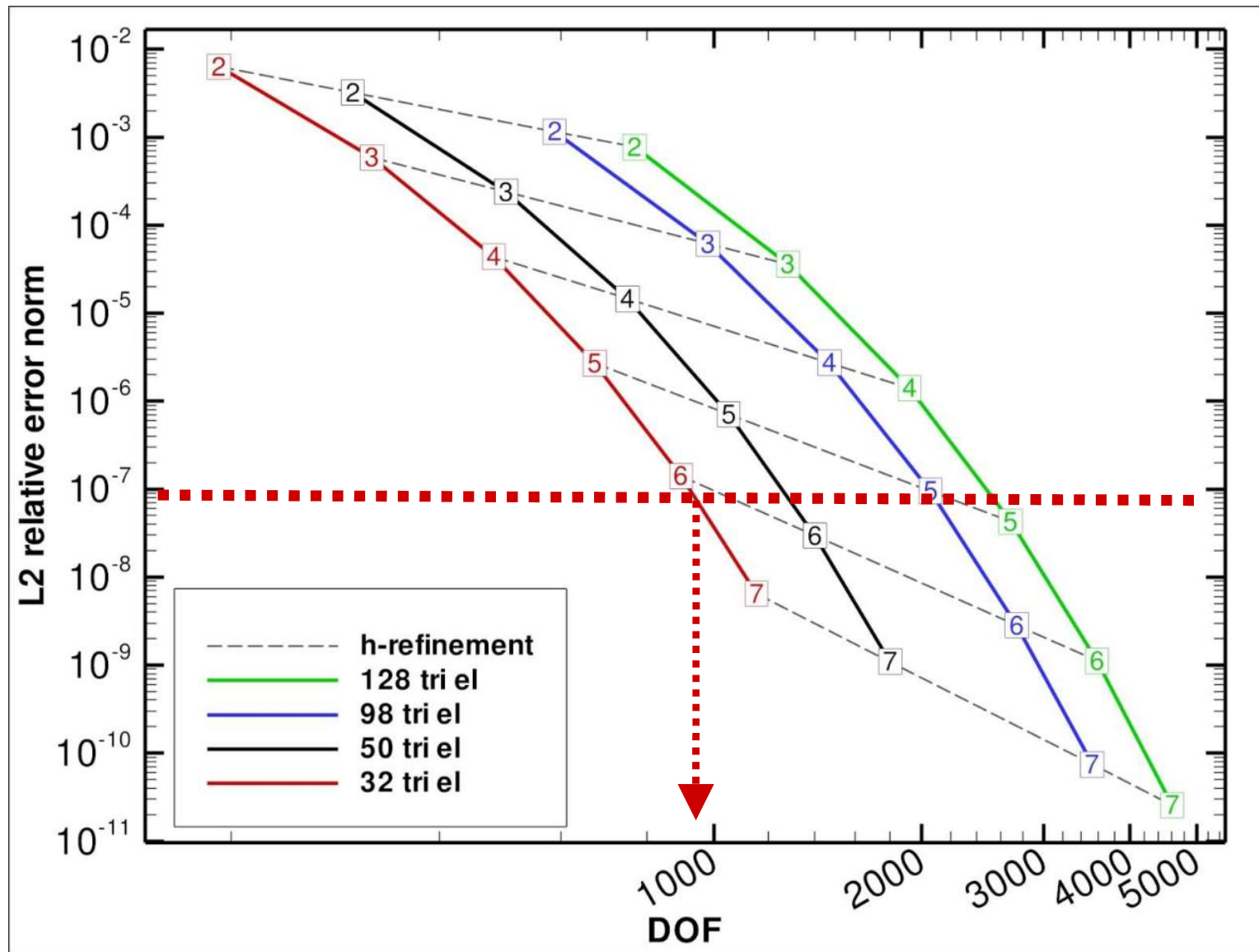
High order methods



High order methods (Poisson eq.)

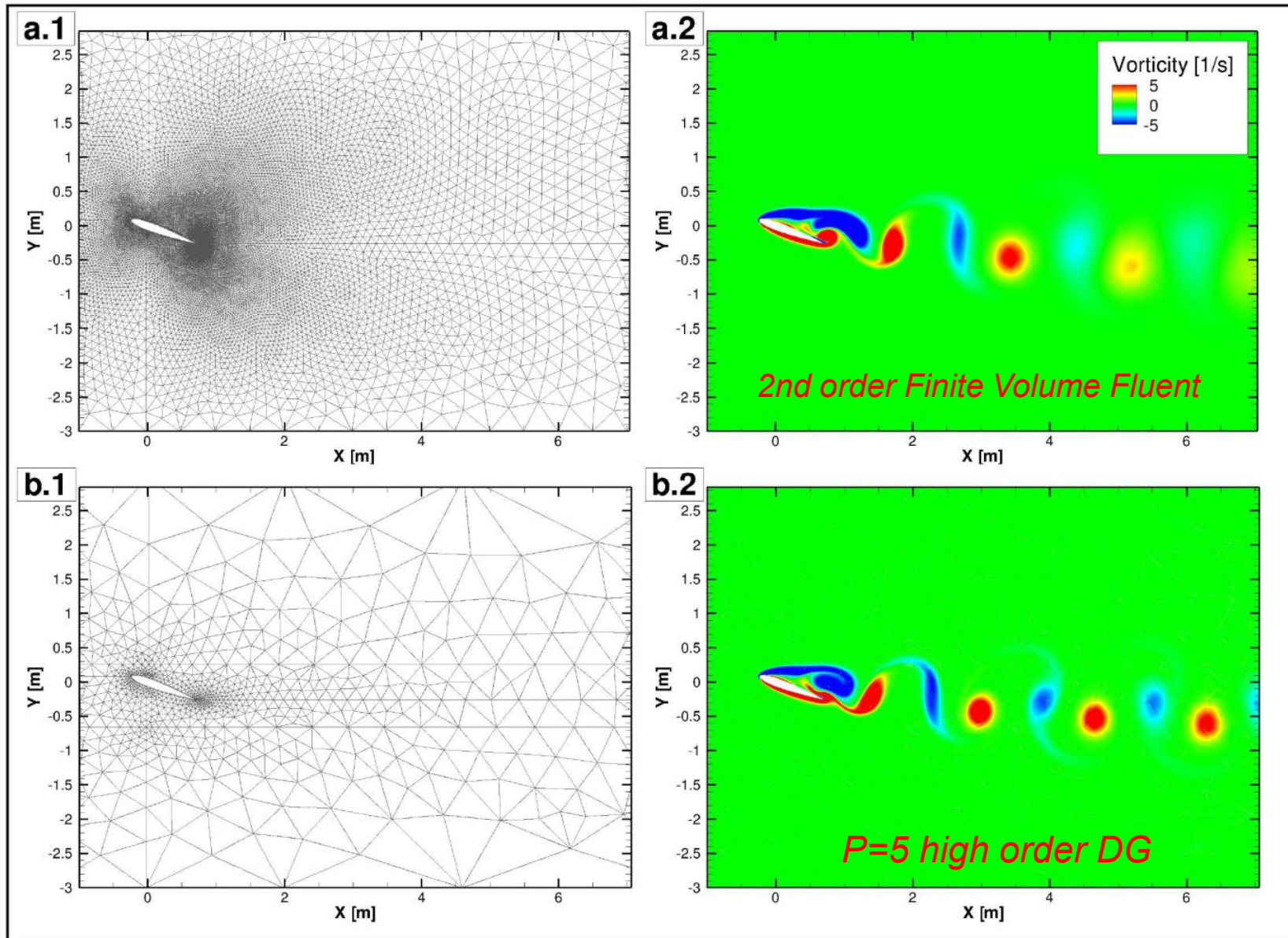


High order methods (Poisson eq.)



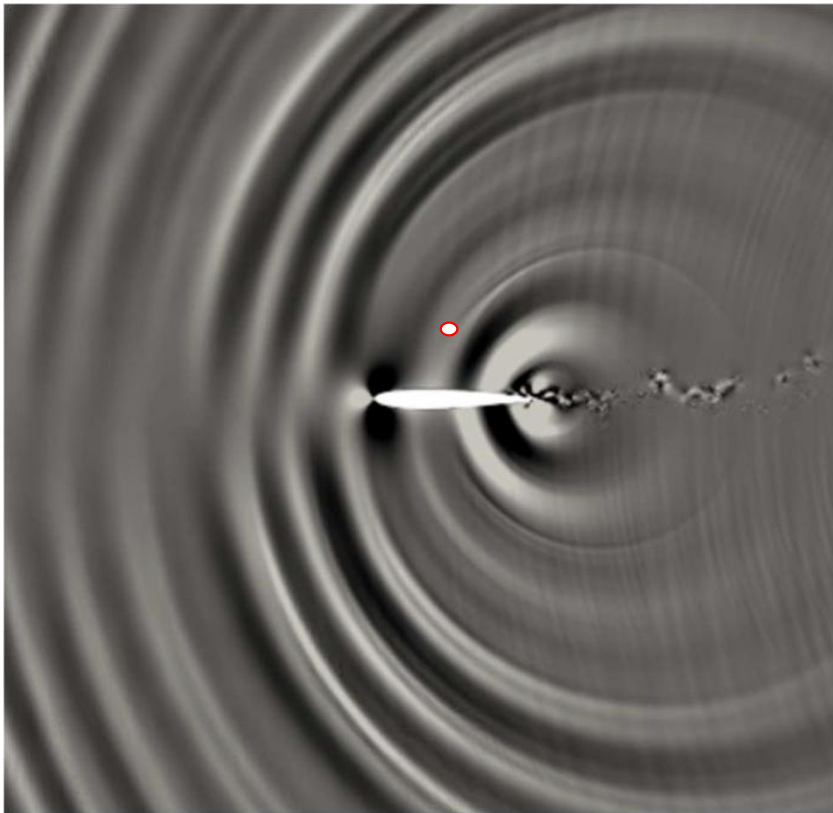


NACA0012 - Re=800 - Laminar flow

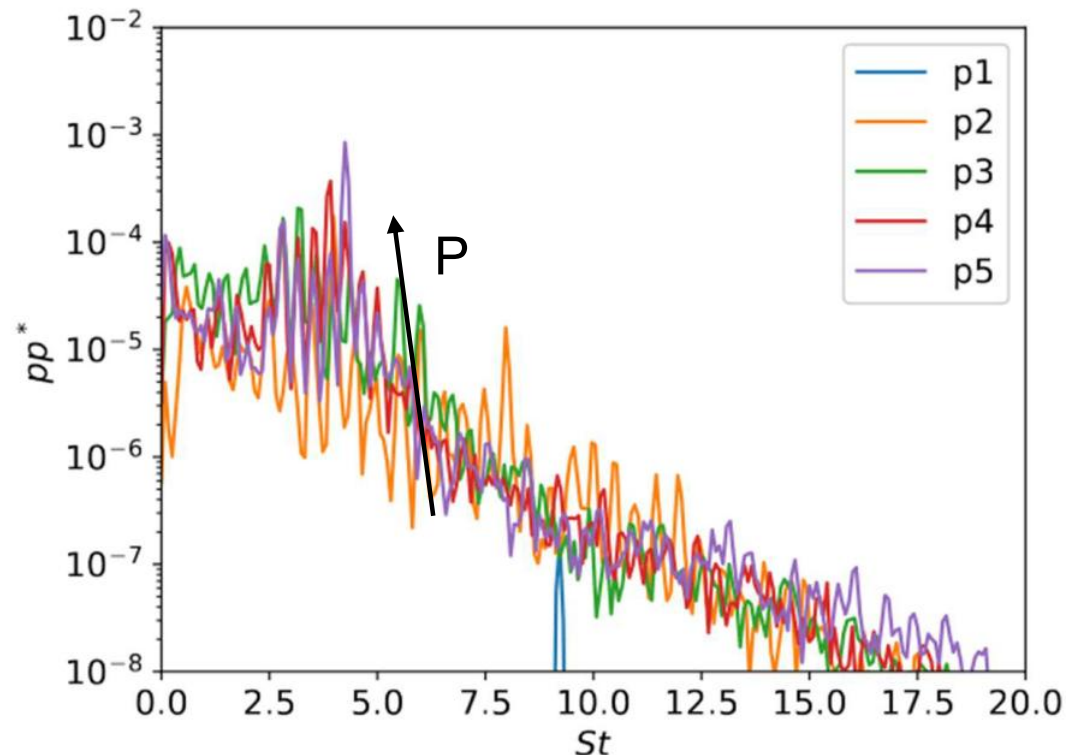


Horses: accuracy

NACA0012 airfoil at $Re = 105$, $M_0 = 0.4$ and $AoA = 0^\circ$



$P \uparrow$: Error decreases exponentially

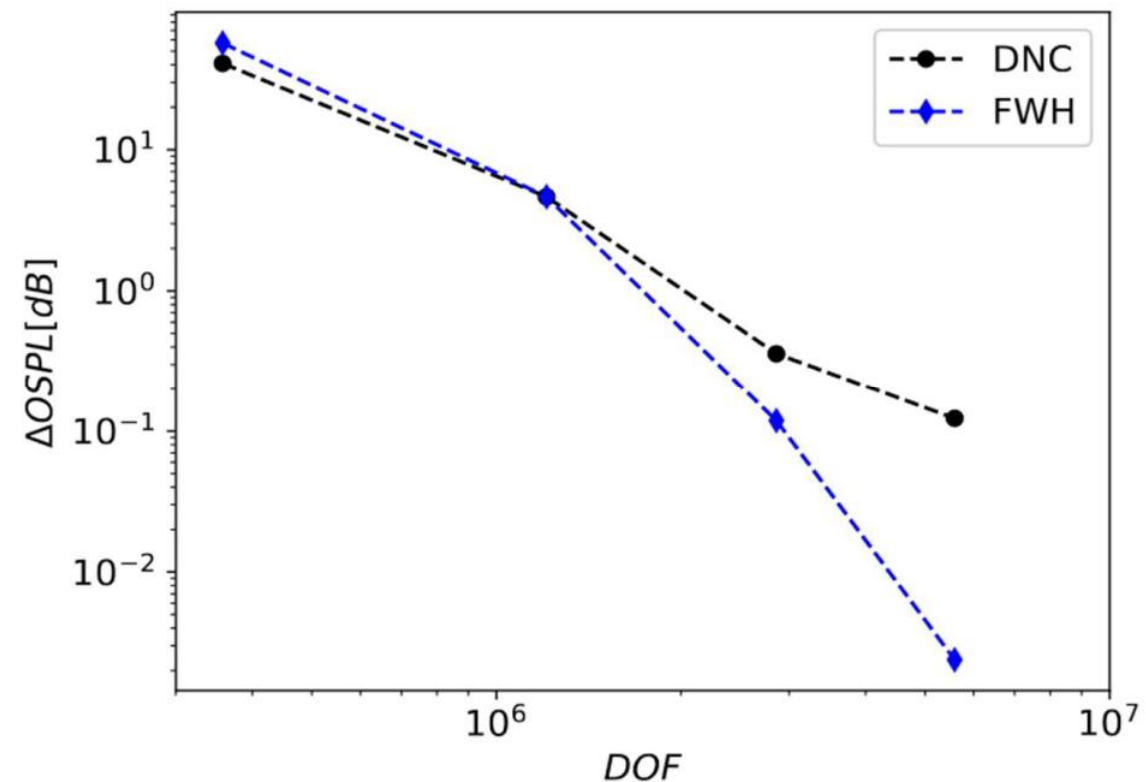
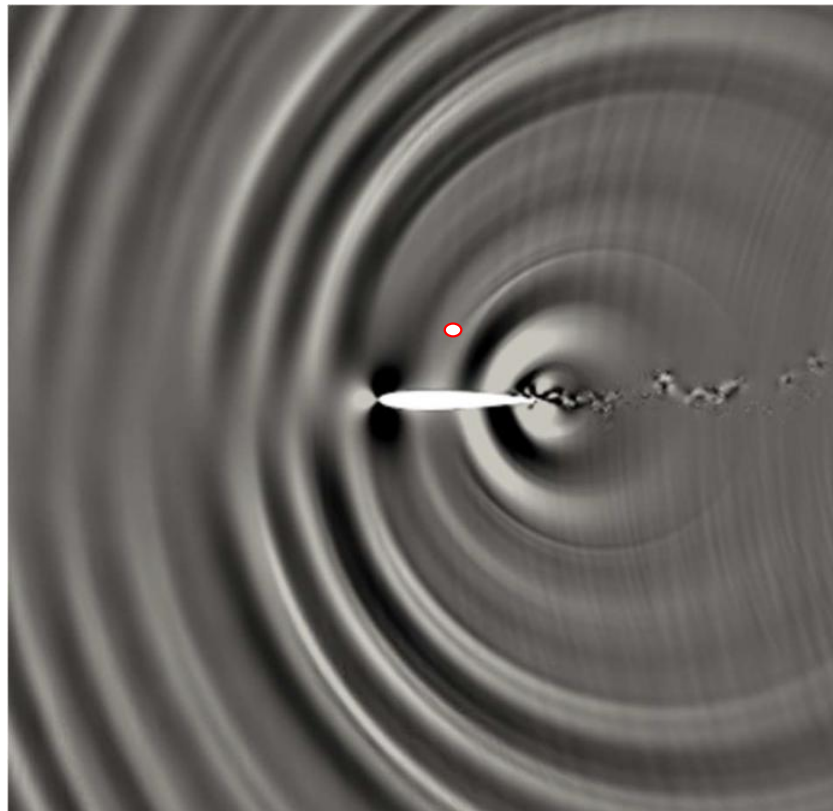


Horses: accuracy

NACA0012 airfoil at $Re = 105$, $M_0 = 0.4$ and $AoA = 0^\circ$



$P \uparrow$: Error decreases **exponentially**

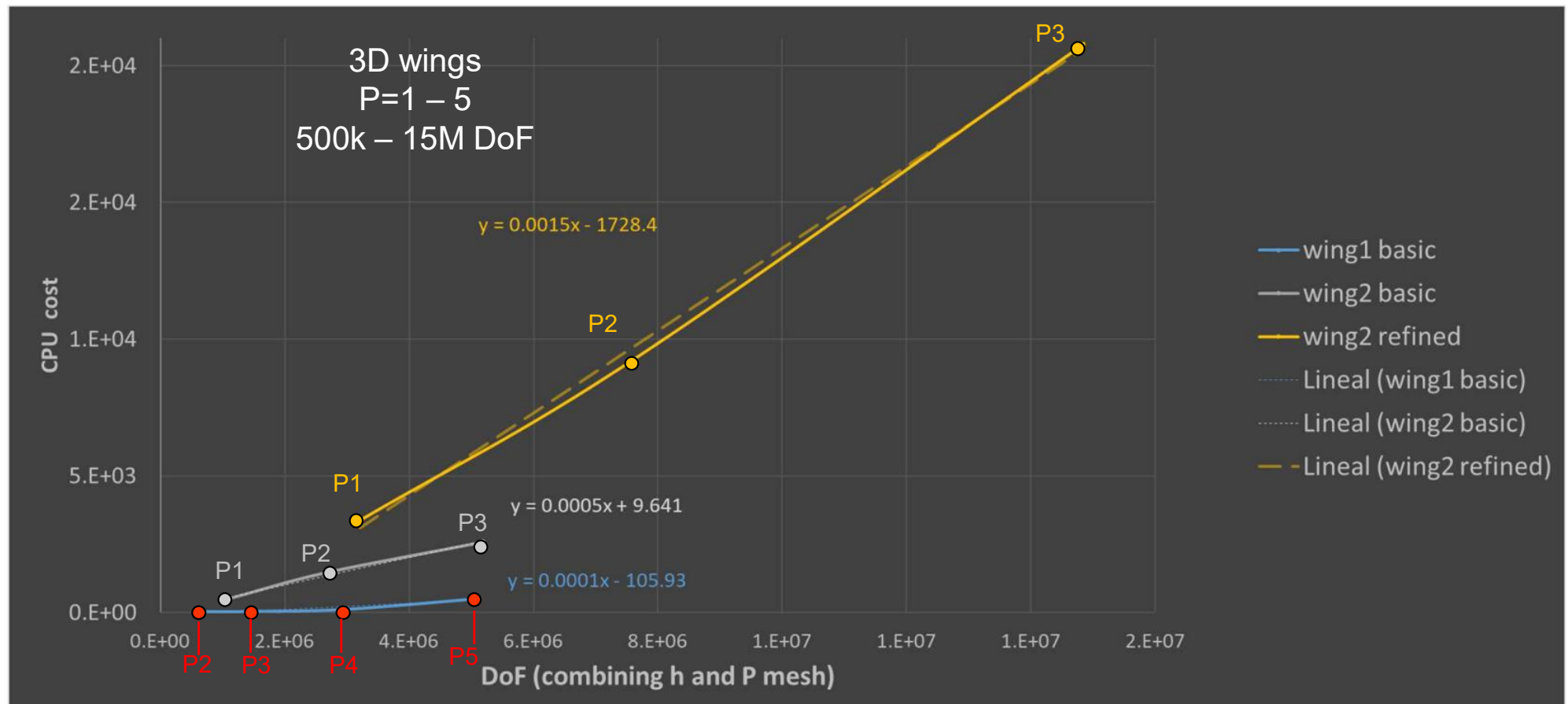


Horses: cost



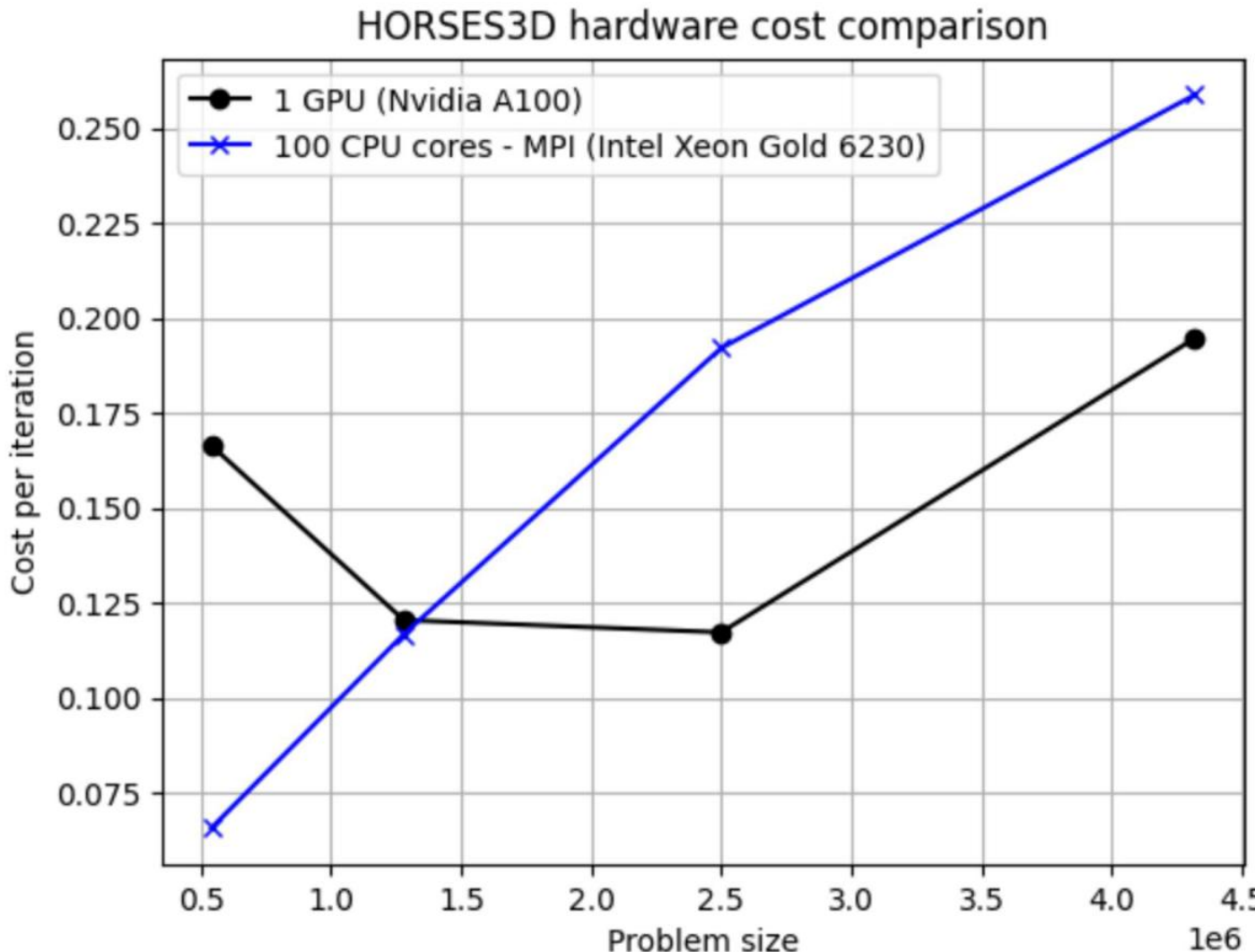
$P \uparrow$: Error decreases **exponentially**

$P \uparrow$: Cost increases **linearly**



Horses: cost → porting to GPUs (openACC on NVIDIA A100)

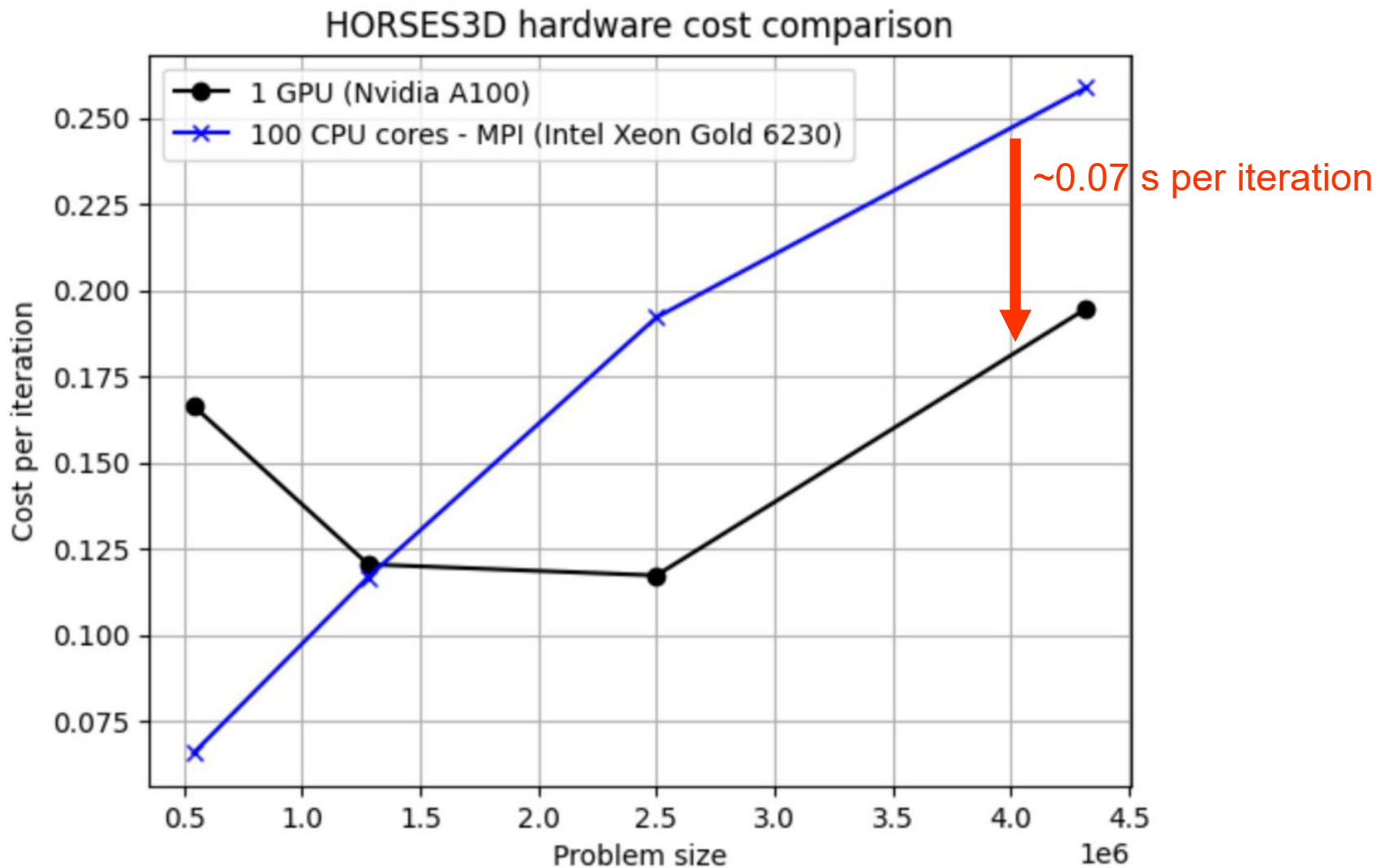
..underway..



*Better performance
than 100 CPU cores*

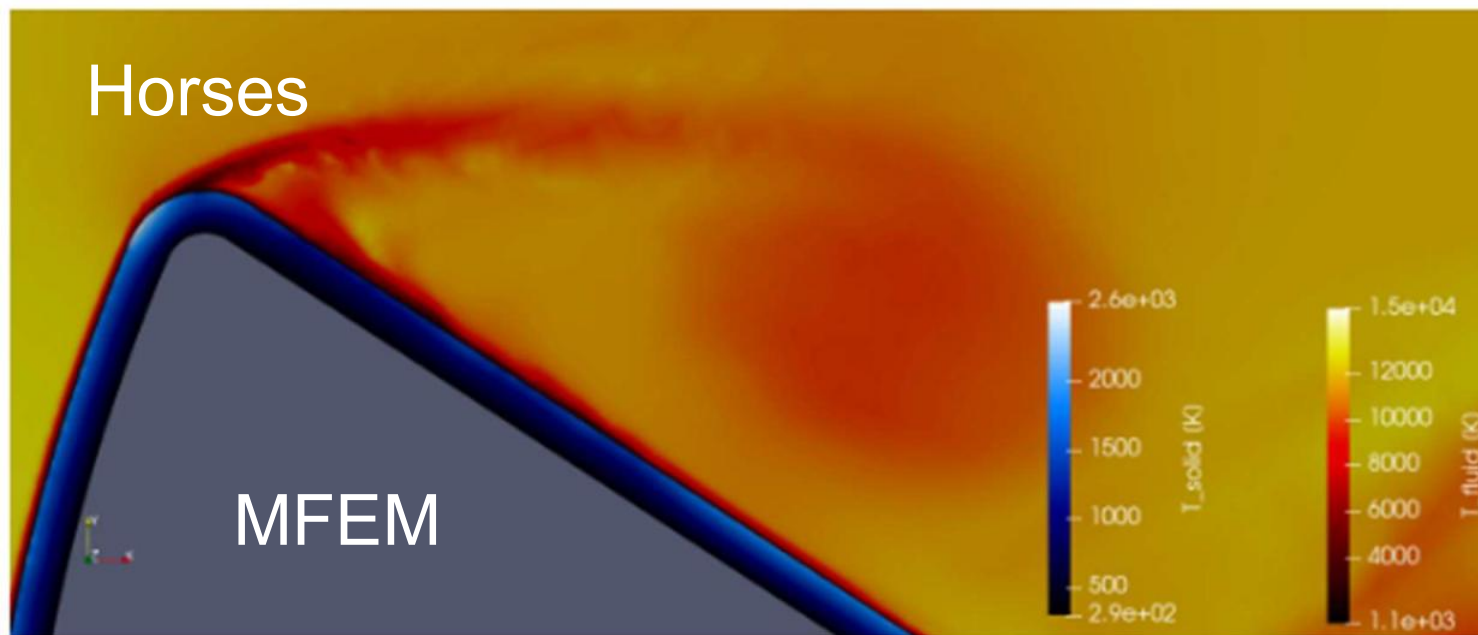
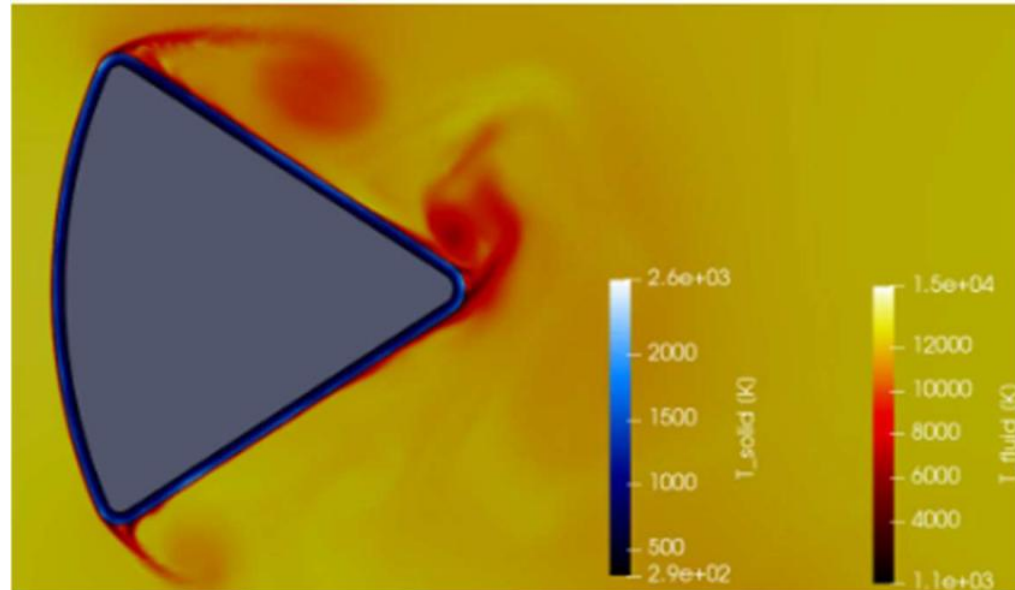
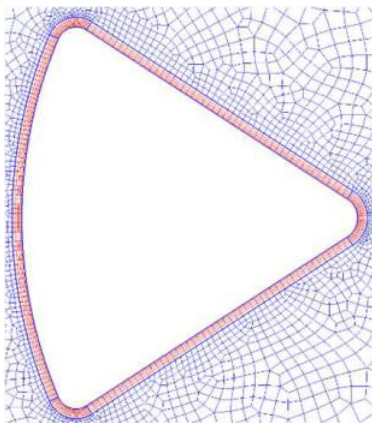
Horses: cost → porting to GPUs (openACC on NVIDIA A100)

..underway..



LES simulation → 1e8 time steps → 81 days faster than 100 CPUs

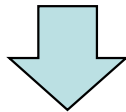
Horses & MFEM (*Python interface*): example 1 - thermal coupling



Horses & MFEM (*Python interface*): example 2 – incompressible solver

$$\frac{\partial \mathbf{u}}{\partial t} = -\nabla \cdot (\mathbf{u}\mathbf{u}) - \frac{1}{\rho_0} \nabla p - \nabla \cdot (\nu \nabla \mathbf{u}) + \frac{\mathbf{f}_{\text{ext}}}{\rho_0}$$

$$\nabla \cdot \mathbf{u} = 0$$



Step 1

$$\frac{\gamma_0 \mathbf{u}^* - \alpha_0 \mathbf{u}^n - \alpha_1 \mathbf{u}^{n-1}}{\Delta t} = -\beta_0 \mathbf{N}(\mathbf{u}^n) - \beta_1 \mathbf{N}(\mathbf{u}^{n-1}),$$

DG/FR-horses

Step 2

$$\nabla \cdot \left(\frac{1}{\rho_0} \nabla p^{n+1} \right) = -\frac{\gamma_0}{\Delta t} \nabla \cdot \mathbf{u}^*$$

DG/CG-MFEM

Step 3

$$-\nabla \cdot (\nu \nabla \mathbf{u}^{n+1}) + \frac{\gamma_0}{\Delta t} \mathbf{u}^{n+1} = \frac{\gamma_0}{\Delta t} \mathbf{u}^* - \frac{\nabla p^{n+1} + \mathbf{f}_{\text{ext}}^n}{\rho_0}$$

DG/CG-MFEM

Summary

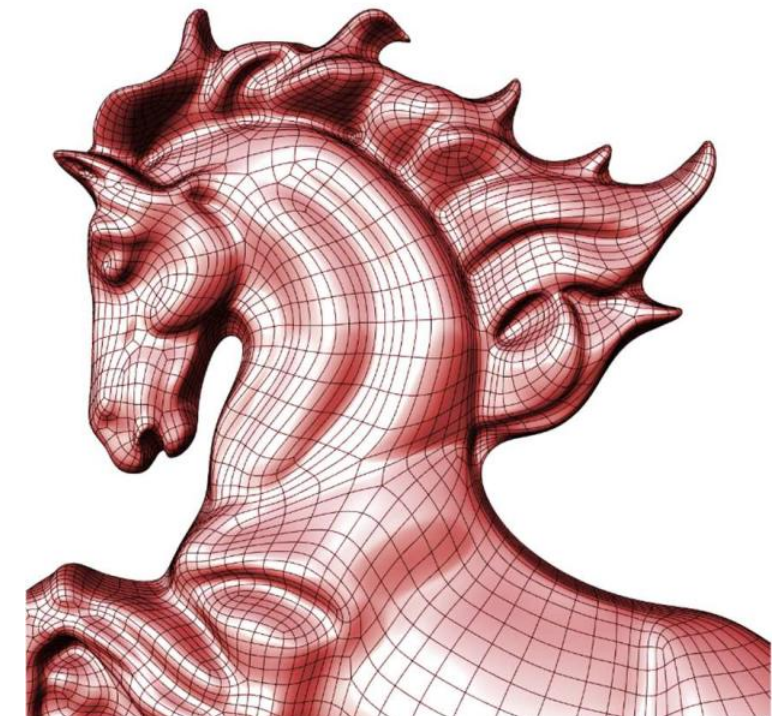
1- Introduction to DG & Horses3d

2- Multiphysics

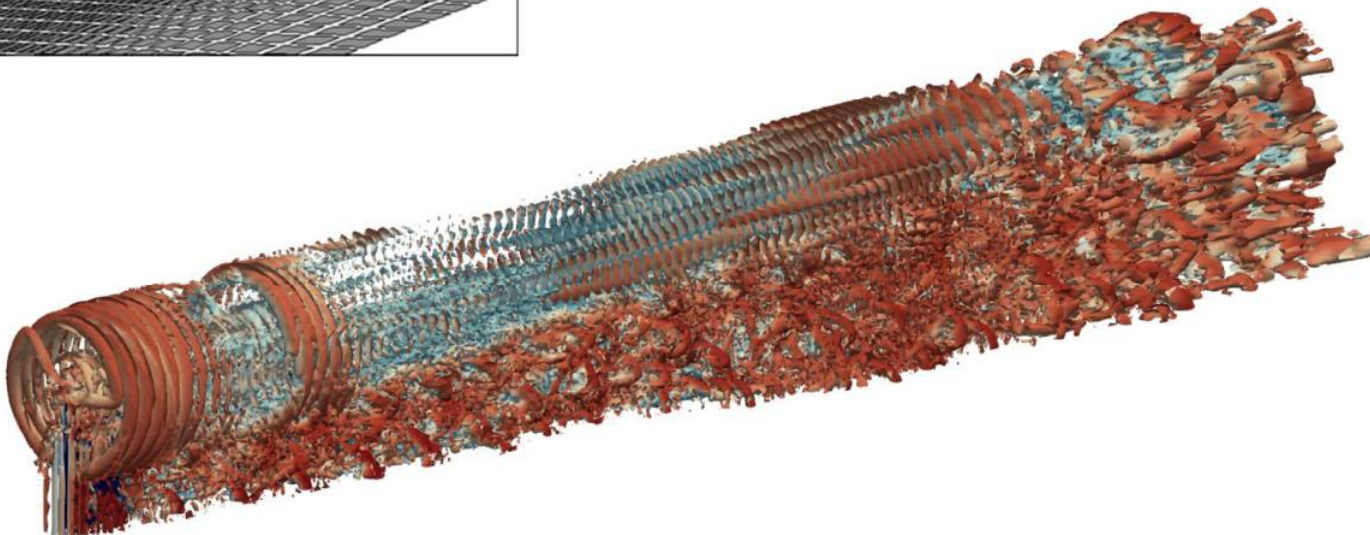
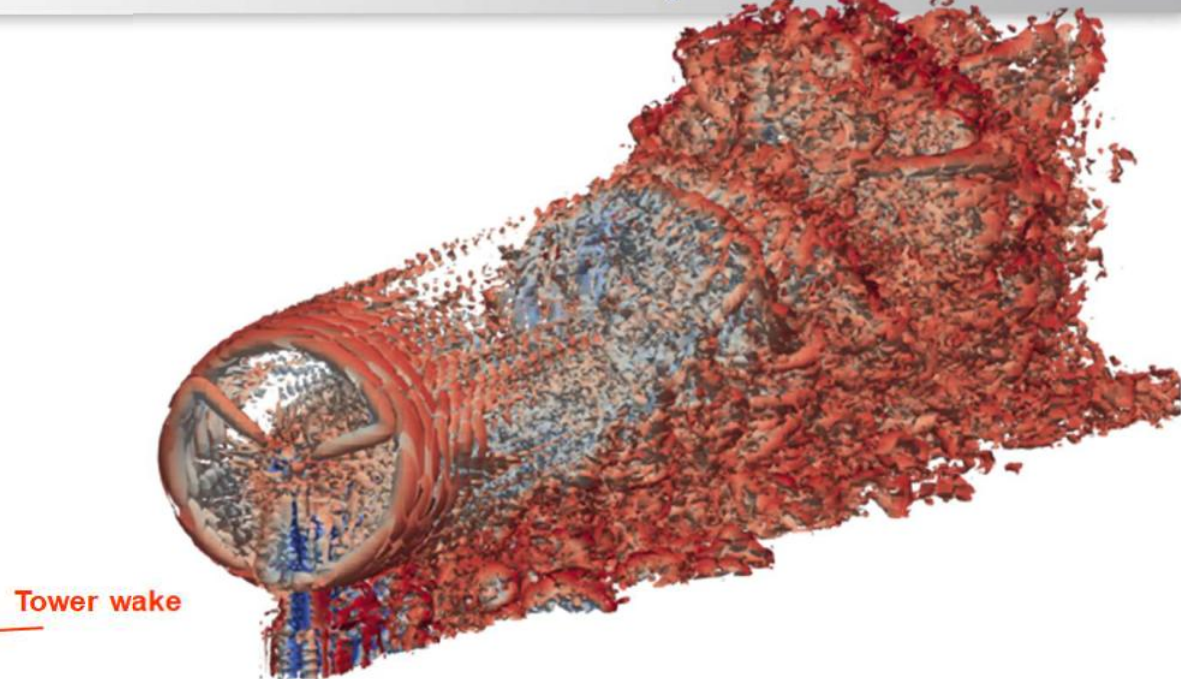
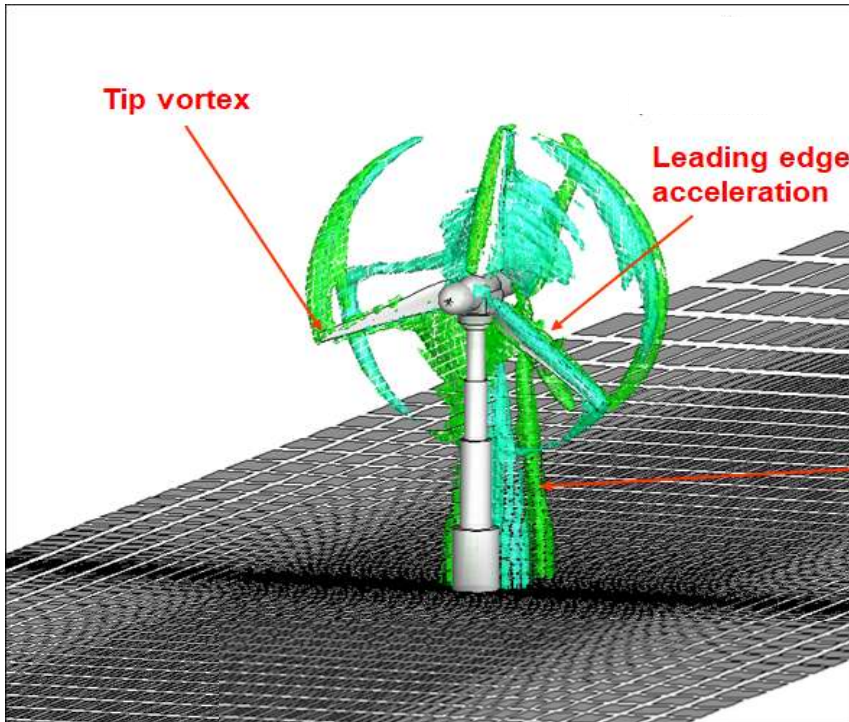
- Wind turbines
- Turbulence

3. Machine Learning + CFD

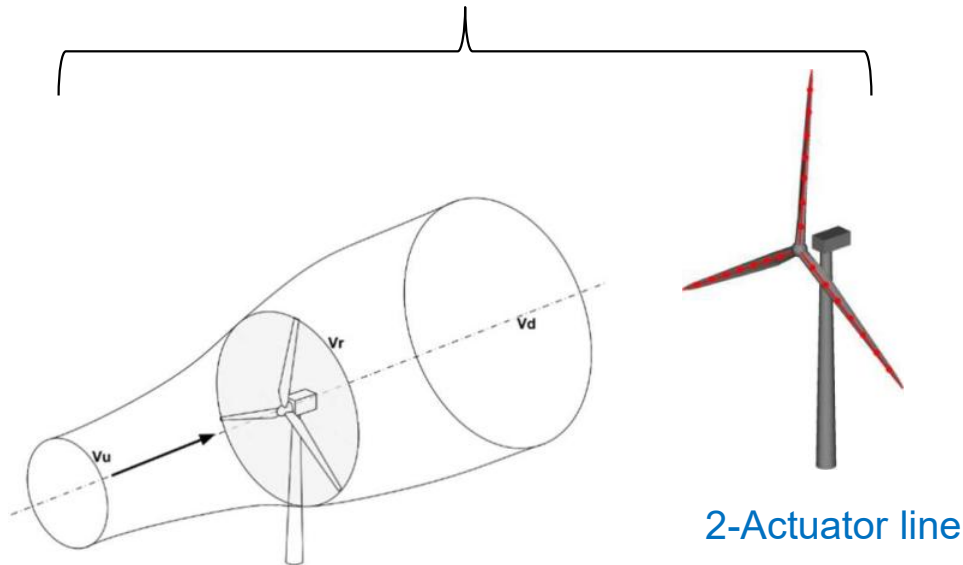
- Mesh adaption
- NN acceleration
- RL for automation



High order wind turbines

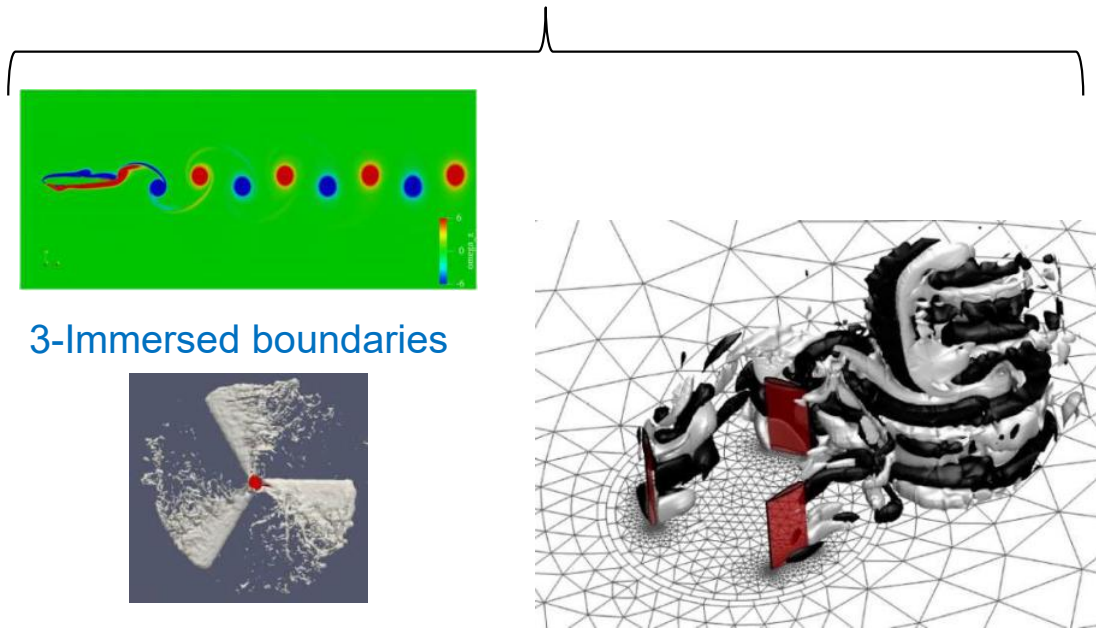


Require 2D aerodynamic data



1-Actuator disc & BEM

Explicit 3D geometry



2-Actuator line

Low

Cost

High

Accuracy

- 4- E Ferrer and RHJ Willden, A high order Discontinuous Galerkin - Fourier incompressible 3D Navier–Stokes solver with **rotating sliding meshes**, *Journal of Computational Physics*, 2012

4- E Ferrer, RHJ Willden, Blade–wake interactions in **cross-flow turbines**, *International Journal of Marine Energy*, 2015

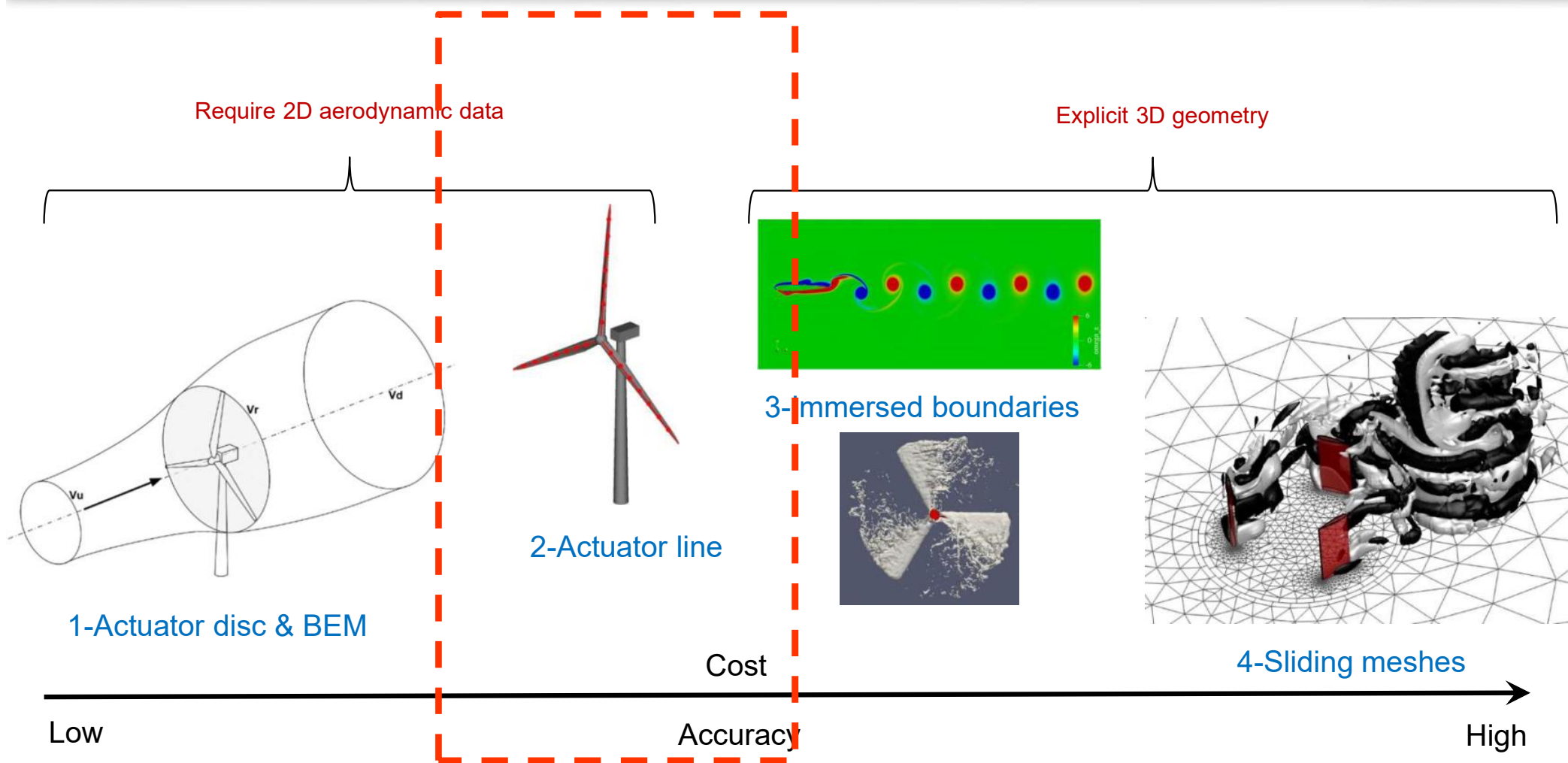
3- J Kou, A Hurtado-de-Mendoza, S Joshi, S Le Clainche, E Ferrer, Eigensolution analysis of **immersed boundaries** for high-order schemes, *Journal of Computational Physics*, 2022

3- J Kou, S Joshi, A Hurtado-de-Mendoza, K Puri, C Hirsch, E Ferrer, An **Immersed boundary** method for high–order flux reconstruction, *Journal of Computational Physics*, 2022

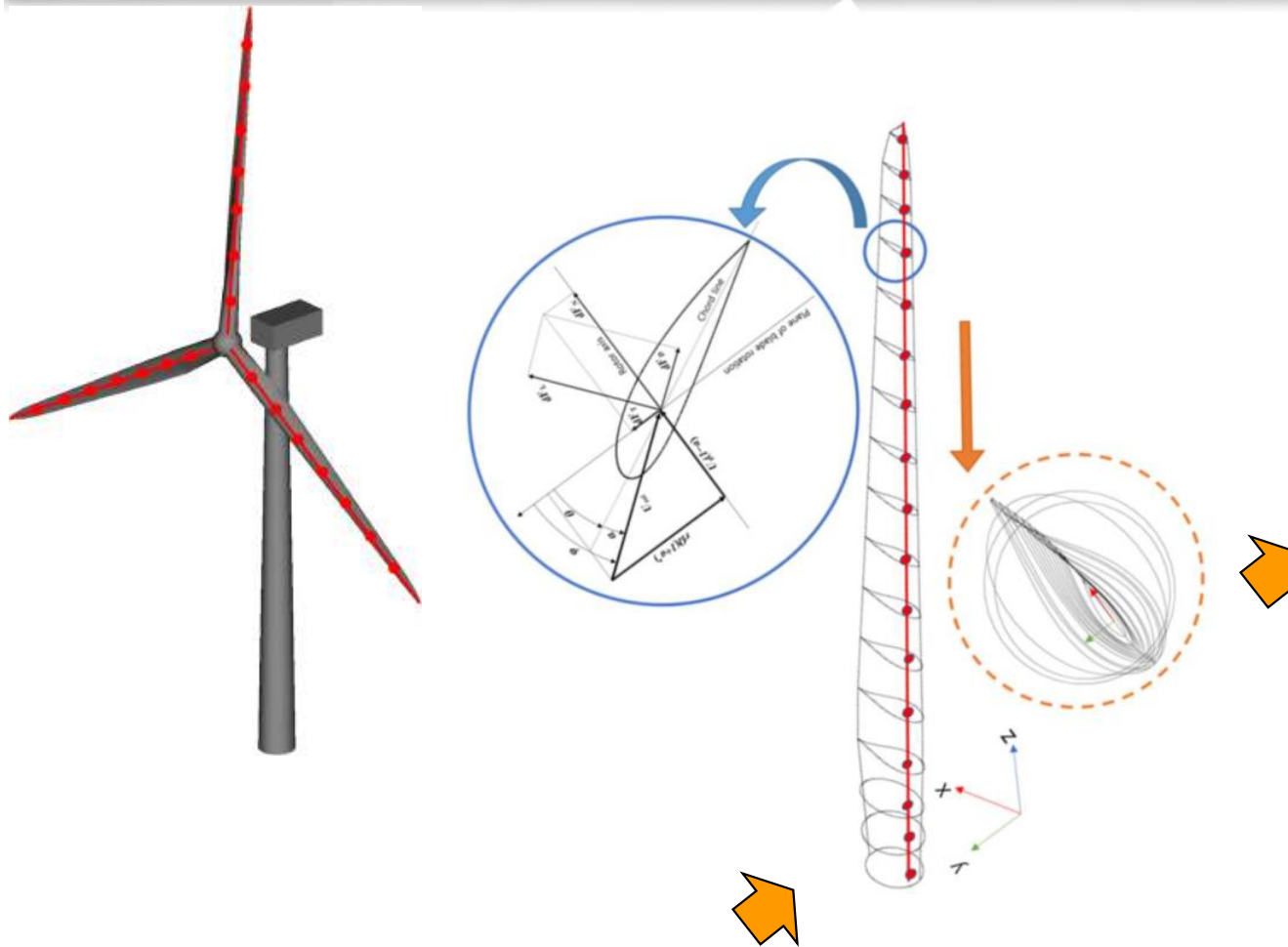
2 & 3- E Ferrer, S Colombo, O Marino, “Aeroacoustic predictions of wind turbines based on **actuator lines and immersed boundaries**”, *Under review at Wind Energy*

1- E Ferrer, S Le Clainche, **Simple models for cross flow turbines**, in *Recent advances in CFD for Wind and Tidal Offshore Turbines*, 2019

1- E Ferrer, OMF Browne, E Valero, Sensitivity analysis to control the far–wake unsteadiness behind **turbines**, *Energies*, 2017

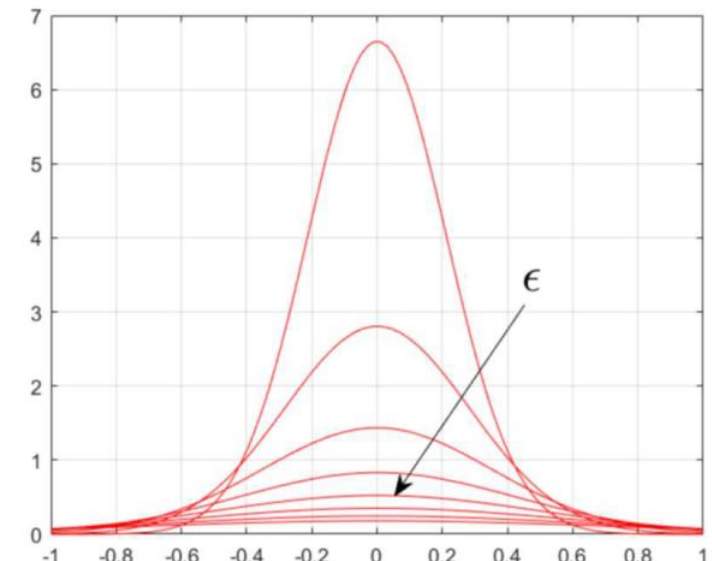


- 4- E Ferrer and RHJ Willden, A high order Discontinuous Galerkin - Fourier incompressible 3D Navier–Stokes solver with **rotating sliding meshes**, *Journal of Computational Physics*, 2012
- 4- E Ferrer, RHJ Willden, Blade–wake interactions in **cross-flow turbines**, *International Journal of Marine Energy*, 2015
- 3- J Kou, A Hurtado-de-Mendoza, S Joshi, S Le Clainche, E Ferrer, Eigensolution analysis of **immersed boundaries** for high-order schemes, *Journal of Computational Physics*, 2022
- 3- J Kou, S Joshi, A Hurtado-de-Mendoza, K Puri, C Hirsch, E Ferrer, An **Immersed boundary** method for high-order flux reconstruction, *Journal of Computational Physics*, 2022
- 2 & 3- E Ferrer, S Colombo, O Marino, “Aeroacoustic predictions of wind turbines based on **actuator lines and immersed boundaries**”, Under review at *Wind Energy*
- 1- E Ferrer, S Le Clainche, **Simple models for cross flow turbines**, in *Recent advances in CFD for Wind and Tidal Offshore Turbines*, 2019
- 1- E Ferrer, OMF Browne, E Valero, Sensitivity analysis to control the far-wake unsteadiness behind **turbines**, *Energies*, 2017



Tabulated data

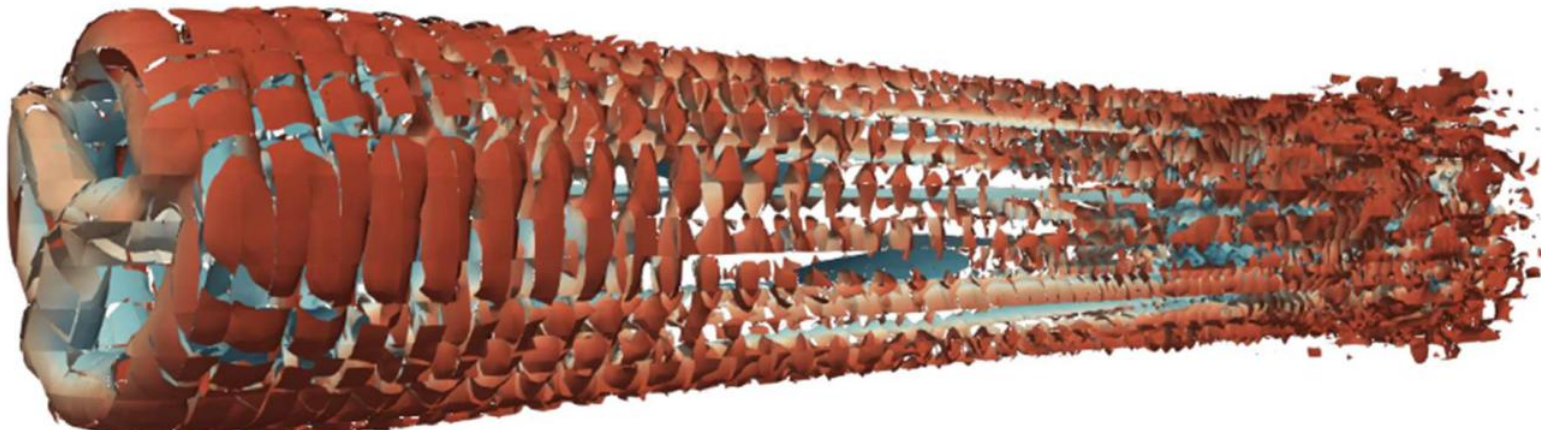
$$f_L = \frac{1}{2} \rho U_{rel}^2 S C_l, \quad f_D = \frac{1}{2} \rho U_{rel}^2 S C_d,$$



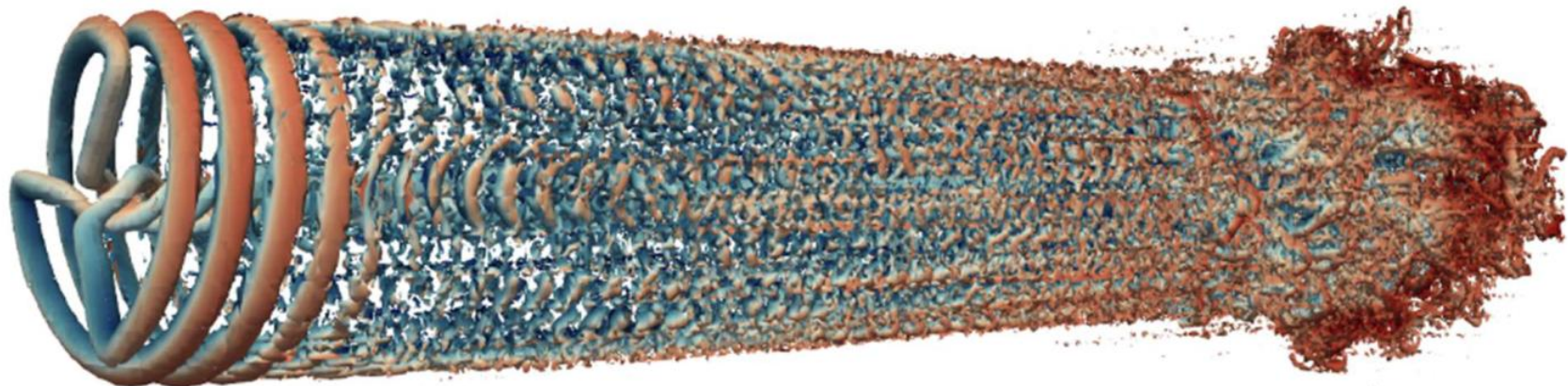
$$\eta_\epsilon = \frac{1}{\epsilon^3 \pi^{\frac{3}{2}}} e^{-(\frac{d}{\epsilon})^2}$$

$$\epsilon_k = k \times \Delta_{grid} = k \times \frac{(\Delta_x \Delta_y \Delta_z)^{\frac{1}{3}}}{p+1}$$

Improved solution using the same h-mesh

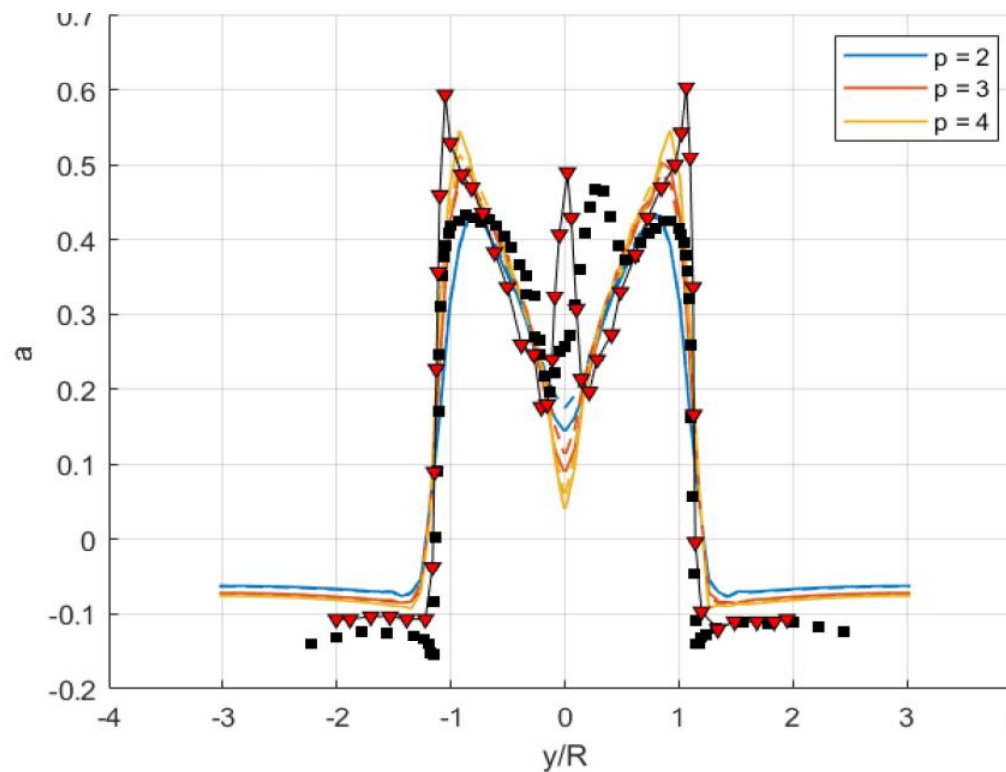
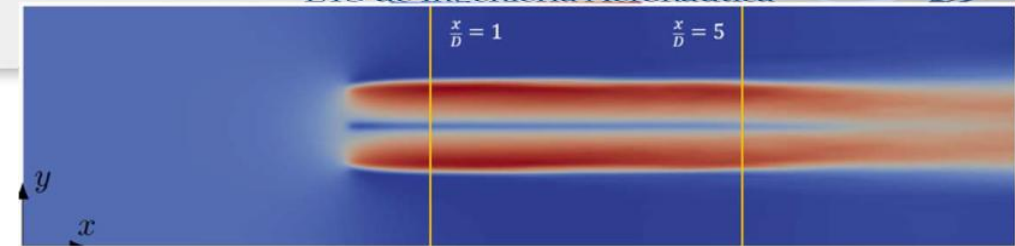


$P = 2$



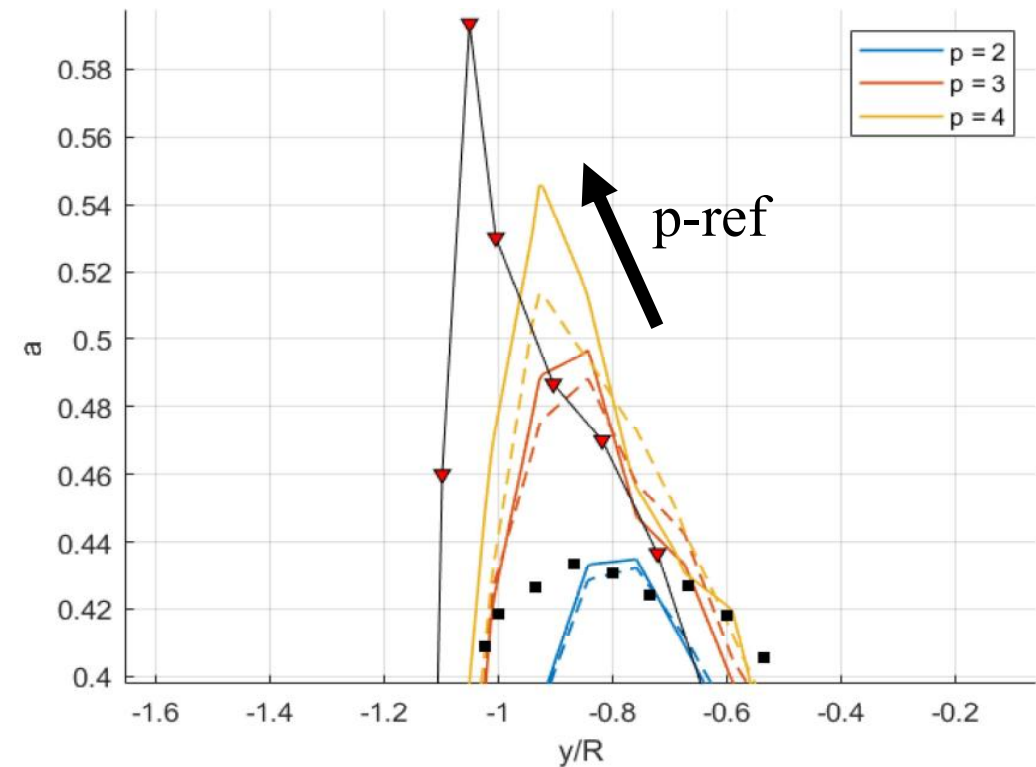
$P = 5$

Averaged velocity deficit



'■' Experimental

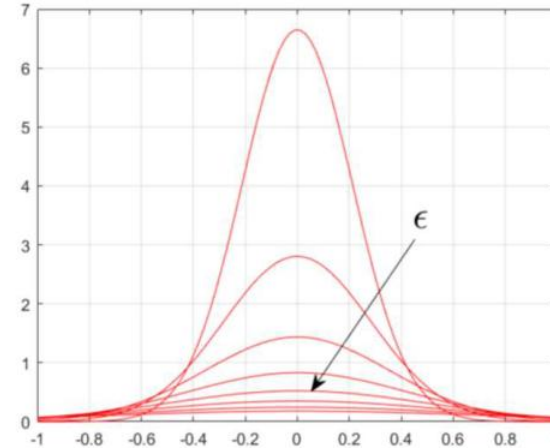
'▽-' OpenFoam-Oxford Fine mesh → 190M elements



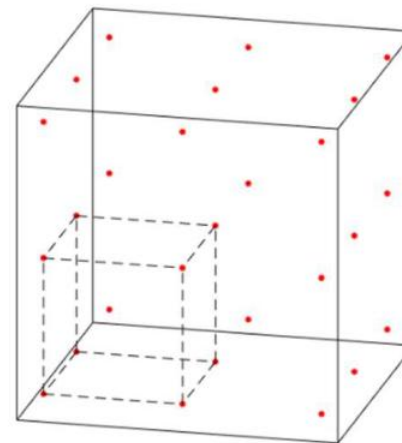


$$f_L = \frac{1}{2} \rho U_{rel}^2 S C_l, \quad f_D = \frac{1}{2} \rho U_{rel}^2 S C_d,$$

cell averaged velocity

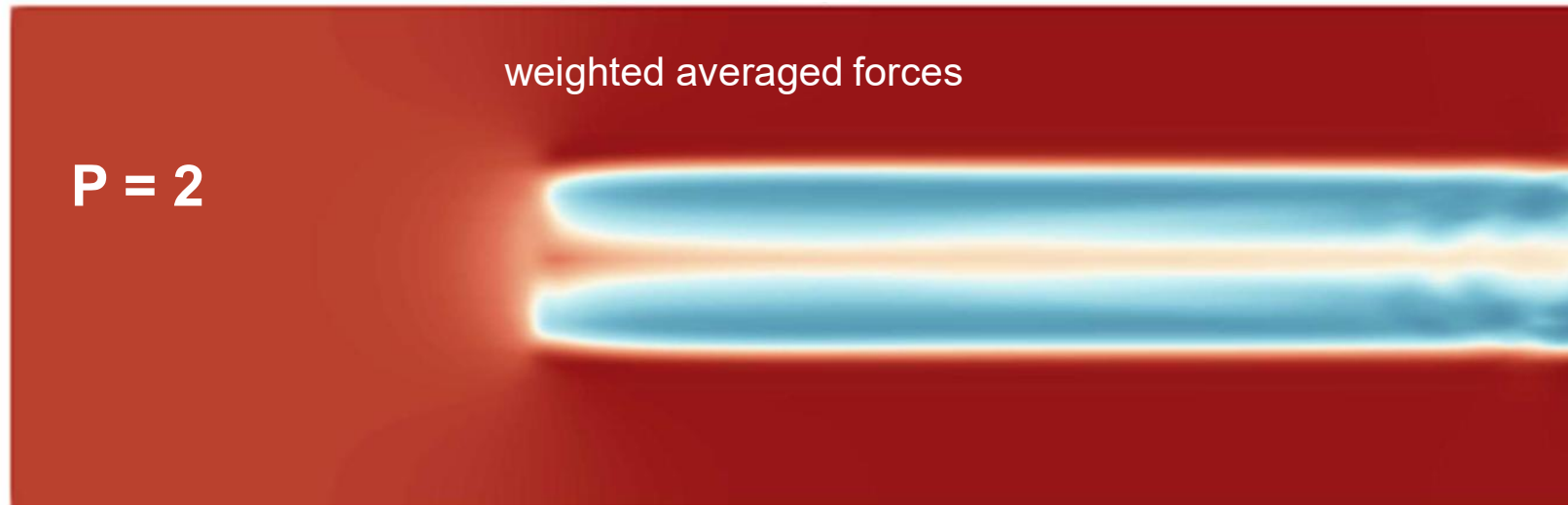
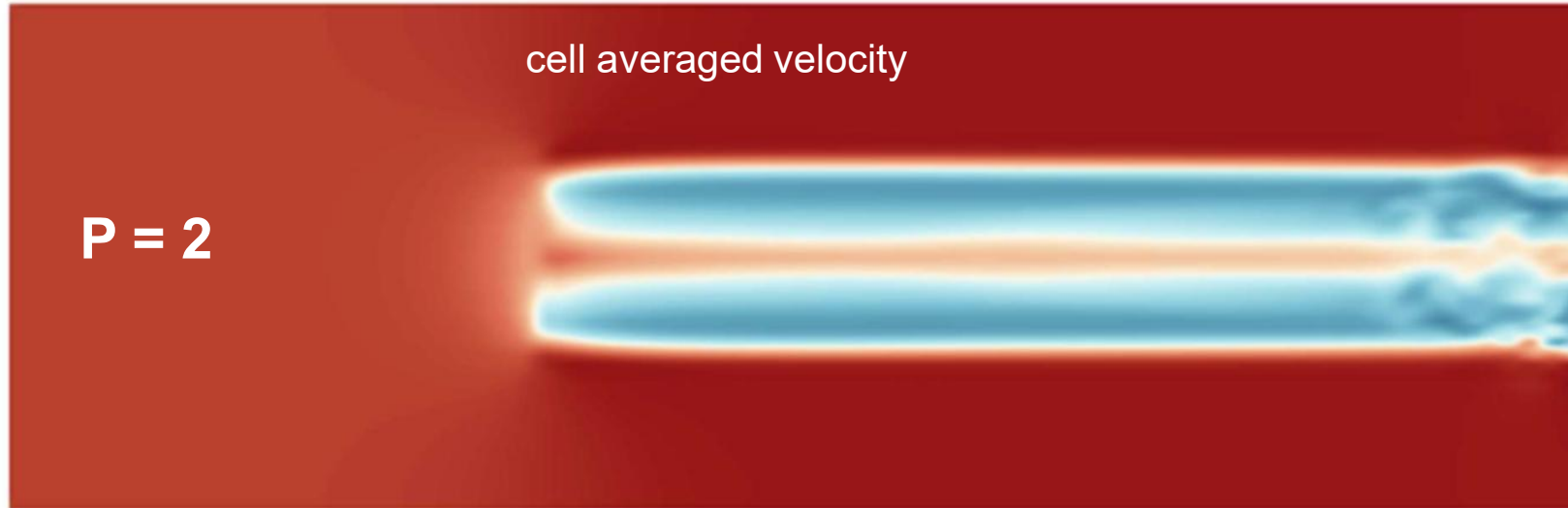


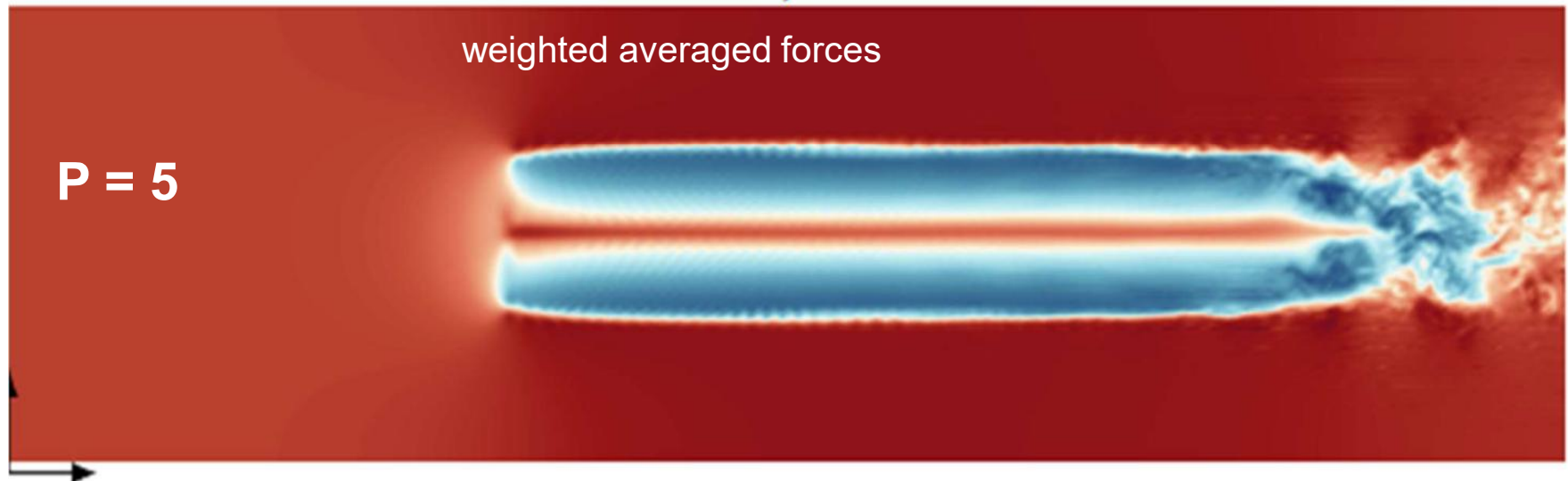
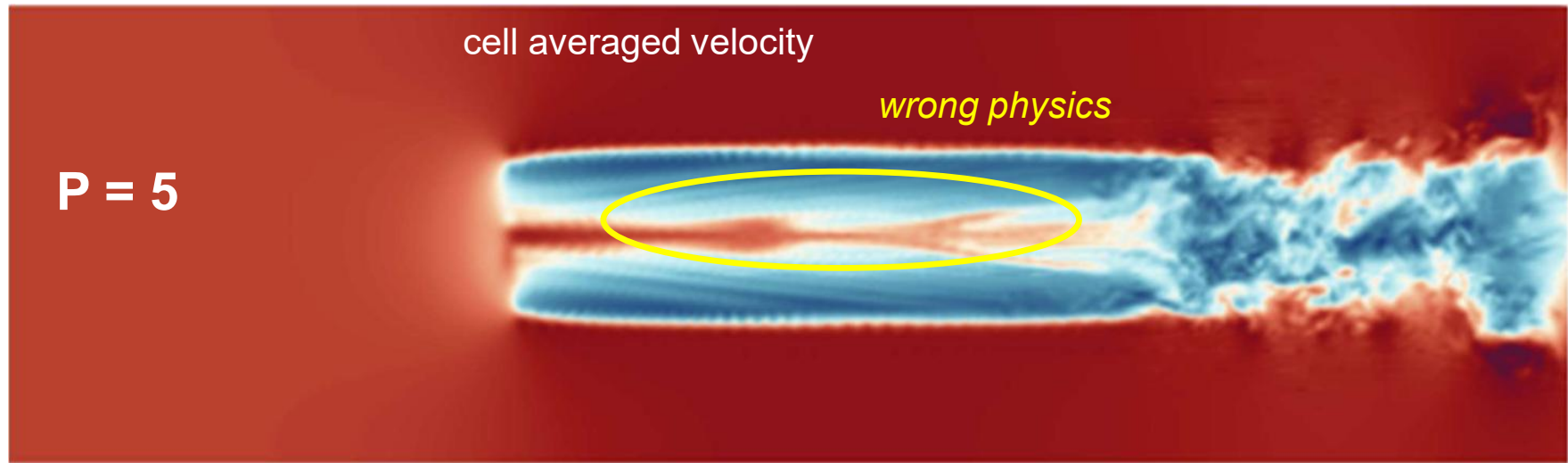
$$\bar{\mathbf{q}_t} = \frac{1}{N} \sum_{i=1}^N \mathbf{q}_{t_i}$$

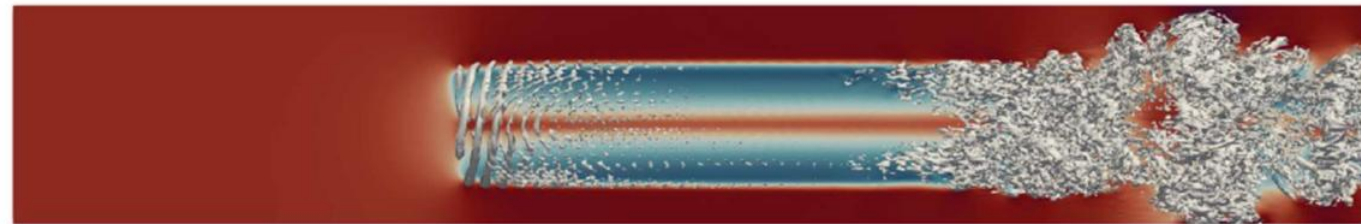


weighted averaged forces

$$\bar{f}_j = \frac{\sum_{i=1}^N \eta_{ji}(d) \cdot f_i}{\sum_{j=1}^{N_a} \sum_{i=1}^N \eta_{ji}(d)}$$



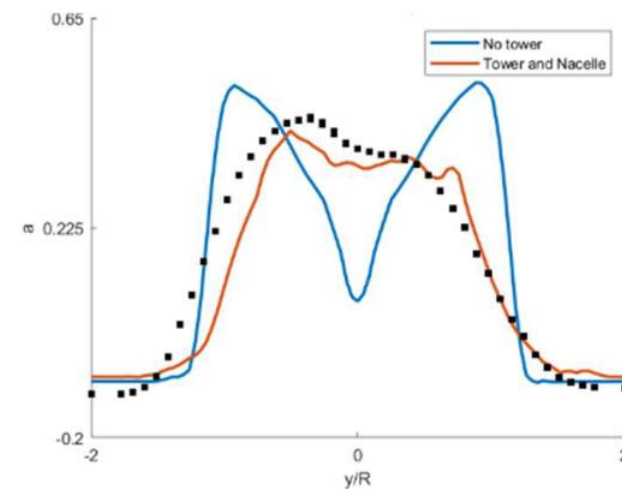
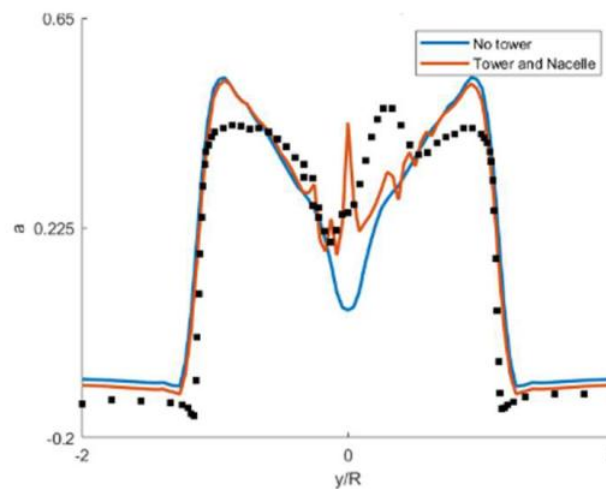




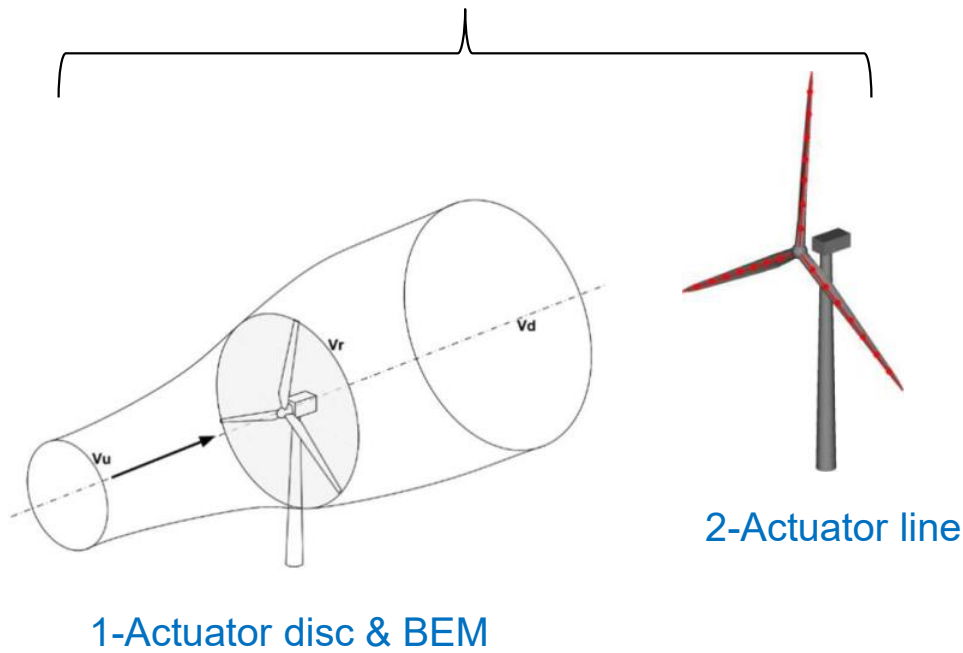
a) Actuator line without tower and nacelle.



b) Actuator line with tower and nacelle, which are modeled using immersed boundaries.



Require 2D aerodynamic data

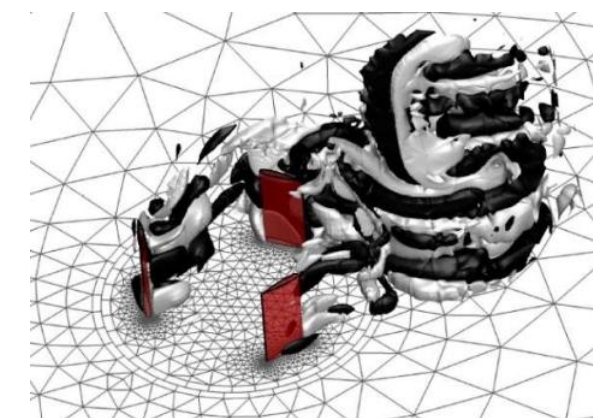
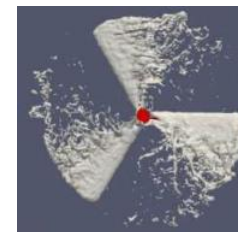


1-Actuator disc & BEM

2-Actuator line

Explicit 3D geometry

3-Immersed boundaries



4-Sliding meshes

Cost

Accuracy

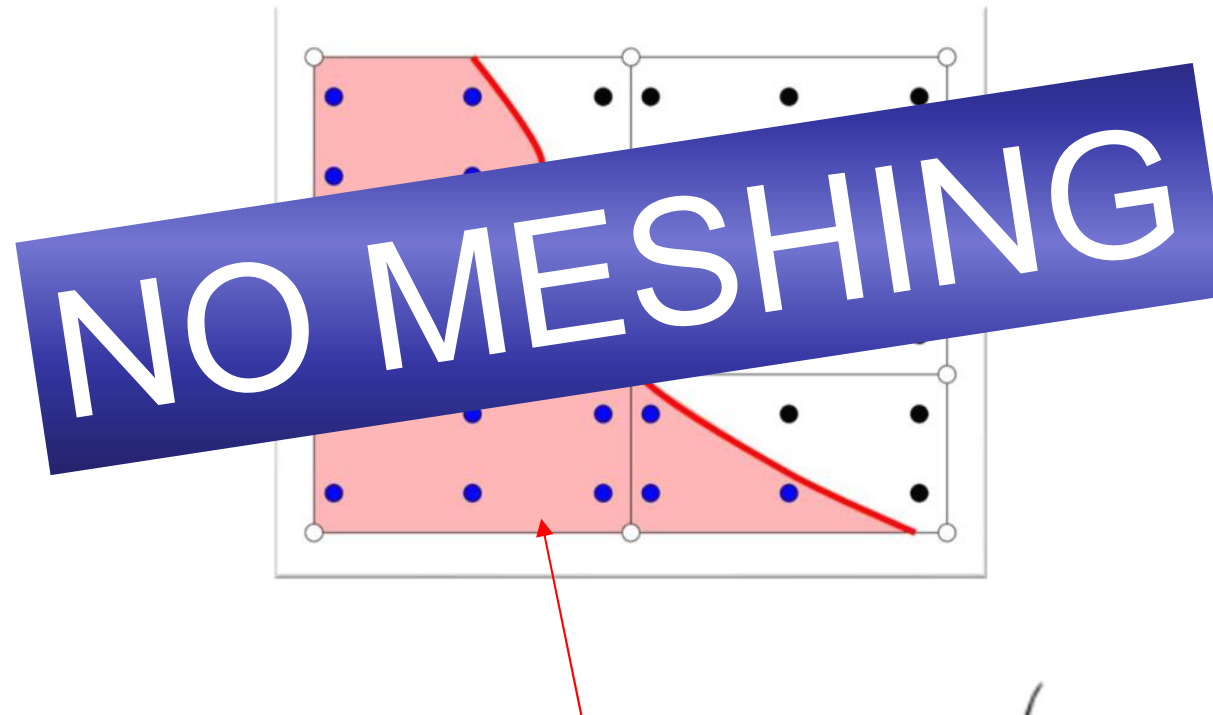
Low

High

- 4- E Ferrer and RHJ Willden, A high order Discontinuous Galerkin - Fourier incompressible 3D Navier–Stokes solver with **rotating sliding meshes**, *Journal of Computational Physics*, 2012
- 4- E Ferrer, RHJ Willden, Blade-wake interactions in **cross-flow turbines**, *International Journal of Marine Energy*, 2015
- 3- J Kou, A Hurtado-de-Mendoza, S Joshi, S Le Clainche, E Ferrer, Eigensolution analysis of **immersed boundaries** for high-order schemes, *Journal of Computational Physics*, 2022
- 3- J Kou, S Joshi, A Hurtado-de-Mendoza, K Puri, C Hirsch, E Ferrer, An **Immersed boundary** method for high-order flux reconstruction, *Journal of Computational Physics*, 2022
- 2 & 3- E Ferrer, S Colombo, O Marino, “Aeroacoustic predictions of wind turbines based on **actuator lines and immersed boundaries**”, *Under review at Wind Energy*
- 1- E Ferrer, S Le Clainche, **Simple models for cross flow turbines**, in *Recent advances in CFD for Wind and Tidal Offshore Turbines*, 2019
- 1- E Ferrer, OMF Browne, E Valero, Sensitivity analysis to control the far-wake unsteadiness behind **turbines**, *Energies*, 2017

Immersed boundary method (penalty) → Mesh Free method

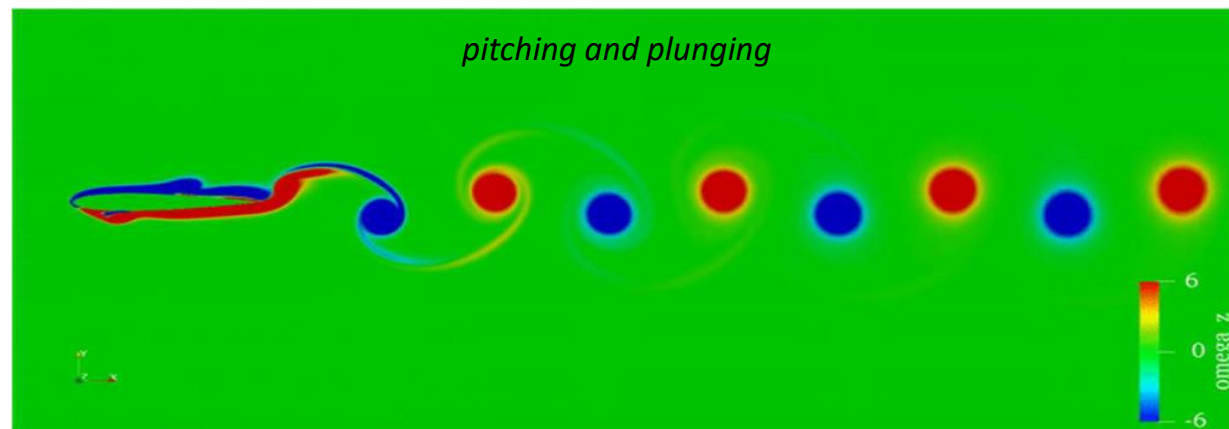
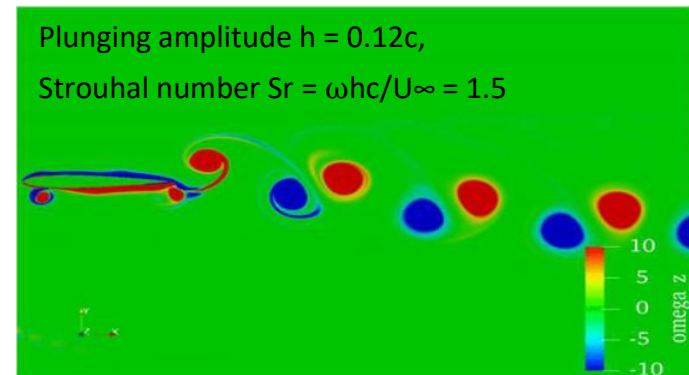
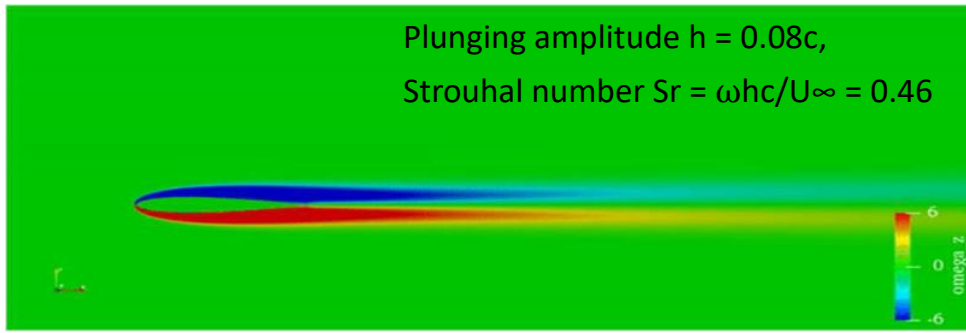
- Simple ‘Cartesian’ grids (with local P refinement)
- Complex geometries
- Moving geometries



$$\frac{\partial \mathbf{U}}{\partial t} + \nabla \cdot \vec{\mathbf{F}}(\mathbf{U}) = \nabla \cdot \vec{\mathbf{G}}(\mathbf{U}, \nabla \mathbf{U}) + \boxed{\mathbf{S}(\mathbf{U})}.$$

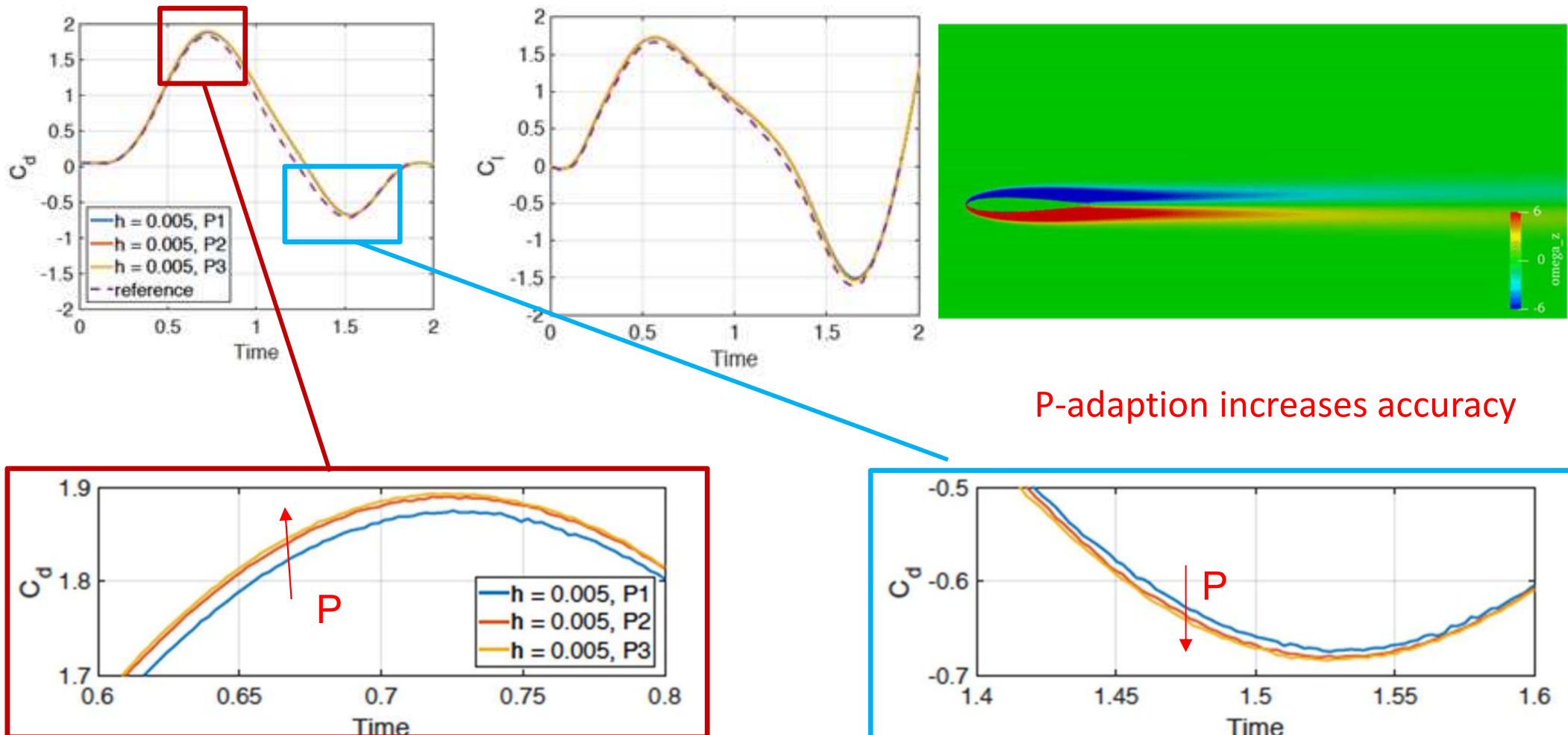
$$\mathbf{S}(\mathbf{U}) = a \times \begin{pmatrix} 0 \\ \rho u_0 - \rho u \\ \rho v_0 - \rho v \\ \rho w_0 - \rho w \\ \frac{\rho}{2}(u_0^2 + v_0^2 + w_0^2) - \frac{\rho}{2}(u^2 + v^2 + w^2) \end{pmatrix}$$

Moving NACA0012 at Reynolds number 1000, *pitching and plunging*:



- J Kou, A Hurtado-de-Mendoza, S Joshi, S Le Clainche, **E Ferrer**, "Eigensolution analysis of immersed boundary method based on volume penalization: applications to high-order schemes", *Journal of Computational Physics*, Vol 449, 110817, 2022
- J Kou, S Joshi, A Hurtado-de-Mendoza, K Puri, C Hirsch, **E Ferrer**, "An Immersed boundary method for high-order flux reconstruction based on volume penalization", *Journal of Computational Physics*, Vol 448, 110721, 2022
- J Kou, VJ Llorente, E Valero, **E Ferrer**, "A Modified Equation Analysis for Immersed Boundary Methods based on Volume Penalization: Applications to Linear Advection-Diffusion and High-Order Discontinuous Galerkin Schemes" *Computers & Fluids*, Vol 257, 105869, 2023
- J Kou, **E Ferrer**, "A combined volume penalization / selective frequency damping for immersed boundary methods applied to high-order schemes" *Journal of Computational Physics*, Vol 472, 111678, 2023

Moving NACA0012 at Reynolds number 1000, *pitching and plunging*:



- J Kou, A Hurtado-de-Mendoza, S Joshi, S Le Clainche, **E Ferrer**, "Eigensolution analysis of immersed boundary method based on volume penalization: applications to high-order schemes", *Journal of Computational Physics*, Vol 449, 110817, 2022
- J Kou, S Joshi, A Hurtado-de-Mendoza, K Puri, C Hirsch, **E Ferrer**, "An Immersed boundary method for high-order flux reconstruction based on volume penalization", *Journal of Computational Physics*, Vol 448, 110721, 2022
- J Kou, VJ Llorente, E Valero, **E Ferrer**, "A Modified Equation Analysis for Immersed Boundary Methods based on Volume Penalization: Applications to Linear Advection-Diffusion and High-Order Discontinuous Galerkin Schemes" *Computers & Fluids*, Vol 257, 105869, 2023
- J Kou, **E Ferrer**, "A combined volume penalization / selective frequency damping for immersed boundary methods applied to high-order schemes" *Journal of Computational Physics*, Vol 472, 111678, 2023

Immersed boundary method (penalty)

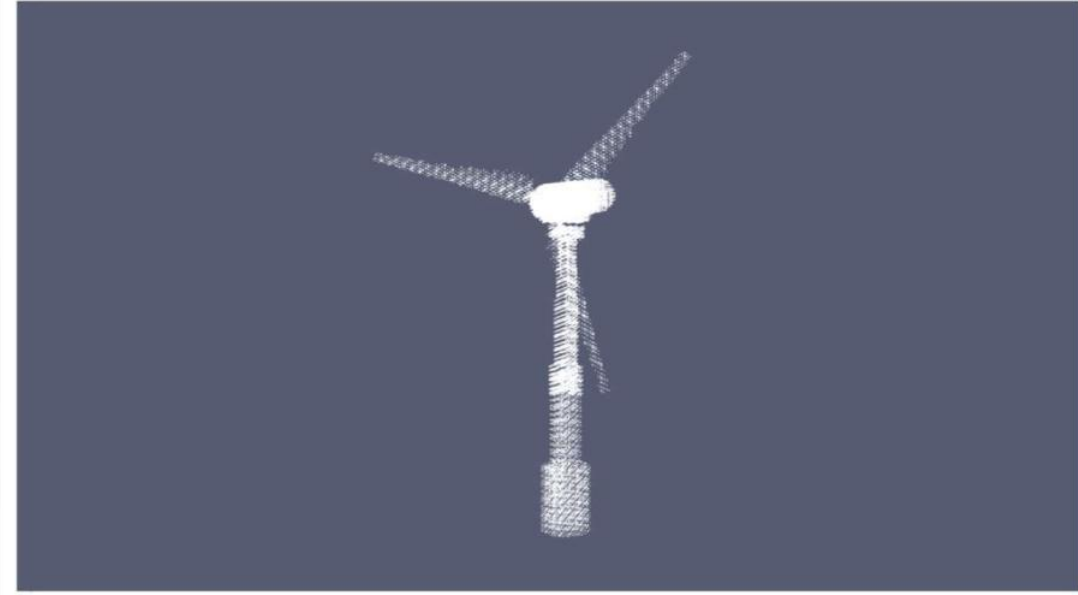
IB for rotating Wind turbine



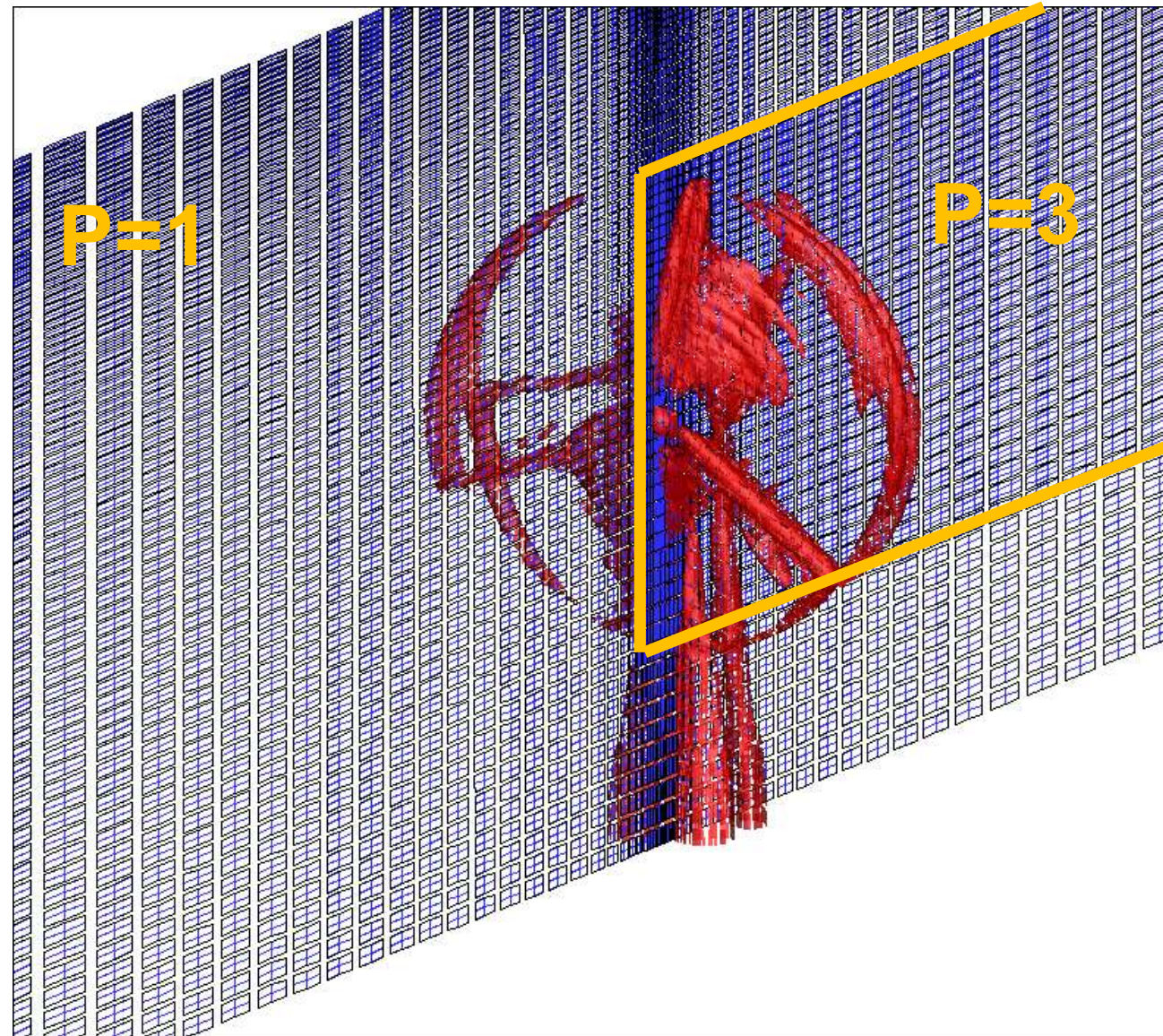
Only CAD '.stl' file
for the wind turbine

&

Simple Cartesian mesh



Penalty points for the wind turbine

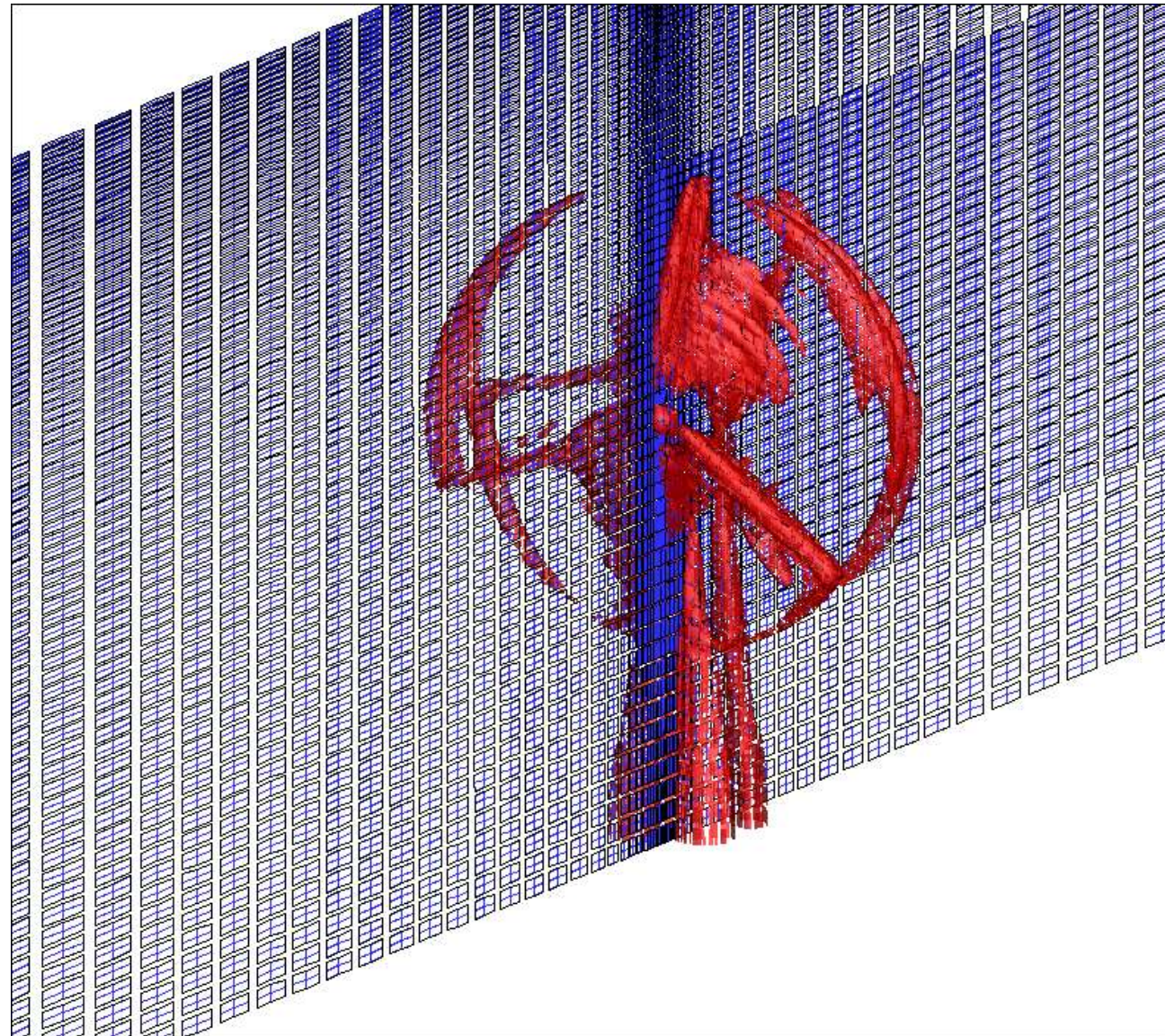


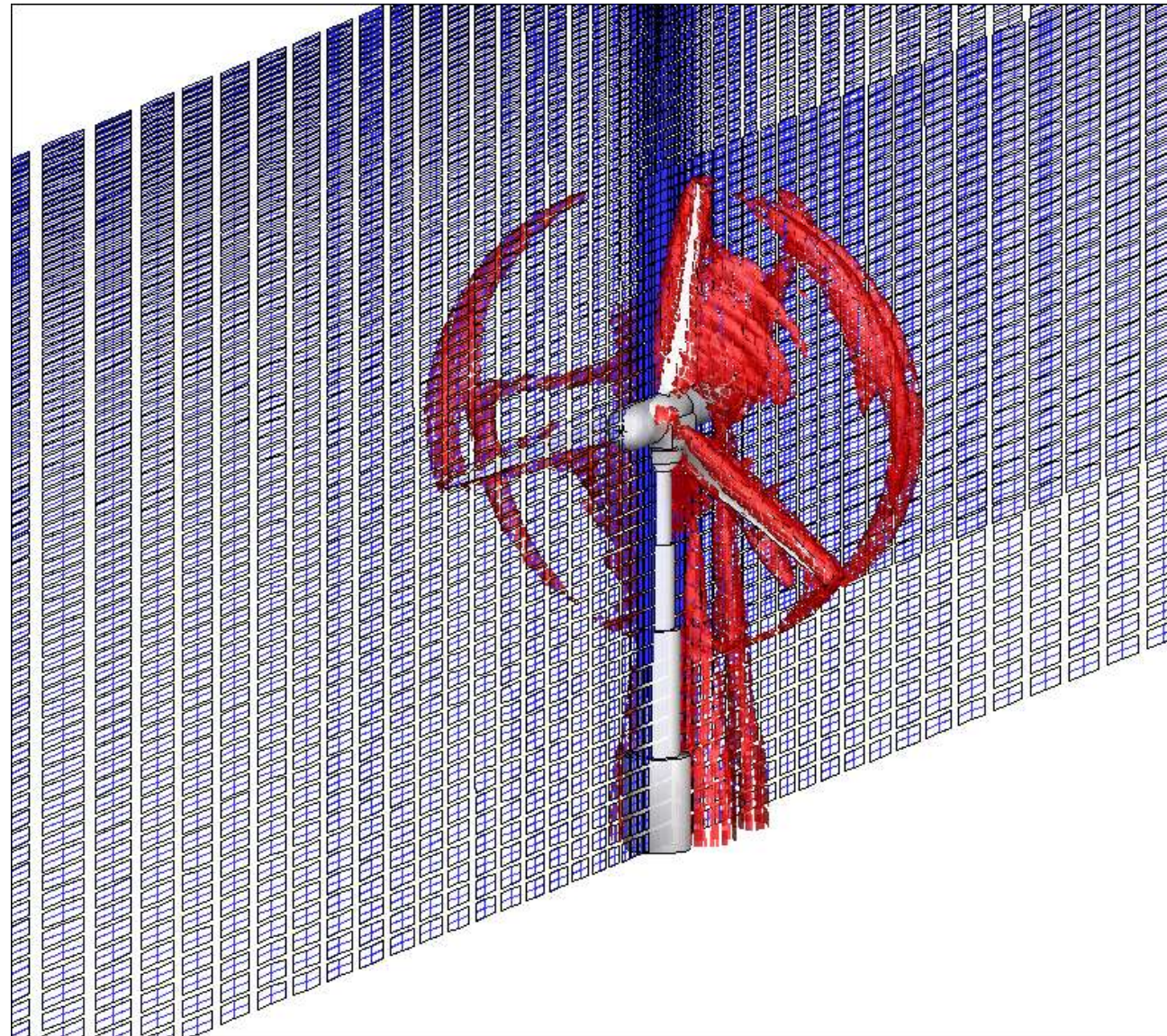


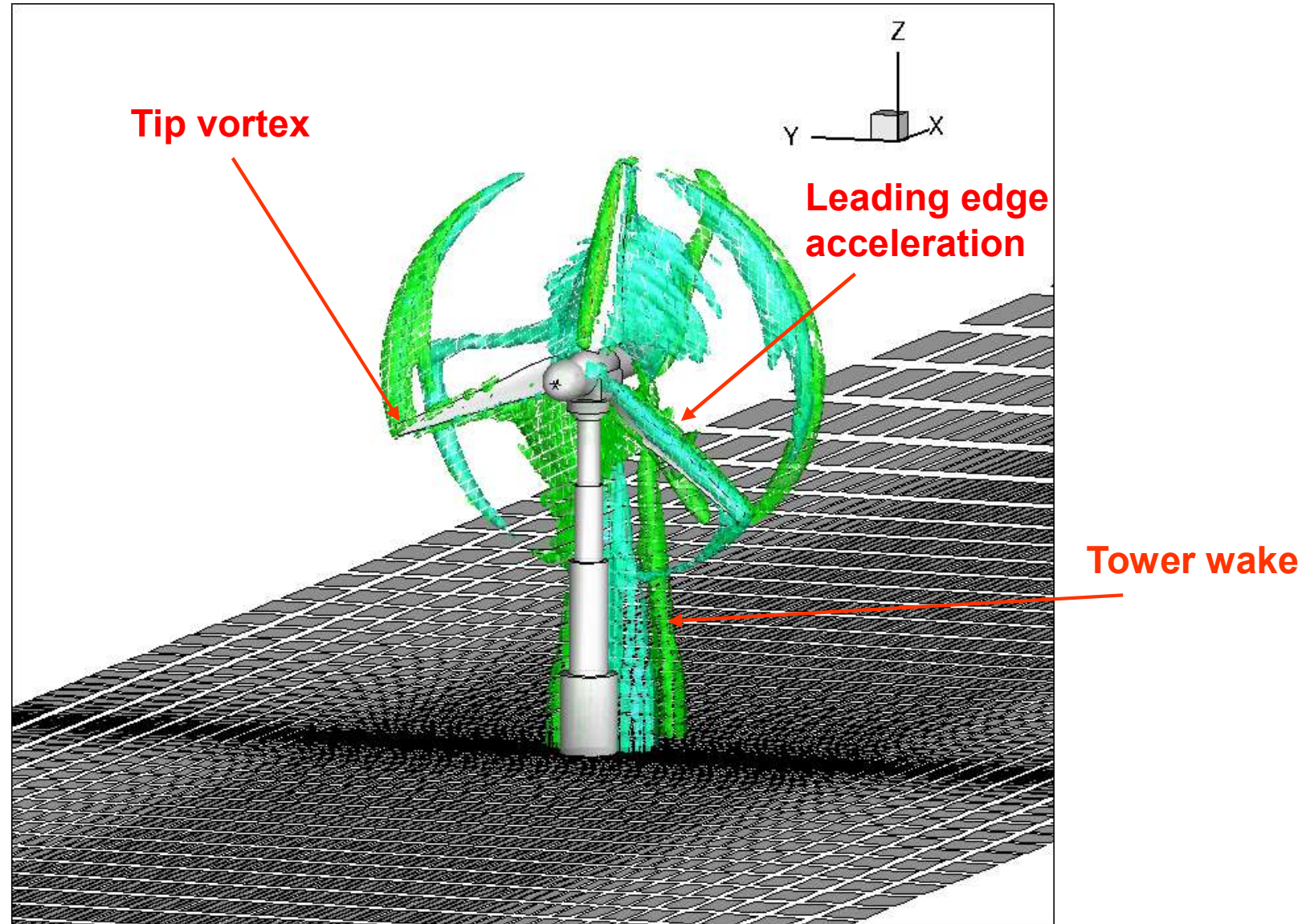
CAMPUS
DE EXCELENCIA
INTERNACIONAL

POLITÉCNICA

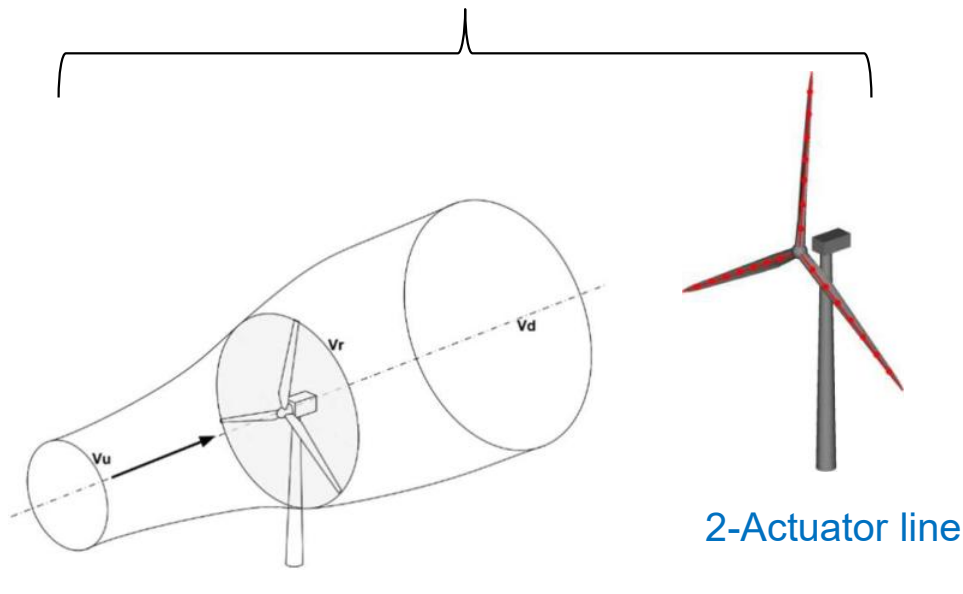
Universidad Politécnica de Madrid
ETS de Ingeniería Aeronáutica
y del Espacio







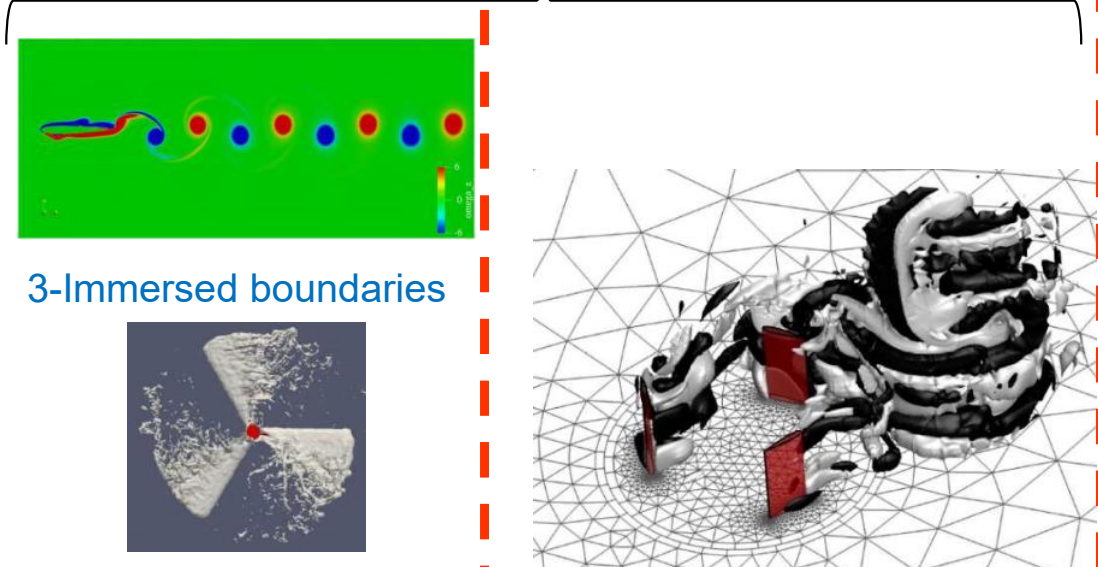
Require 2D aerodynamic data



1-Actuator disc & BEM

2-Actuator line

Explicit 3D geometry



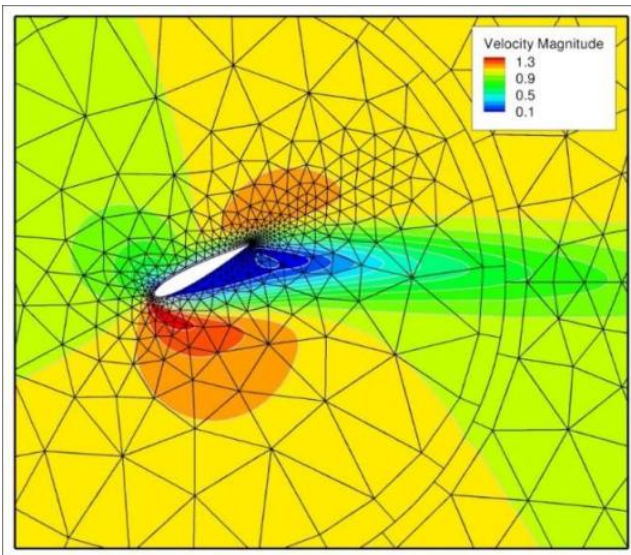
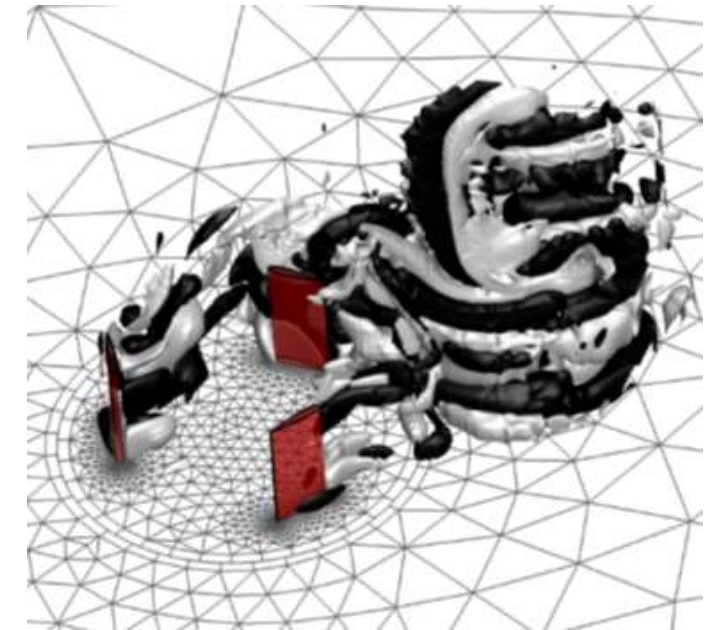
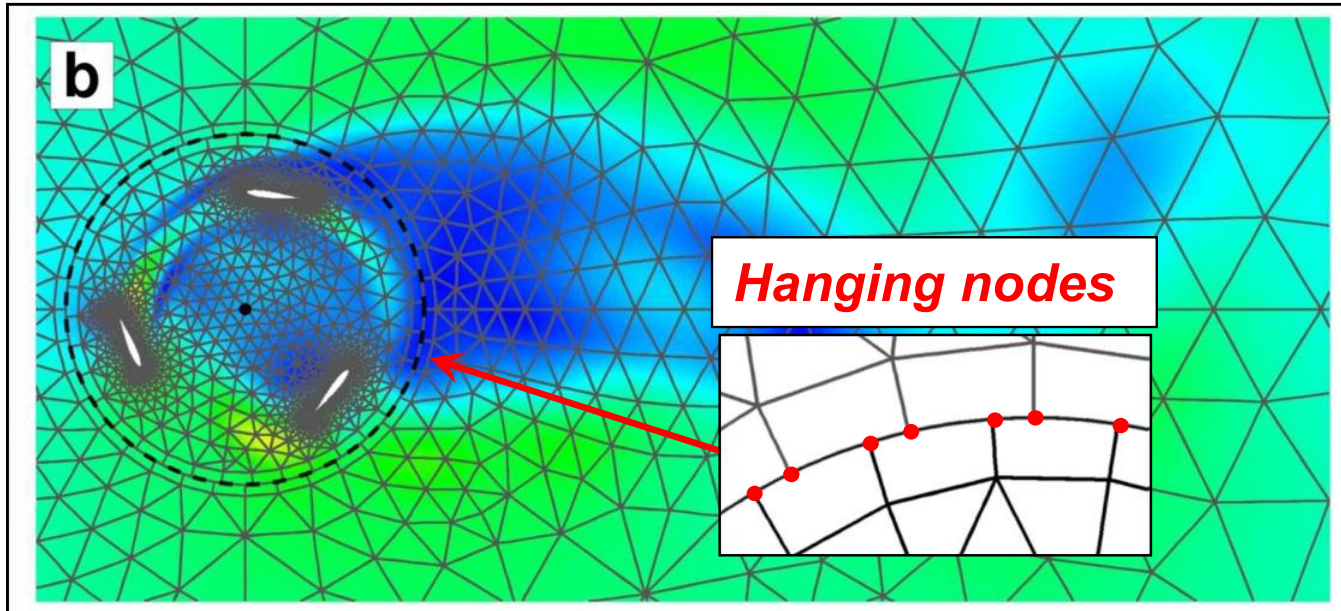
Cost

Accuracy

4-Sliding meshes

- 4- E Ferrer and RHJ Willden, A high order Discontinuous Galerkin - Fourier incompressible 3D Navier–Stokes solver with **rotating sliding meshes**, *Journal of Computational Physics*, 2012
- 4- E Ferrer, RHJ Willden, Blade–wake interactions in **cross-flow turbines**, *International Journal of Marine Energy*, 2015
- 3- J Kou, A Hurtado-de-Mendoza, S Joshi, S Le Clainche, E Ferrer, Eigensolution analysis of **immersed boundaries** for high-order schemes, *Journal of Computational Physics*, 2022
- 3- J Kou, S Joshi, A Hurtado-de-Mendoza, K Puri, C Hirsch, E Ferrer, An **Immersed boundary** method for high-order flux reconstruction, *Journal of Computational Physics*, 2022
- 2 & 3- E Ferrer, S Colombo, O Marino, “Aeroacoustic predictions of wind turbines based on **actuator lines and immersed boundaries**”, Under review at *Wind Energy*
- 1- E Ferrer, S Le Clainche, **Simple models for cross flow turbines**, in *Recent advances in CFD for Wind and Tidal Offshore Turbines*, 2019
- 1- E Ferrer, OMF Browne, E Valero, Sensitivity analysis to control the far–wake unsteadiness behind **turbines**, *Energies*, 2017

High order sliding meshes



DG solution
Rotating NACA0015
Re=100
Rot speed=0.3
polynomial order
k=5

Summary

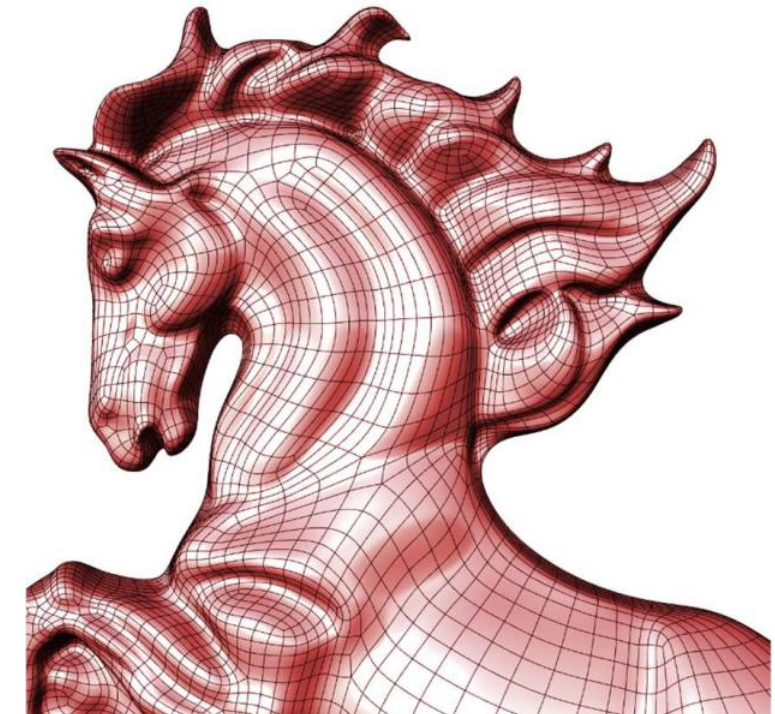
1- Introduction to DG & Horses3d

2- Multiphysics

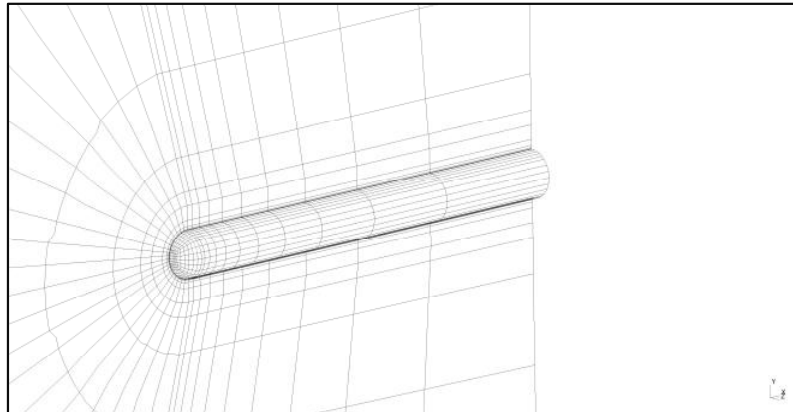
- Wind turbines
- Turbulence

3. Machine Learning + CFD

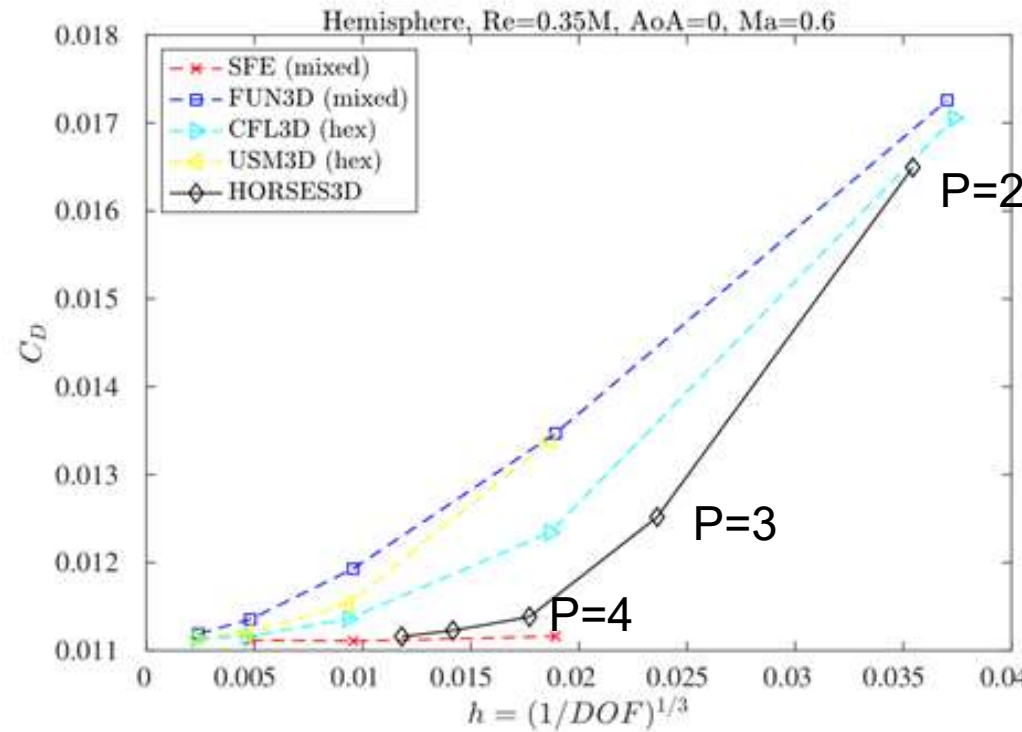
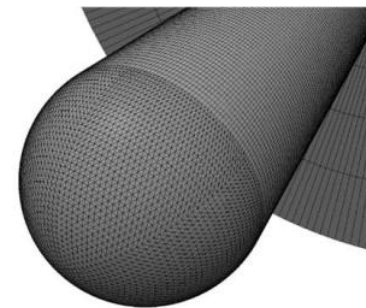
- Mesh adaption
- NN acceleration
- RL for automation



High order RANS (SAneg)

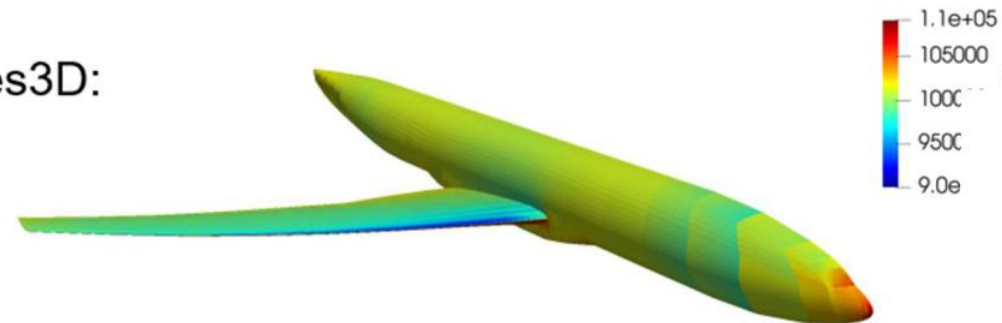


NASA workshop
https://turbmodels.larc.nasa.gov/hc3dnumerics_val.html

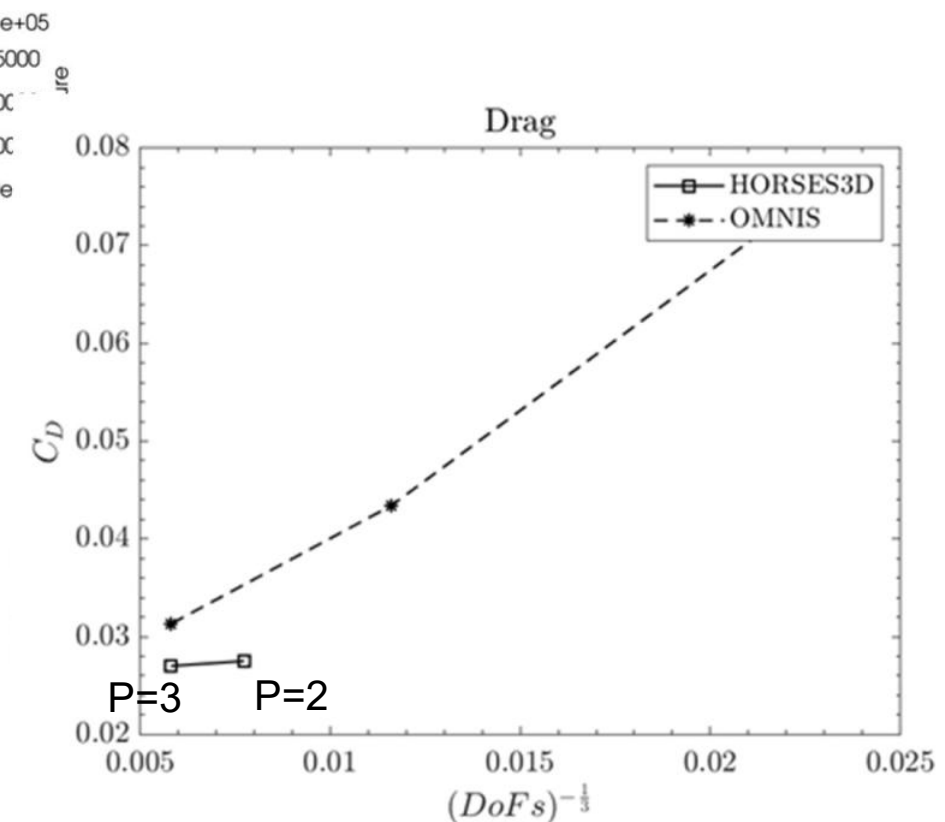
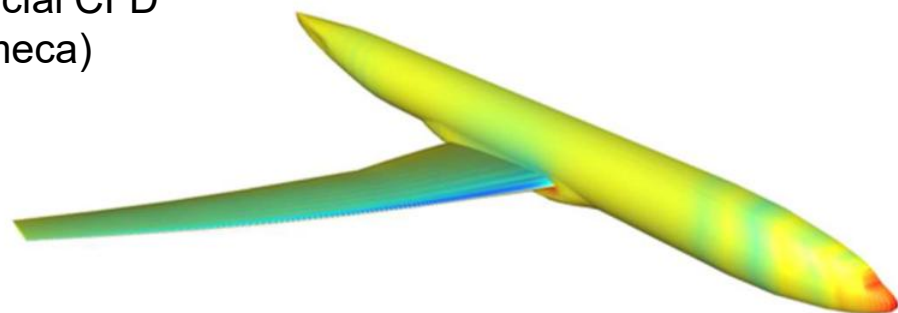


High order RANS (SAneg)

Horses3D:



Commercial CFD
(Numeca)



CRM Family Of Models

From Left to Right: High-Speed CRM, High-Lift CRM, CRM with NLF wing and Icing Research Tunnel CRM.

$Re=1.000.000$
 $AoA = 0 \text{ deg}$



$Re=1.000.000$
 $AoA = 5 \text{ deg}$



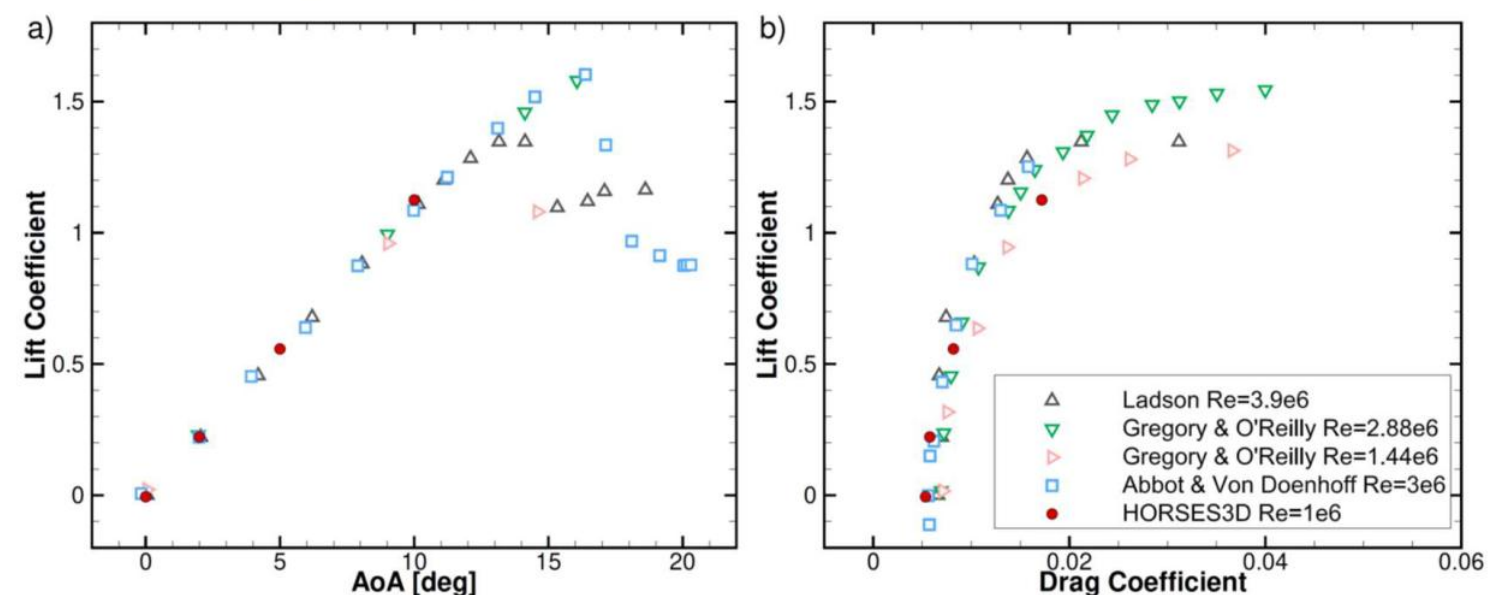
contours of velocity: [0.85; 1.2]

Implicit LES

$Re=1.000.000$
 $AoA = 10 \text{ deg}$

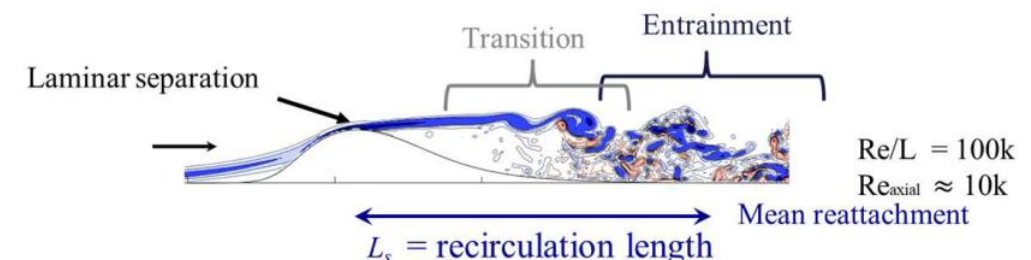
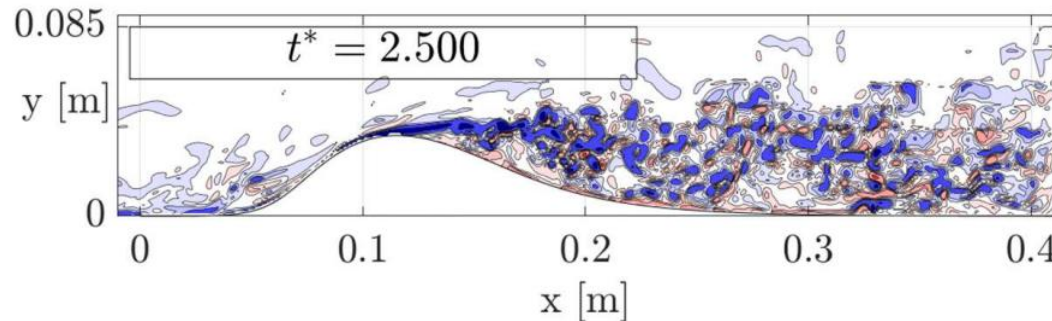


NACA0012 at various AoAs

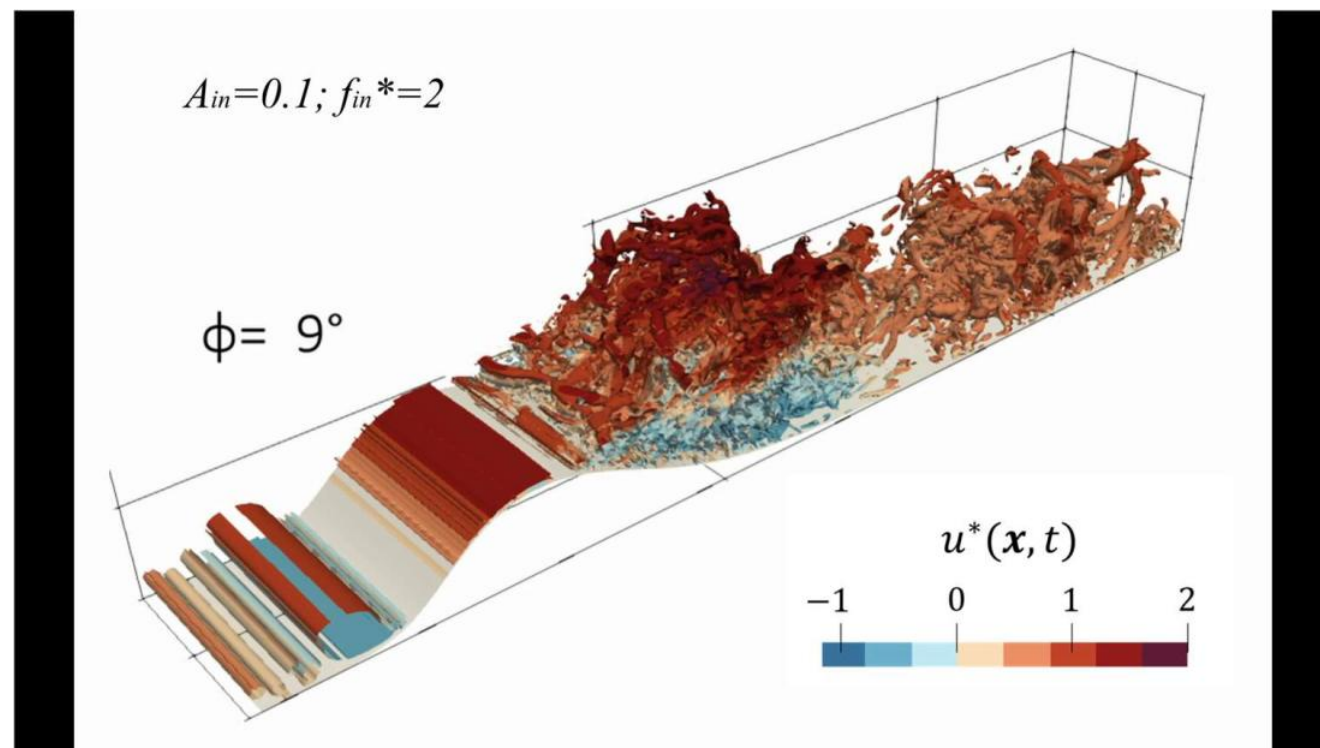


HORSES3D: Compressible DGSEM – energy-stable - SBP-SAT & Roe fluxes & BR1

E Ferrer, J Manzanero, AM Rueda-Ramirez, G Rubio, E Valero, "Implicit large eddy simulations for NACA0012 airfoils using compressible and incompressible DG solvers", *Spectral and High Order Methods for Partial Differential Equations ICOSAHOM 2018, Lecture Notes in Computational Science and Engineering*, Springer

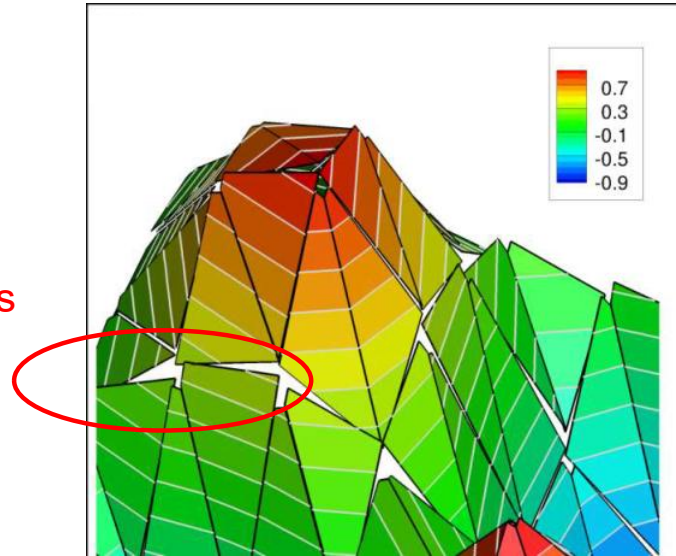


Implicit LES

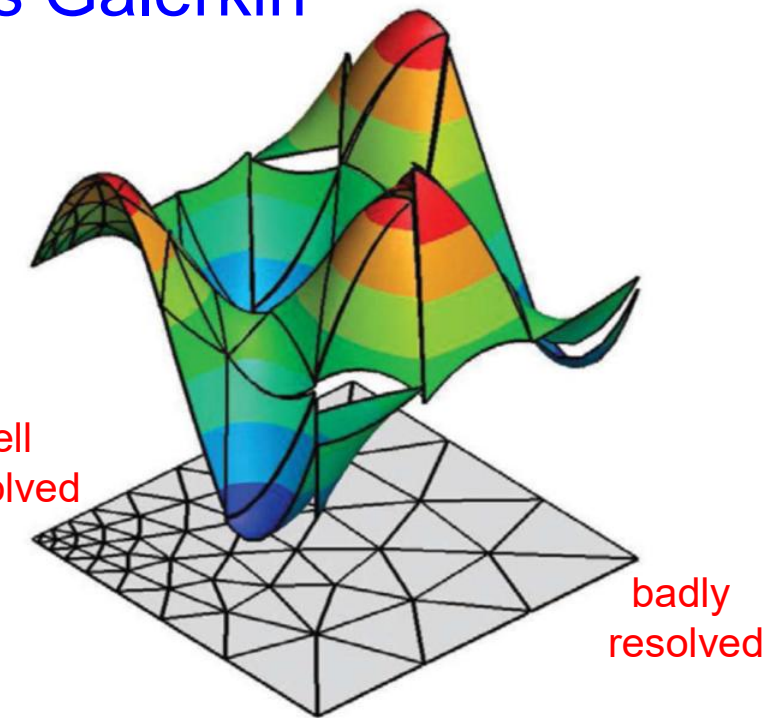


New turbulent models for discontinuous Galerkin

Discontinuous
solutions



well
resolved

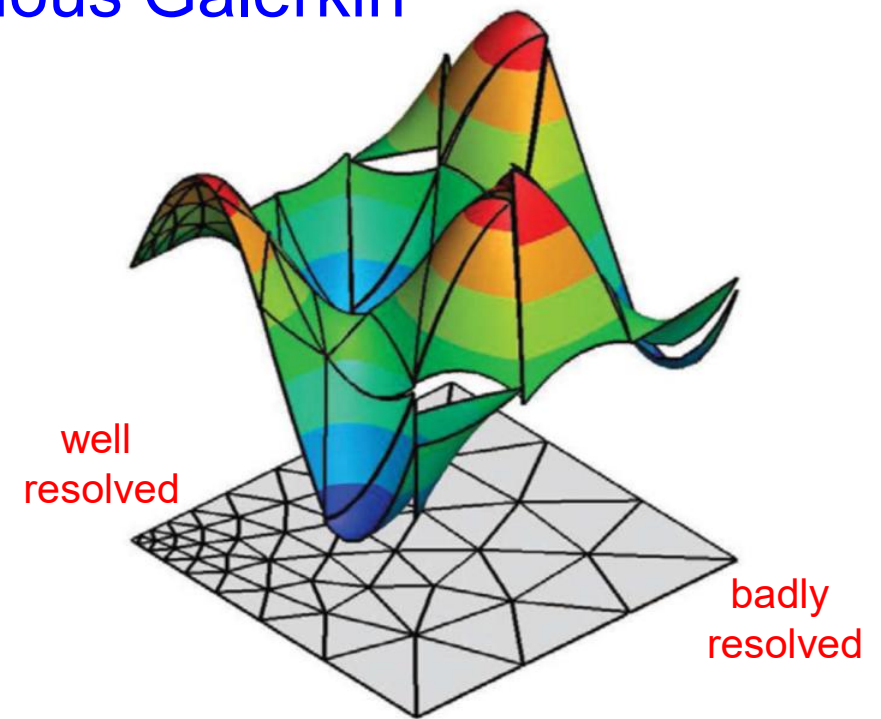
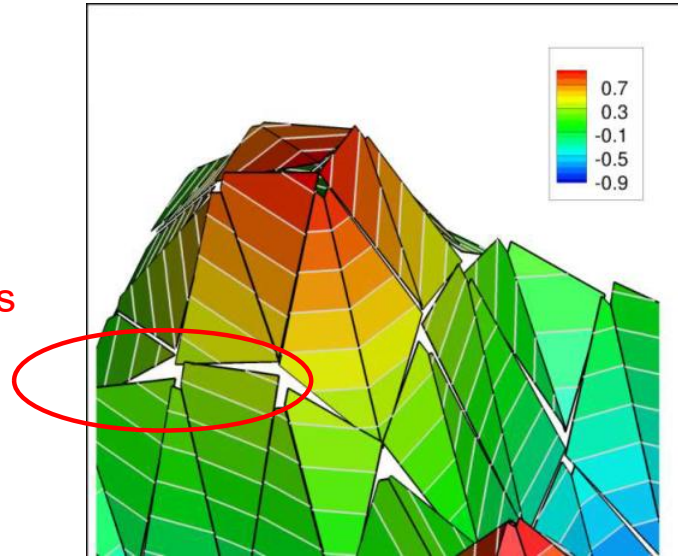


J Kou, OA Marino, **E Ferrer**, "Jump penalty stabilisation techniques for under-resolved turbulence in DG schemes" *Journal of Computational Physics*, Vol 491, 112399, 2023

E Ferrer, "An interior penalty stabilised incompressible DG–Fourier solver for implicit Large Eddy Simulations", *Journal of Computational Physics*, Vol 348, 2017

New turbulent models for discontinuous Galerkin

Discontinuous
solutions



Viscosity proportional to jumps (associated to under-resolution)

Solution: $\frac{\tau_s}{Re} \int_{\partial\Omega_n} [\tilde{\mathbf{q}}] \phi_i.$

Ferrer 2017

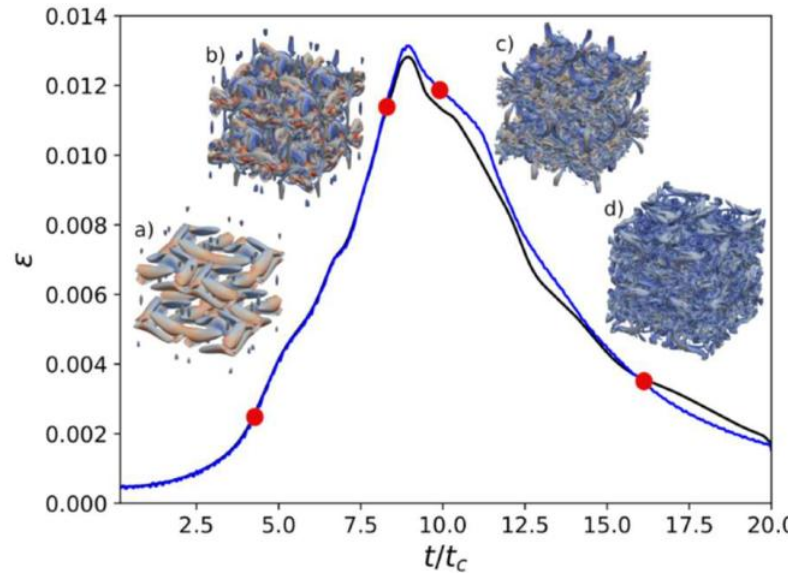
Gradients: $- \frac{\tau_g h^2}{Re} \int_{\partial\Omega_n} [\nabla \tilde{\mathbf{q}}] \nabla \phi_i \cdot \mathbf{n}$

Burman et al 2010
Moura et al 2022

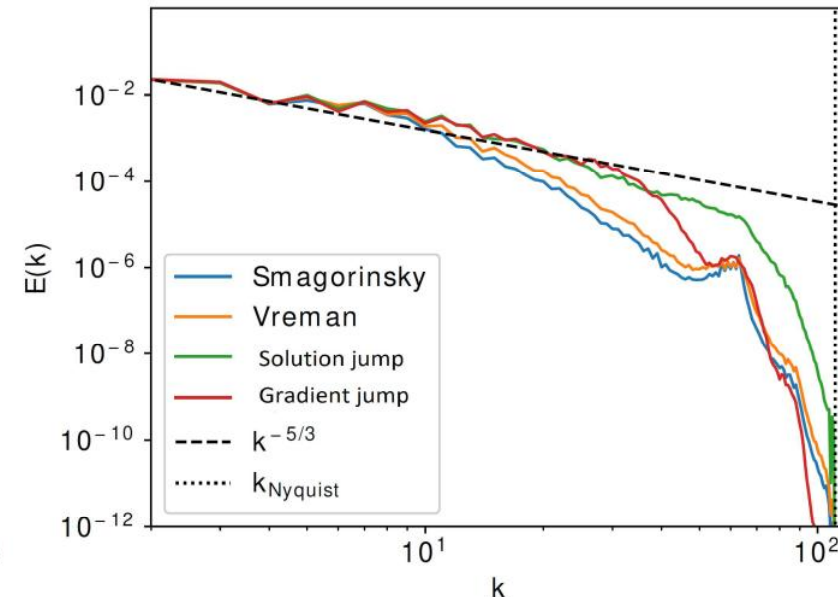
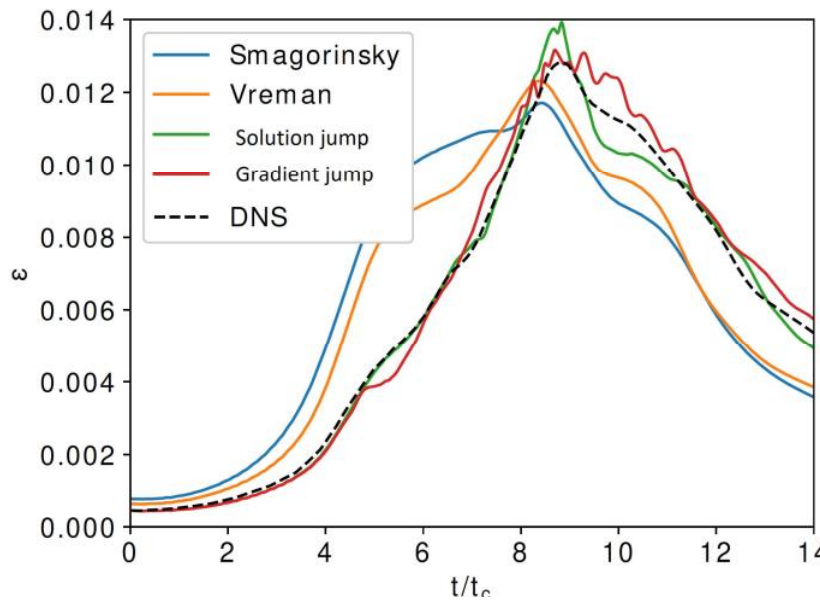
J Kou, OA Marino, **E Ferrer**, "Jump penalty stabilisation techniques for under-resolved turbulence in DG schemes" *Journal of Computational Physics*, Vol 491, 112399, 2023

E Ferrer, "An interior penalty stabilised incompressible DG–Fourier solver for implicit Large Eddy Simulations", *Journal of Computational Physics*, Vol 348, 2017

New turbulent models for discontinuous Galerkin



Taylor Green Vortex
Re=1600

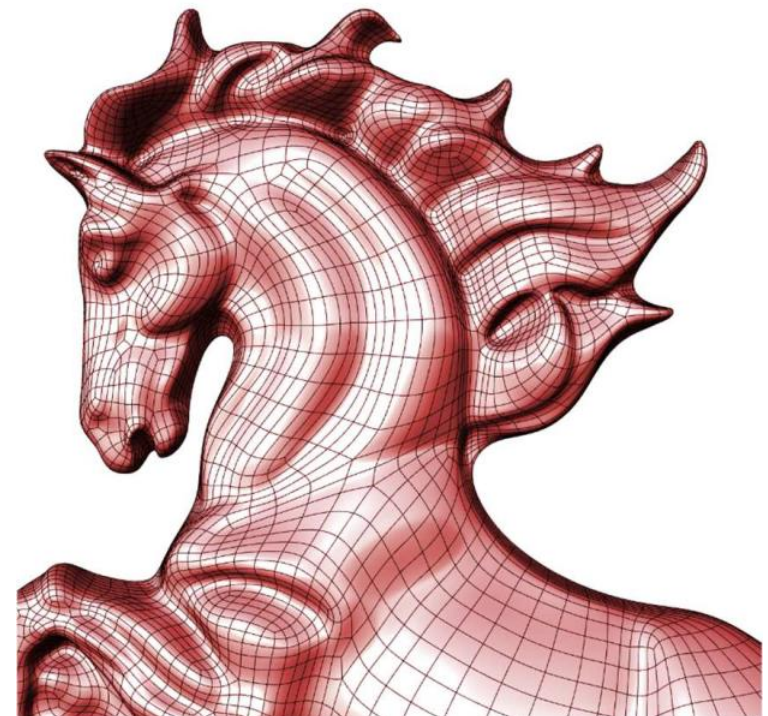


Summary

1- Introduction to DG & Horses3d

2- Multiphysics

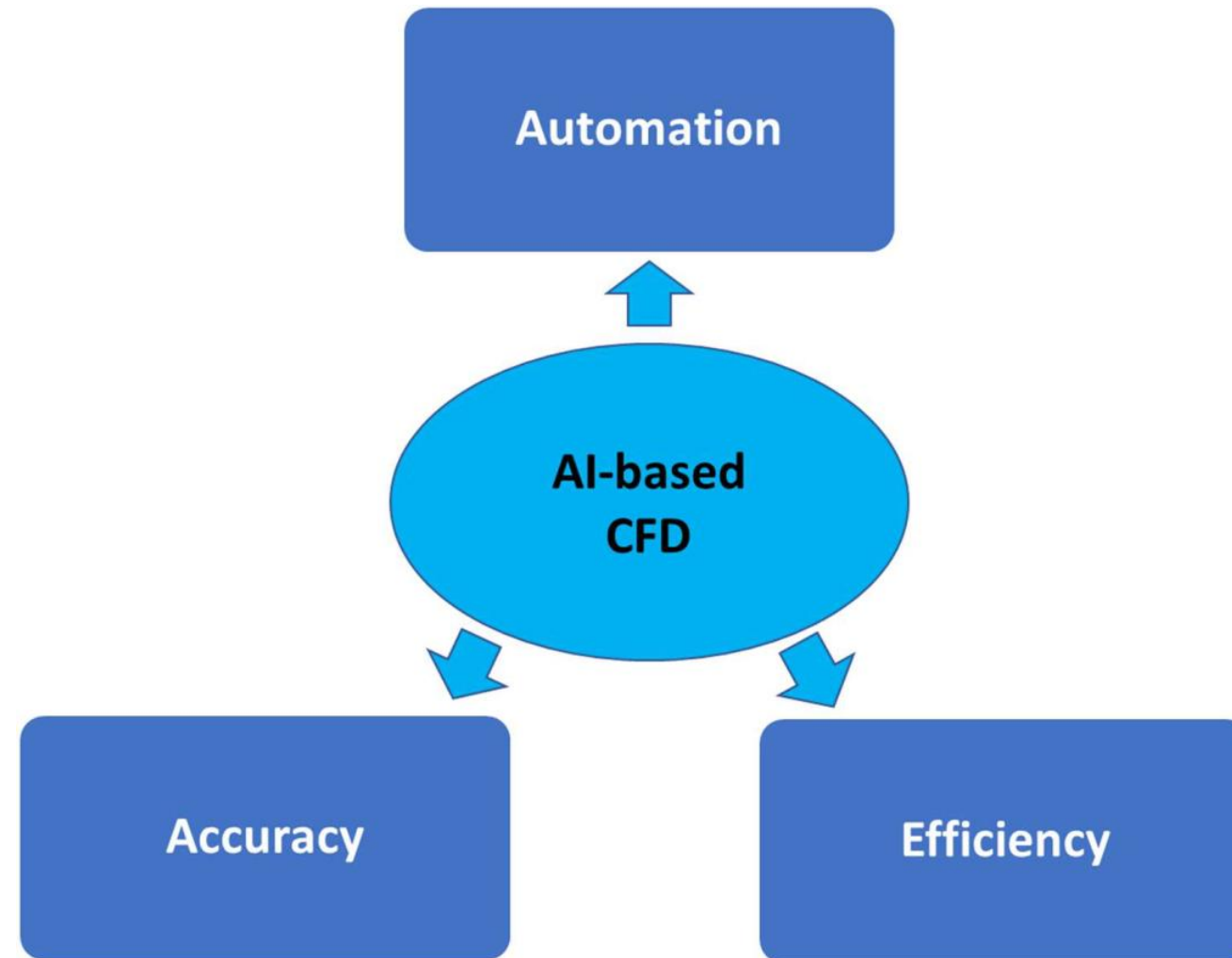
- Wind turbines
- Turbulence



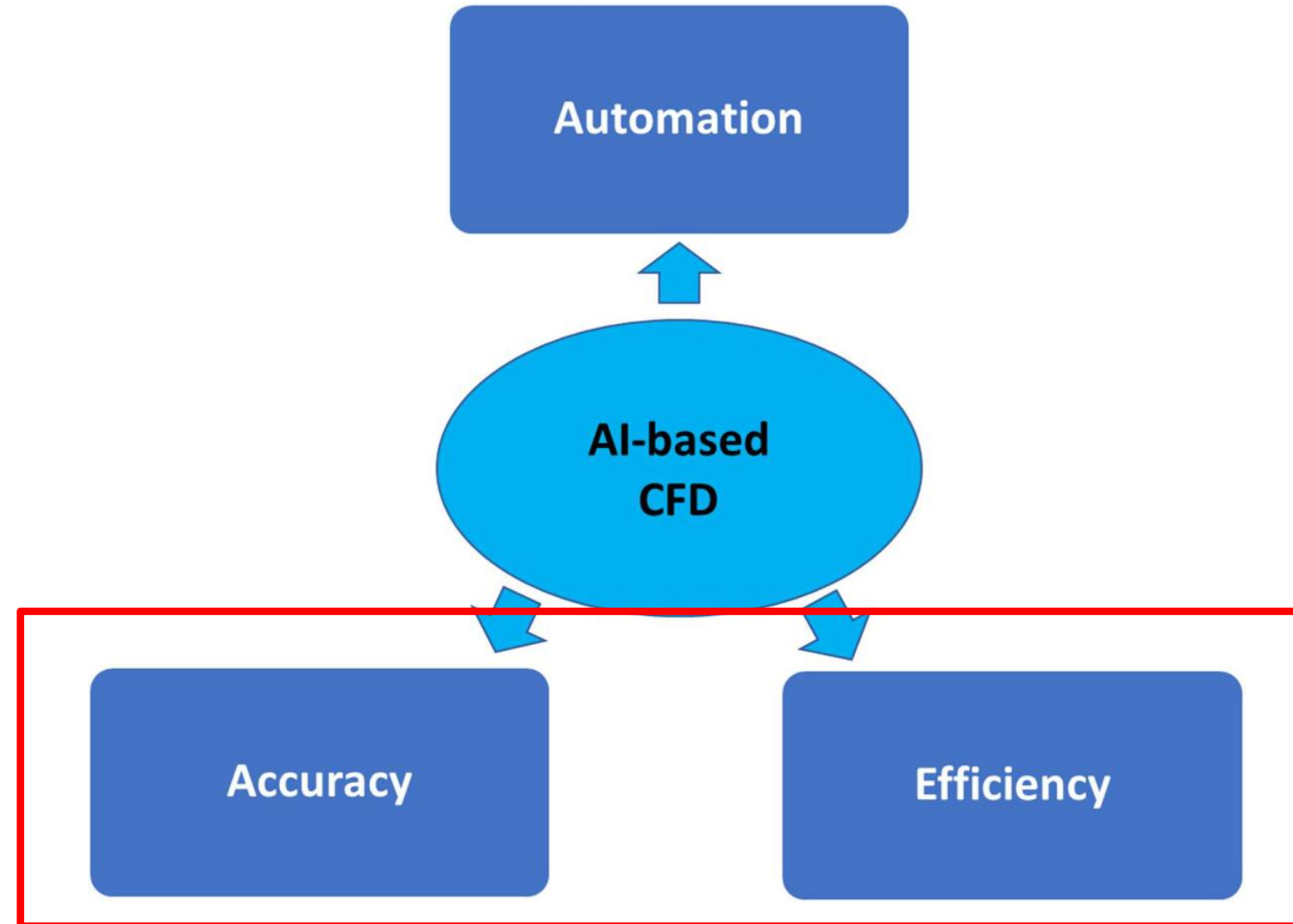
3. Machine Learning + CFD

- Mesh adaption
- NN acceleration
- RL for automation

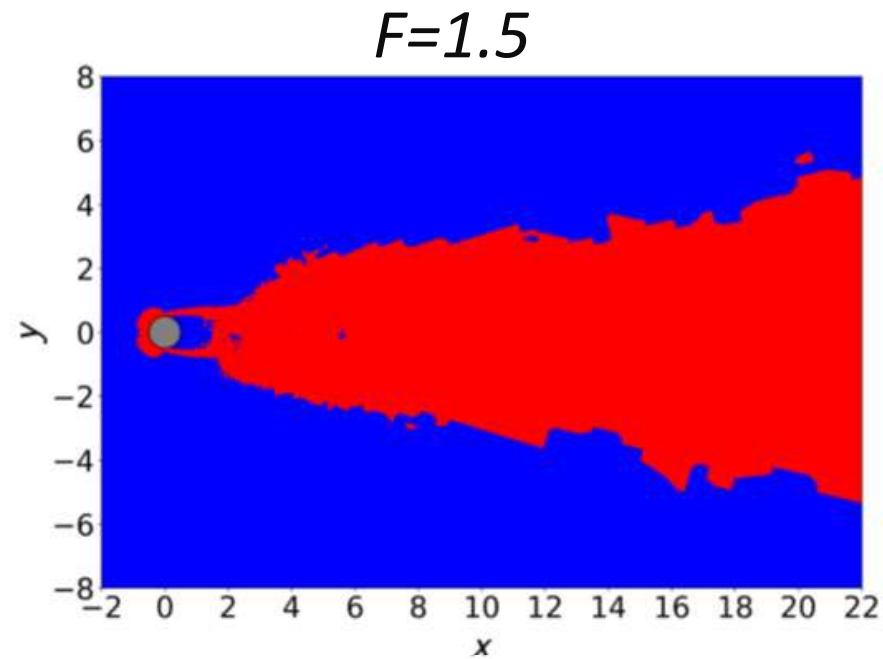
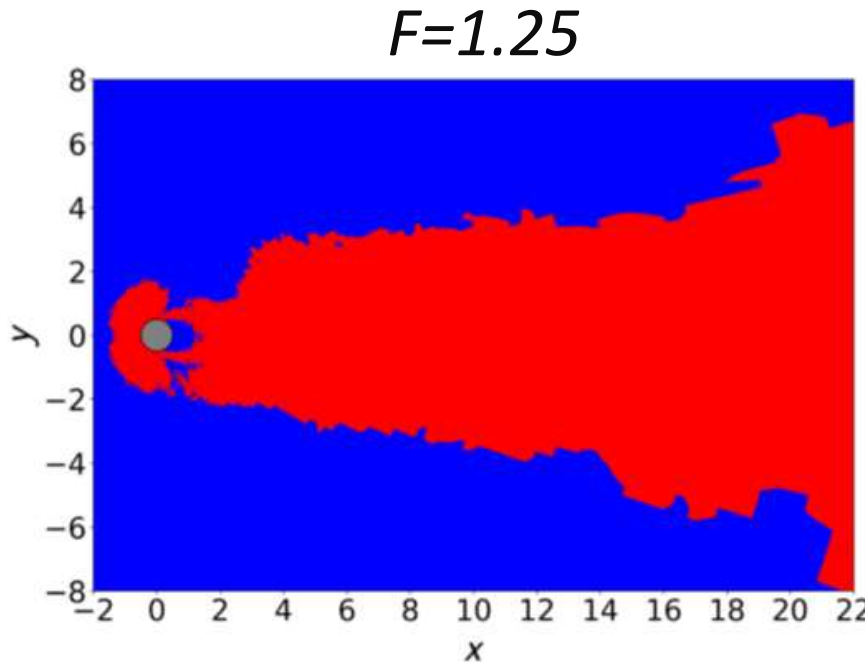
Towards AI-based Computational Fluid Dynamics



Towards AI-based Computational Fluid Dynamics

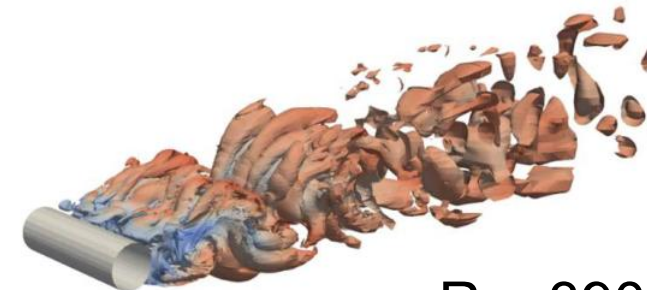
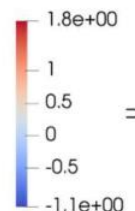


Machine Learning to detect flow regions



Feature based sensors
Eddy viscosity sensor

$$F_{\mu_t} = \frac{\mu + \mu_t}{\mu}$$

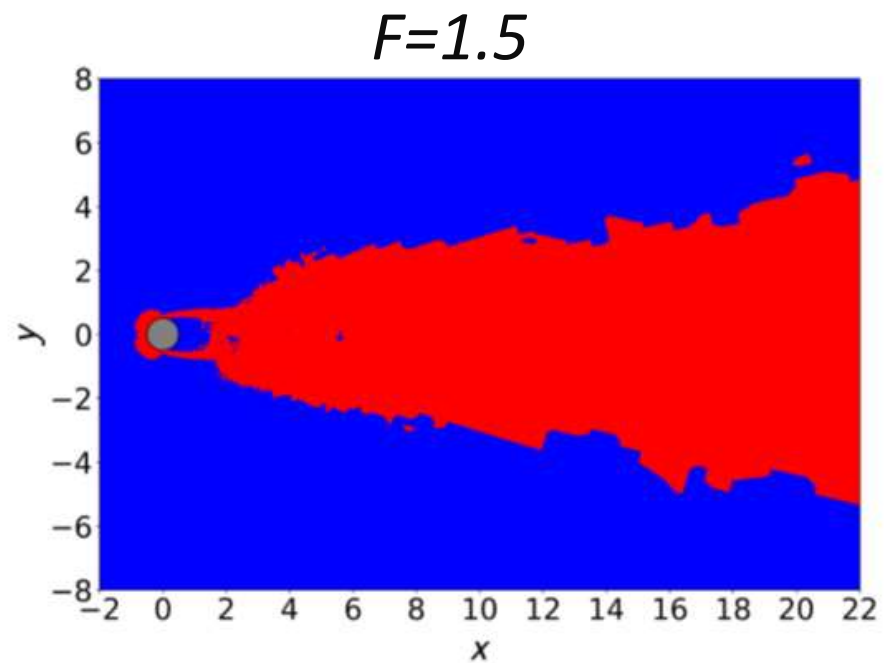
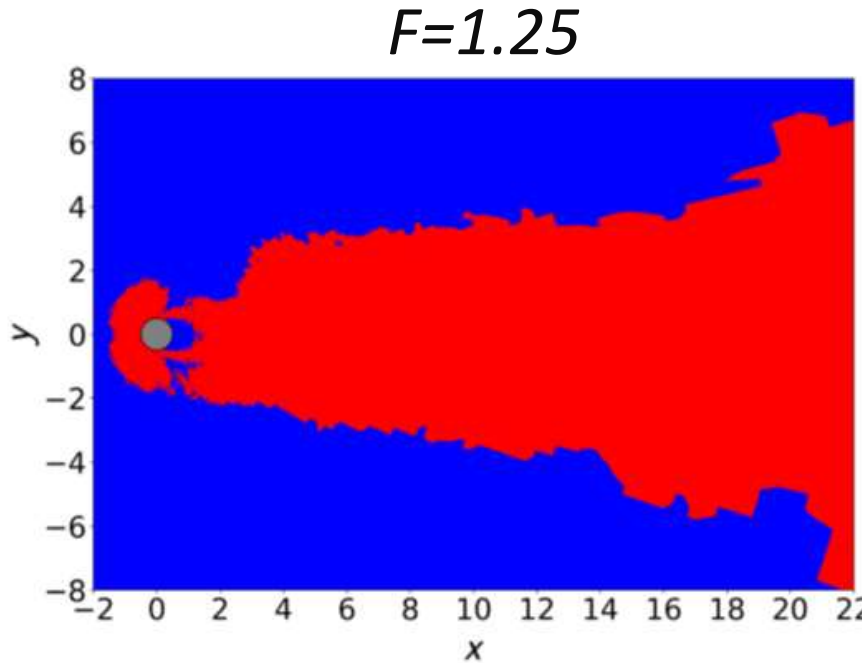


$Re=3900$

-KE Otmani, G Ntoukas, E Ferrer, "Towards a robust detection of flow regions using unsupervised machine learning", Vol 35, 027112, 2023

-K Tlales, KE Otmani, G Ntoukas, G Rubio, E Ferrer, "Machine learning mesh-adaptation for laminar and turbulent flows: applications to high order discontinuous Galerkin solvers", Engineering with Computers, 2024

Machine Learning to detect flow regions



Feature based sensors
Eddy viscosity sensor

- **Very sensitive to threshold**
- **Cannot detect mixed regions
(e.g. laminar-turbulent)**

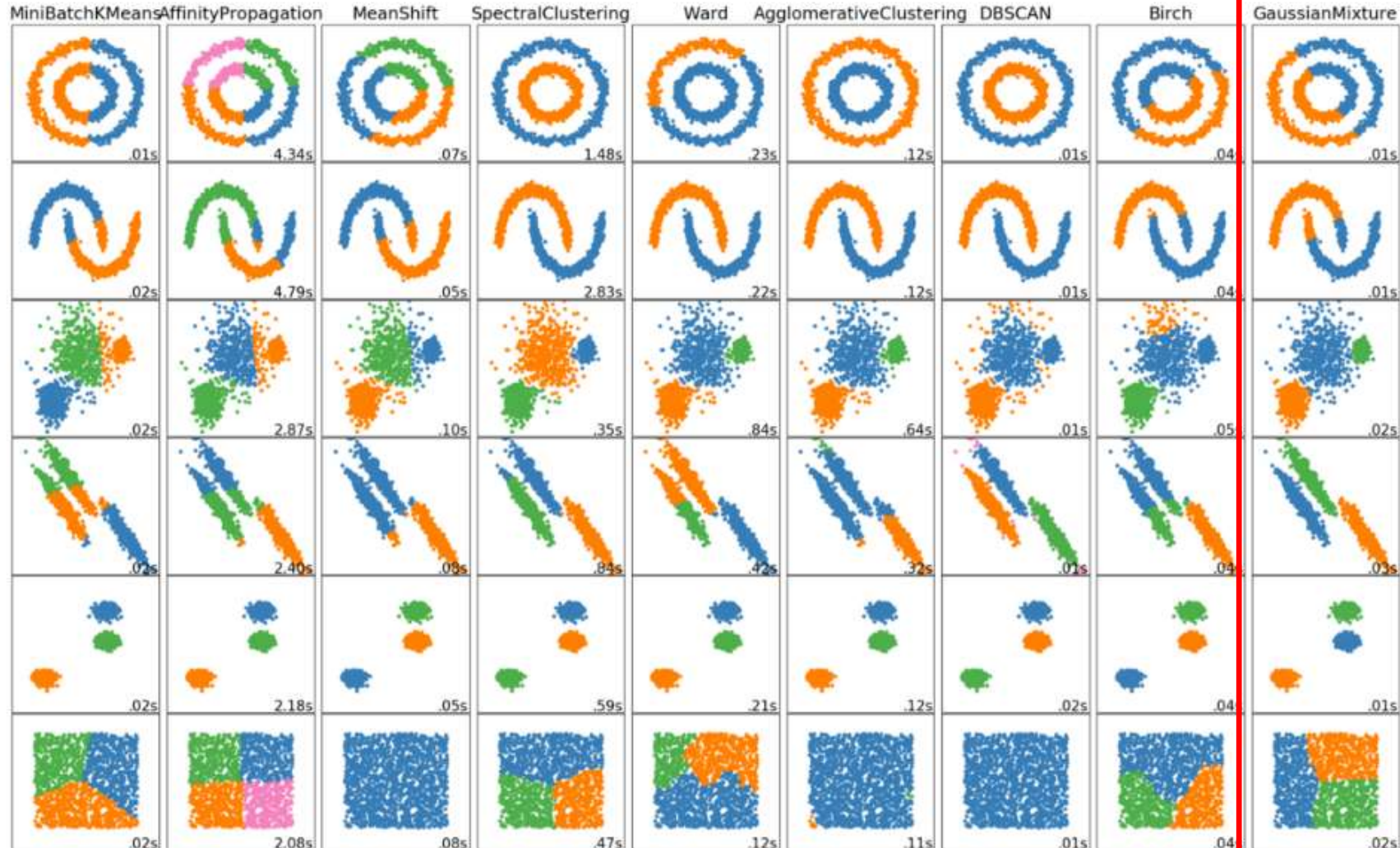
$$F_{\mu_t} = \frac{\mu + \mu_t}{\mu}$$

-KE Otmani, G Ntoukas, E Ferrer, "Towards a robust detection of flow regions using unsupervised machine learning", Vol 35, 027112, 2023

-K Tlales, KE Otmani, G Ntoukas, G Rubio, E Ferrer, "Machine learning mesh-adaptation for laminar and turbulent flows: applications to high order discontinuous Galerkin solvers", Engineering with Computers, 2024

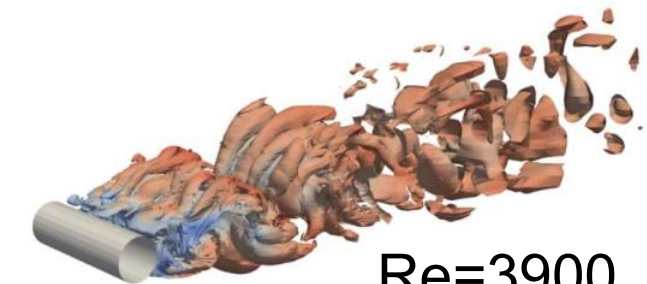
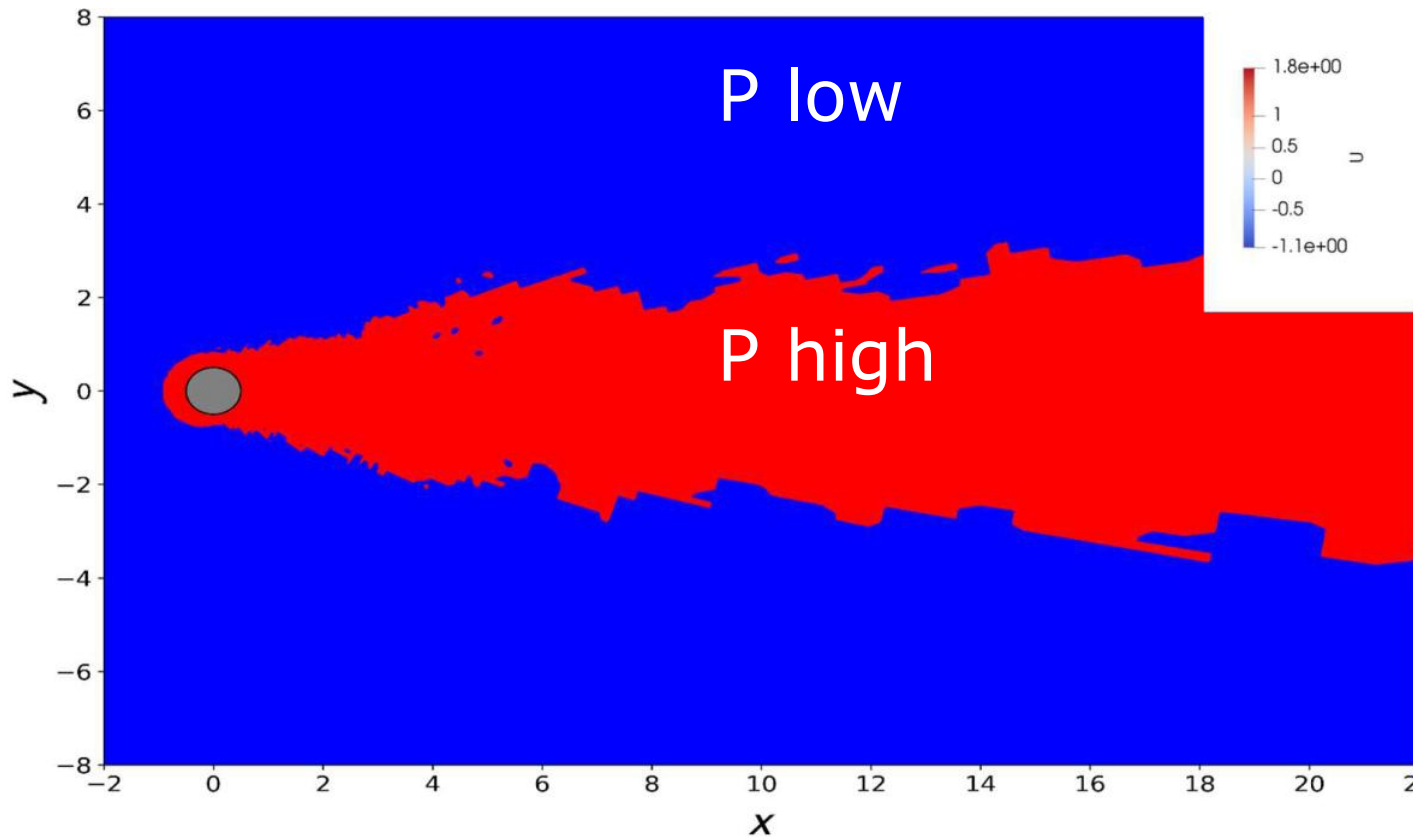
Machine Learning to detect flow regions

Clustering (classify data): Gaussian mixture model



Machine Learning to detect flow regions

Clustering (classify data): Gaussian mixture model



Automate the detection
(no thresholds)

**Use a robust feature space
for a variety of Re**

Invariants of strain and rotational
rate tensors

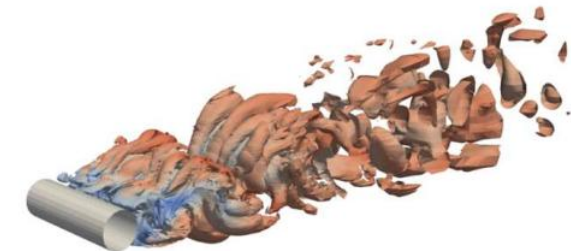
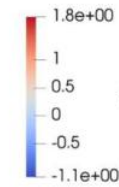
-KE Otmani, G Ntoukas, E Ferrer, "Towards a robust detection of flow regions using unsupervised machine learning", Vol 35, 027112, 2023

-K Tlales, KE Otmani, G Ntoukas, G Rubio, E Ferrer, "Machine learning mesh-adaptation for laminar and turbulent flows: applications to high order discontinuous Galerkin solvers", Engineering with Computers, 2024

Machine Learning to detect flow regions

Clustering: Gaussian mixture model

	St	C _d	L _r	L _{z\backslash D}
Uniform P3	0.202	0.7844	1.36	π
Uniform P4	0.203	0.9513	1.64	π
Cluster-Adapt P4-P2	0.204	0.9506	1.63	π
Parnadeau et al.[40]	0.208	-	1.56	π
Snyder and Degrez [45]	0.207	1.09	1.30	π
Kravchenko and Moin[46]	0.210	1.04	1.35	π
Breuer [47]	-	1.07	1.20	π
Franke and Frank [48]	0.209	0.98	1.64	π
(DNS) Ma et al. [41]	0.219	1.59	-	π
Ouvrard et al. [49]	0.223	0.94	1.56	π



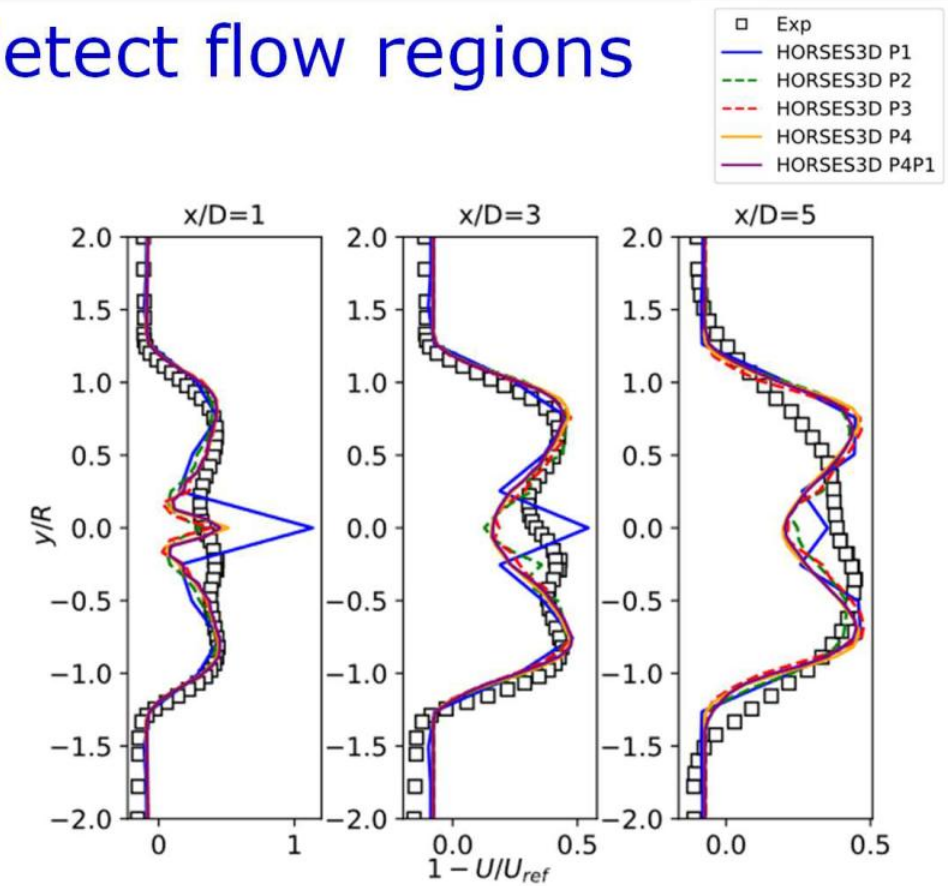
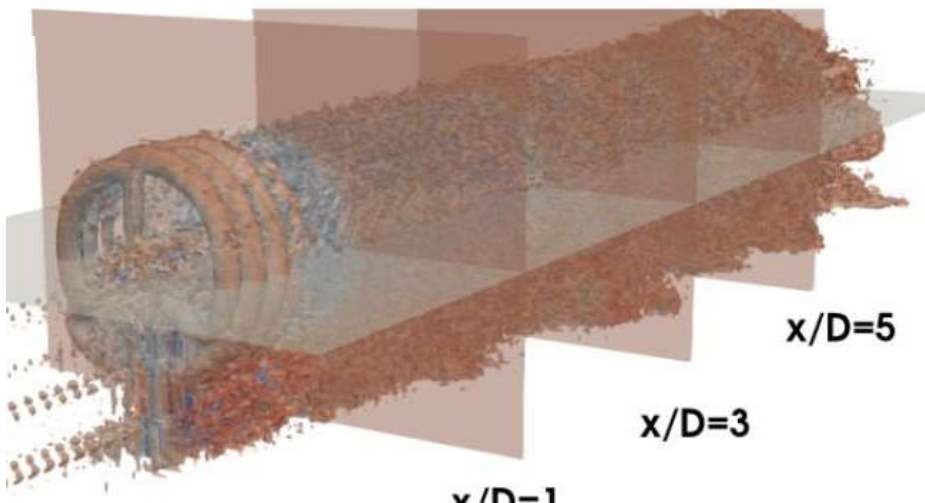
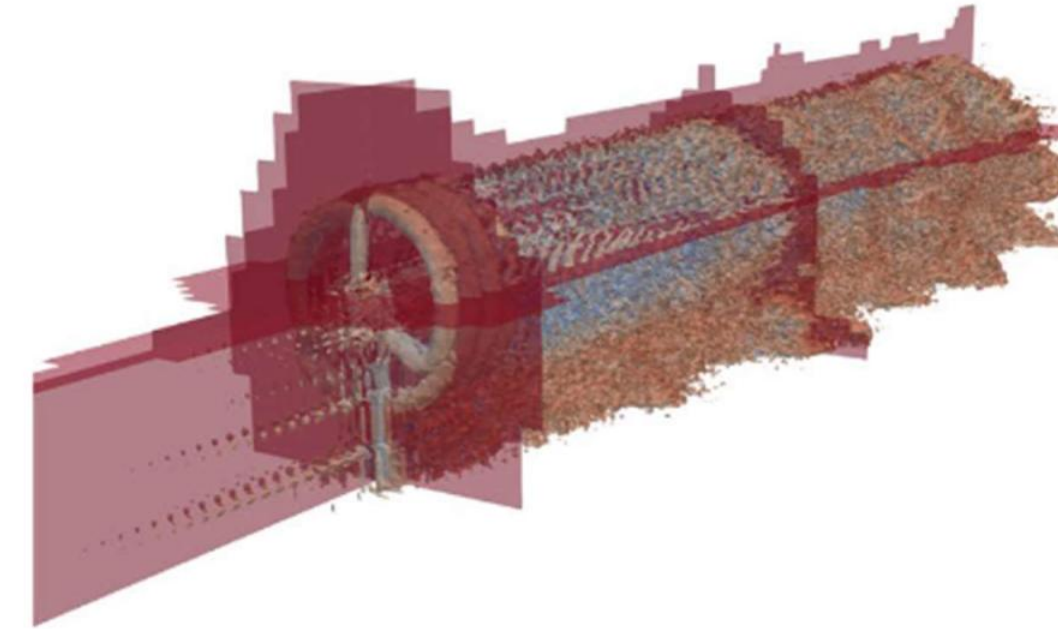
Re=3900

	DoFs	reduction of DoFs	reduction of comp. time
Cluster-Adapt P4-P2	1.55M	41%	33%

-KE Otmani, G Ntoukas, **E Ferrer**, "Towards a robust detection of flow regions using unsupervised machine learning", Vol 35, 027112, 2023

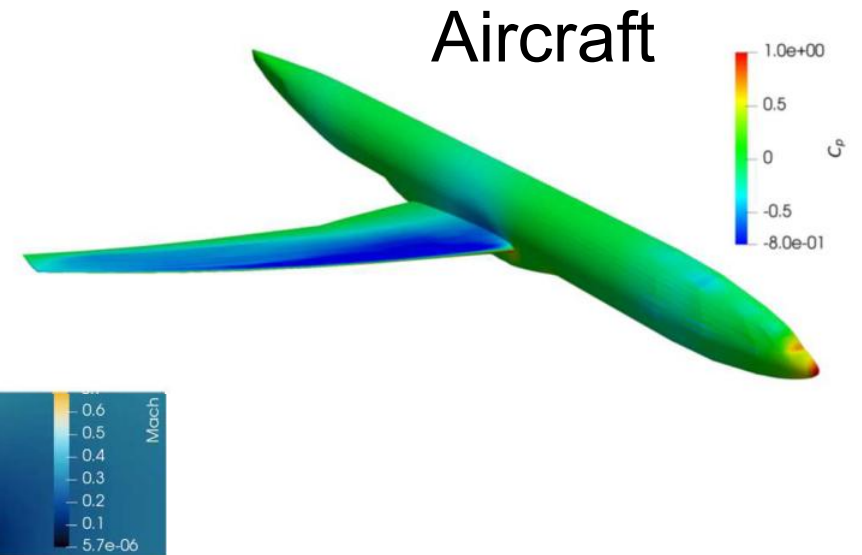
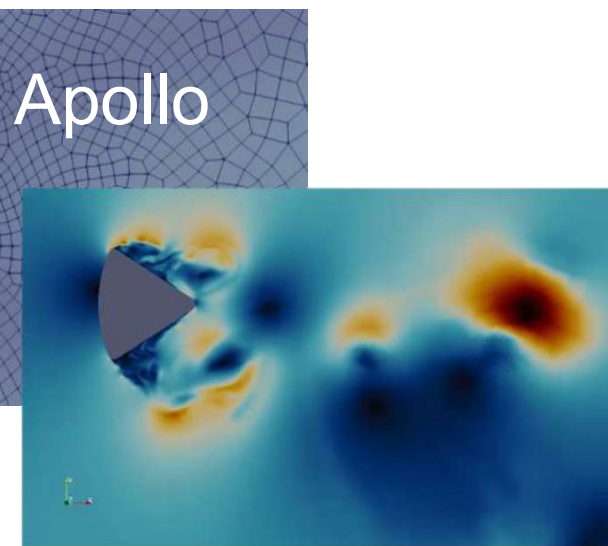
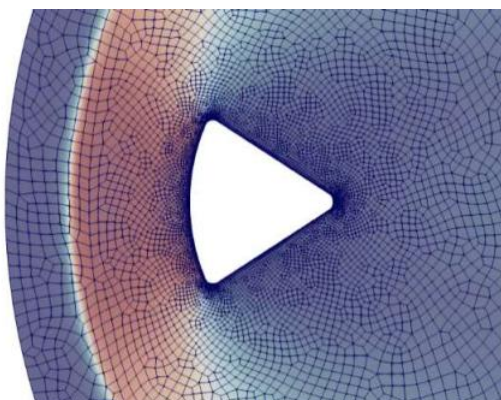
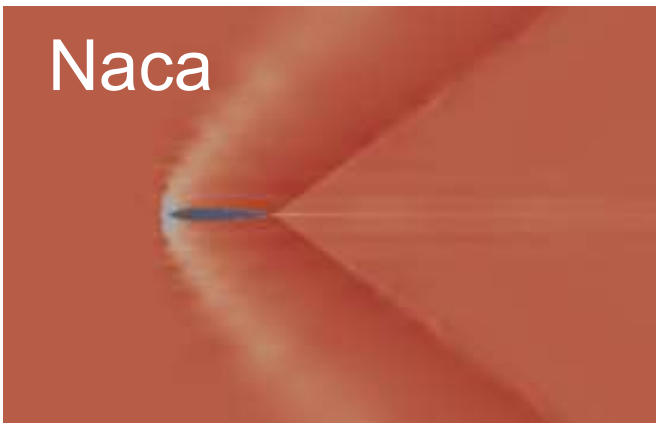
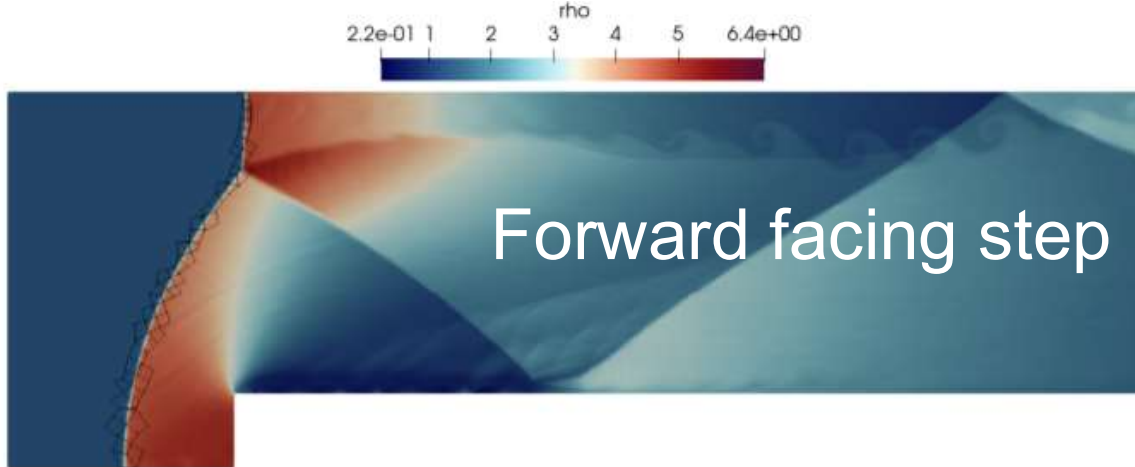
-K Tlales, KE Otmani, G Ntoukas, G Rubio, **E Ferrer**, "Machine learning mesh-adaptation for laminar and turbulent flows: applications to high order discontinuous Galerkin solvers", Engineering with Computers, 2024

Machine Learning to detect flow regions



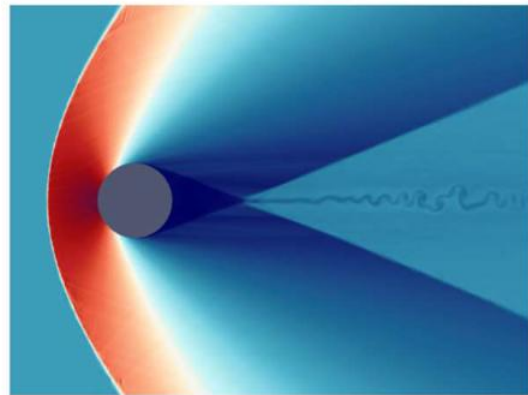
	DoFs	reduction of DoFs	reduction of comp. time
Uniform P1	0.59M	93.6%	92.7%
Uniform P2	1.99M	78.2%	86.5%
Uniform P3	4.72M	48.7%	54.1%
Uniform P4	9.22M	-	-
Cluster-Adapt P4-P1	3.58M	61%	43%

Supersonic & Shock capturing

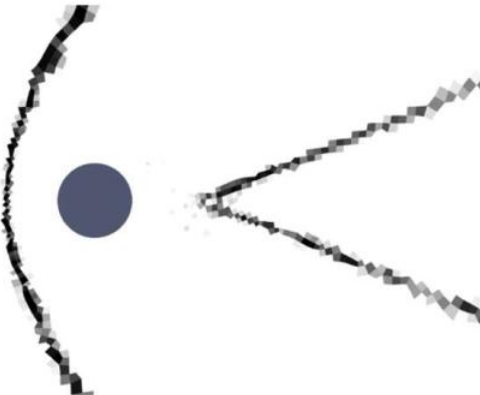


What about shocks?

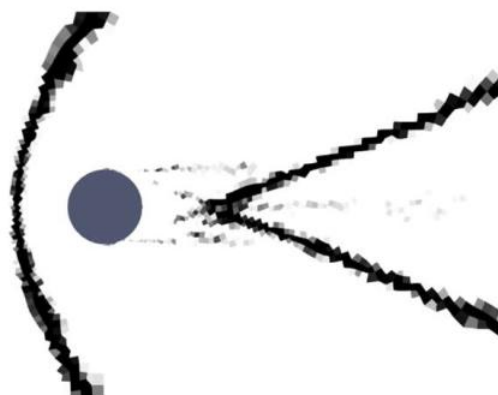
Classic feature based sensors (fine tuned)



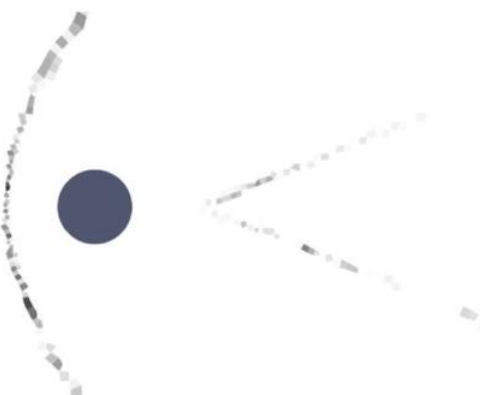
(a)



(b)

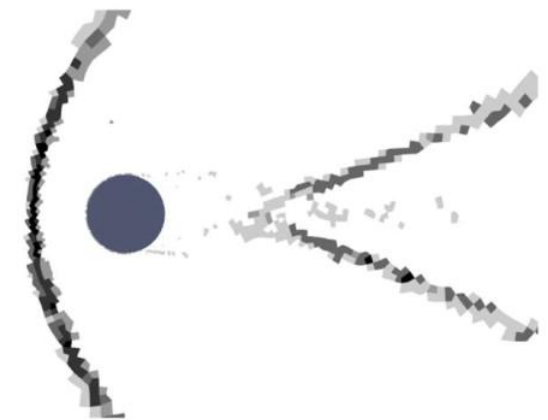


(c)



(d)

GMM
(no tuning)

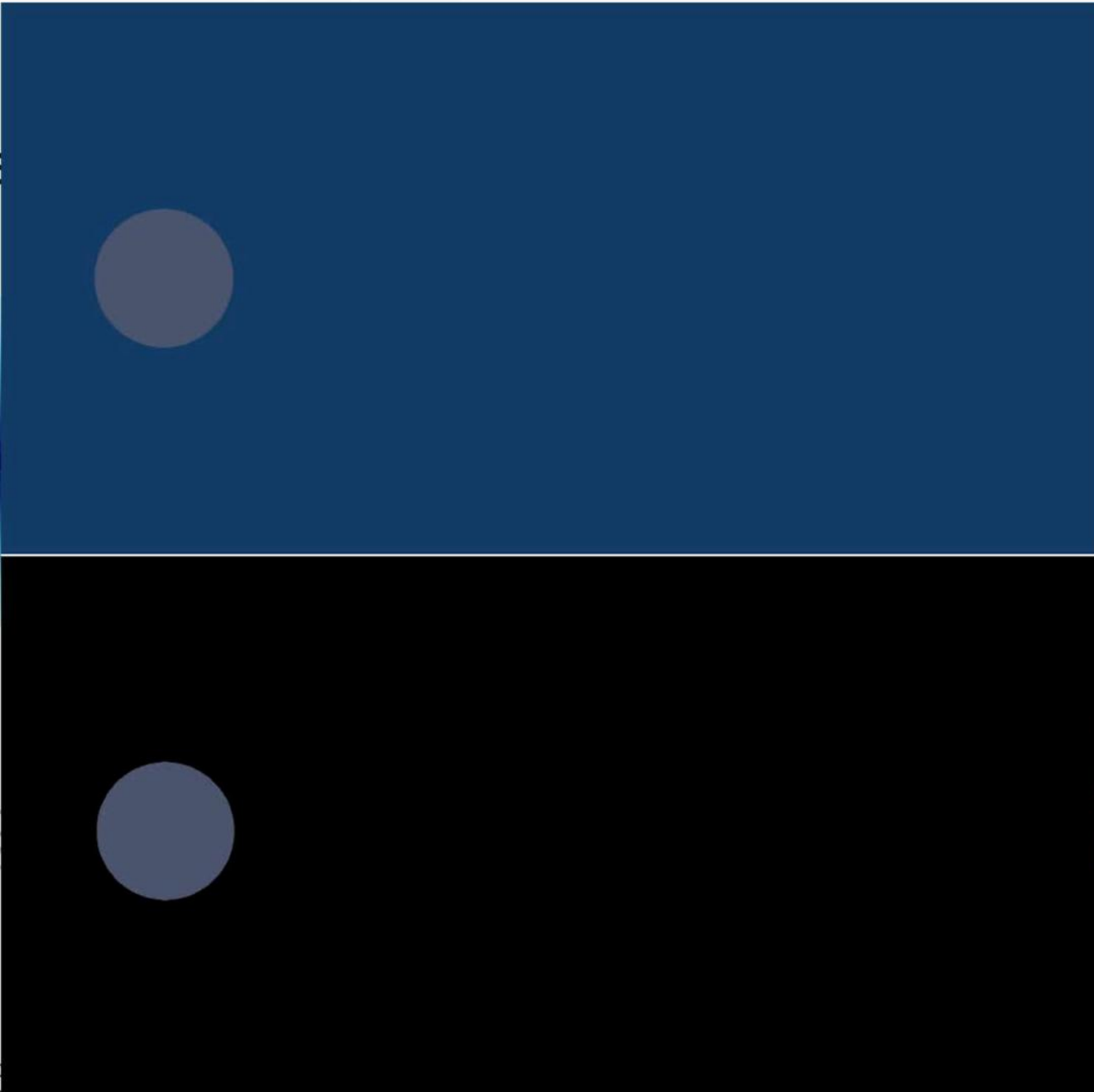
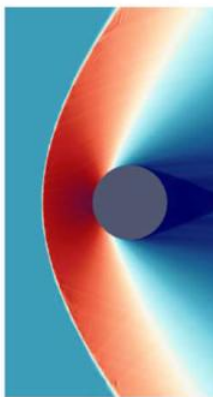


Similar result to state of the art without tuning!

FIG. 10. Viscous case after 300,000 iterations with the modal sensor of section IV A, using $p\rho$. a) density field, b) sensor with $s_0 = -2.5$ and $\Delta s = 1$. Sensor applied to the last iteration with $s_0 = -3.5$, $\Delta s = 1$ (c), and with $s_0 = -1.5$, $\Delta s = 1$ (d).

Classic finite difference CFD

MM
(no tuning)



similar result to
state of the art
without tuning!

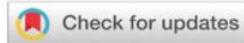
FIG. 10. Viscous case after 3000 iterations. Initial conditions: $s_0 = -2.5$ and $\Delta s = 1$. Sensors located at $x = 0$.



RESEARCH ARTICLE | FEBRUARY 08 2023

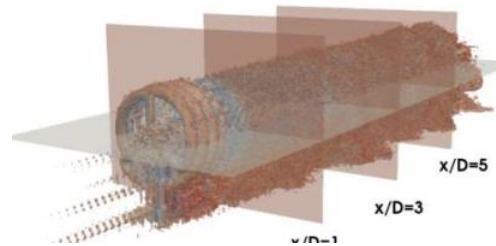
Toward a robust detection of viscous and turbulent flow regions using unsupervised machine learning

Kheir-Eddine Otmani ; Gerasimos Ntoukas ; Oscar A. Mariño ; Esteban Ferrer 



Physics of Fluids 35, 027112 (2023)

<https://doi.org/10.1063/5.0138626>



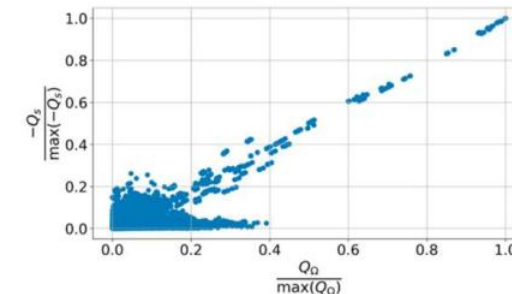
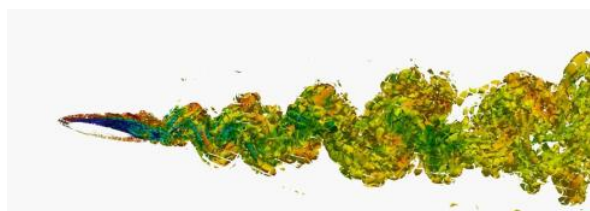
An unsupervised machine-learning-based shock sensor for high-order supersonic flow solvers

Andrés Mateo-Gabín,^{1,a)} Kenza Tlales,¹ Eusebio Valero,^{1,2} Esteban Ferrer,^{1,2} and Gonzalo Rubio^{1,2}

¹⁾ETSIAE-UPM-School of Aeronautics, Universidad Politécnica de Madrid, Madrid-Spain

²⁾Center for Computational Simulation, Universidad Politécnica de Madrid, Madrid-Spain

(Dated: 10 October 2023)



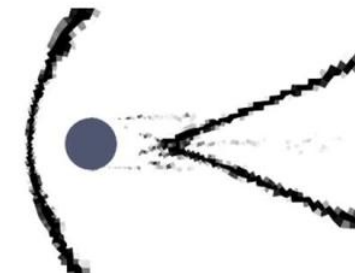
Engineering with Computers
<https://doi.org/10.1007/s00366-024-01950-y>

ORIGINAL ARTICLE



Machine learning mesh-adaptation for laminar and turbulent flows: applications to high-order discontinuous Galerkin solvers

Kenza Tlales¹ · Kheir-Eddine Otmani¹ · Gerasimos Ntoukas¹ · Gonzalo Rubio^{1,2} · Esteban Ferrer^{1,2}



Accelerating high order discontinuous Galerkin solvers through a clustering-based viscous/turbulent-inviscid domain decomposition

Kheir-Eddine Otmani^{*1}, Andrés Mateo-Gabín¹, Gonzalo Rubio^{1,2}, and Esteban Ferrer^{1,2}

¹⁾ETSIAE-UPM-School of Aeronautics, Universidad Politécnica de Madrid, Plaza Cardenal Cisneros 3, E-28040 Madrid, Spain

²⁾Center for Computational Simulation, Universidad Politécnica de Madrid, Campus de Montegancedo, Boadilla del Monte, 28660 Madrid, Spain

Summary

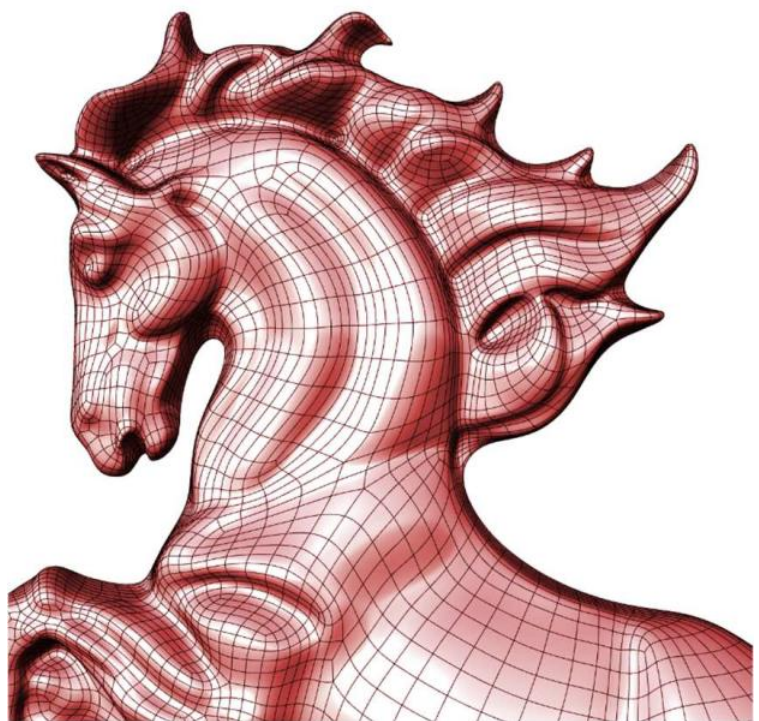
1- Introduction to DG & Horses3d

2- Multiphysics

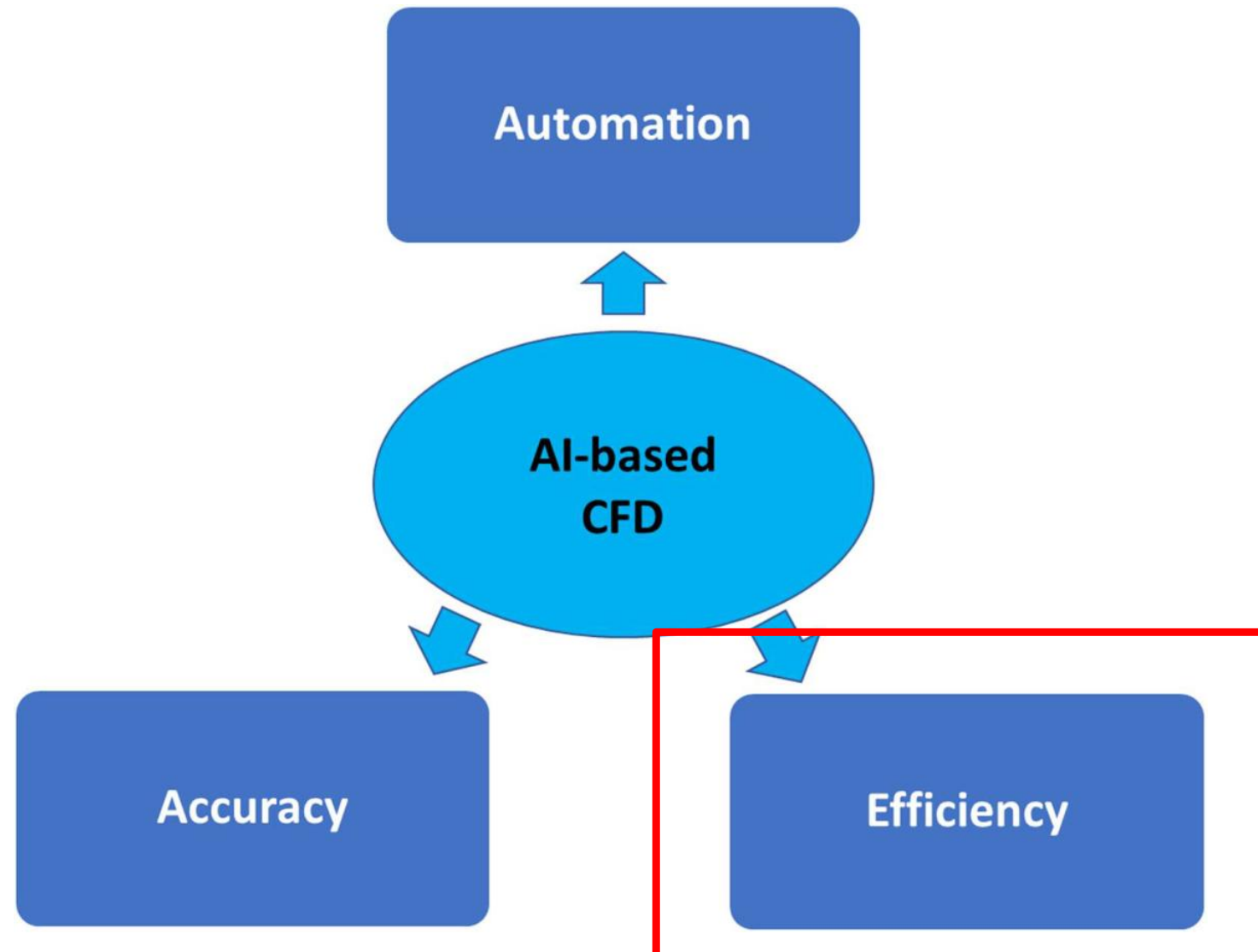
- Wind turbines
- Turbulence

3. Machine Learning + CFD

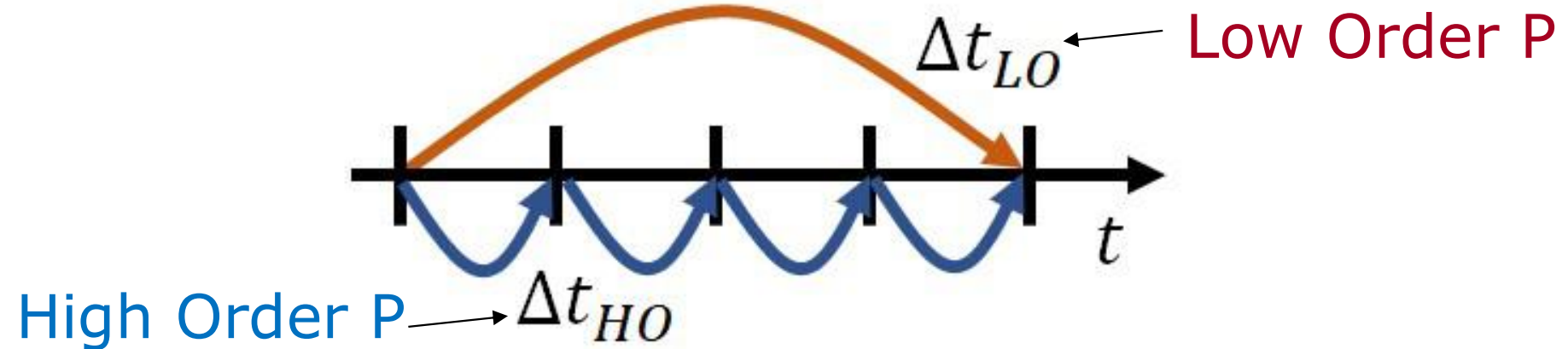
- Mesh adaption
- NN acceleration
- RL for automation



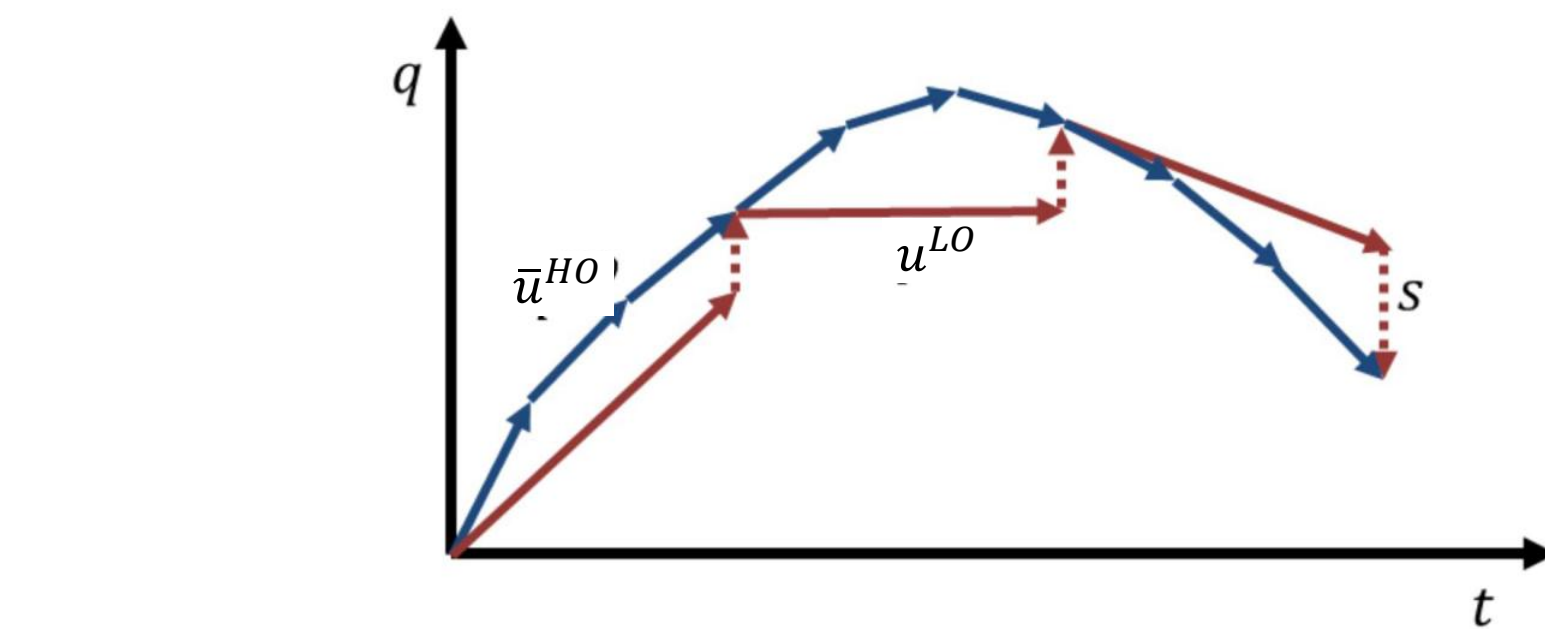
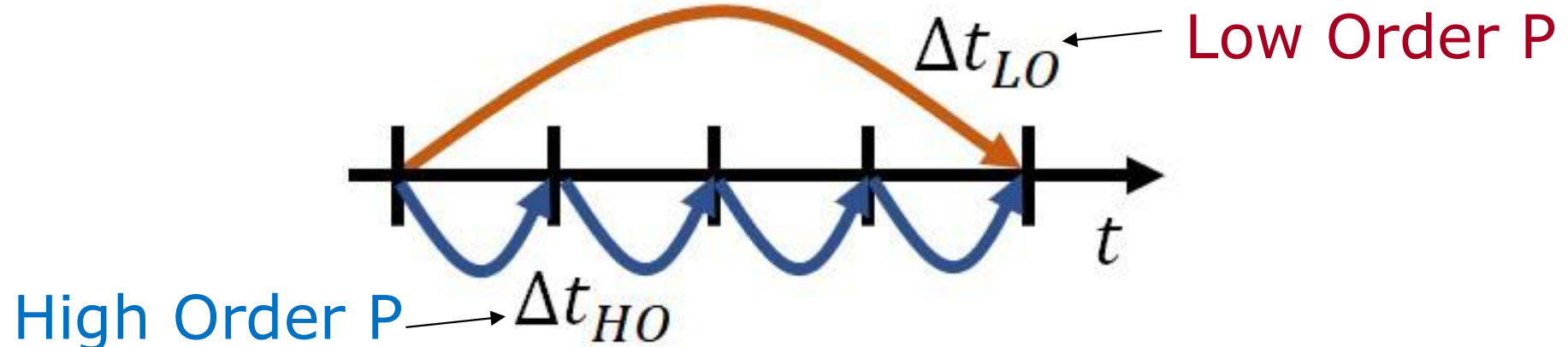
Towards AI-based Computational Fluid Dynamics



Machine Learning to accelerate CFD



Machine Learning to accelerate CFD



Machine Learning to accelerate CFD

LO evolution:

$$u_{n+1}^{LO} = u_n^{LO} + \Delta t_n q^{LO}(u_n^{LO}; t_n)$$

Filtered HO:

$$\bar{u}_{n+1}^{HO} = \bar{u}_n^{HO} + \Delta t_n \bar{q}^{HO}(u_n^{HO}; t_n)$$

Machine Learning to accelerate CFD

LO evolution:

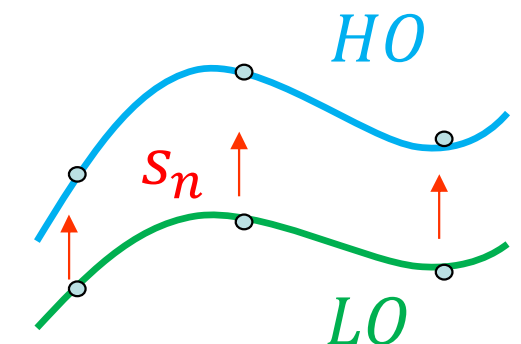
$$u_{n+1}^{LO} = u_n^{LO} + \Delta t_n q^{LO}(u_n^{LO}; t_n)$$

Filtered HO:

$$\bar{u}_{n+1}^{HO} = \bar{u}_n^{HO} + \Delta t_n \bar{q}^{HO}(u_n^{HO}; t_n)$$

LO-NN corrected:

$$u_{n+1}^{NN} = u_n^{NN} + \Delta t_n [q^{LO}(u_n^{NN}; t_n) + s_n]$$



Machine Learning to accelerate CFD

LO evolution:

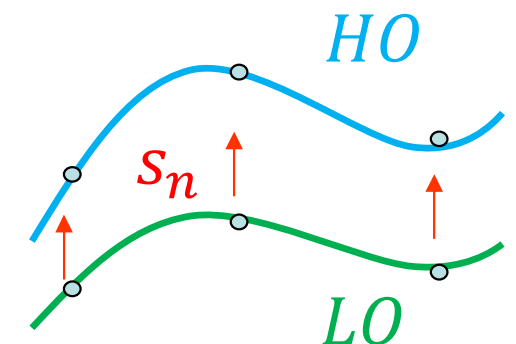
$$u_{n+1}^{LO} = u_n^{LO} + \Delta t_n q^{LO}(u_n^{LO}; t_n)$$

Filtered HO:

$$\bar{u}_{n+1}^{HO} = \bar{u}_n^{HO} + \Delta t_n \bar{q}^{HO}(u_n^{HO}; t_n)$$

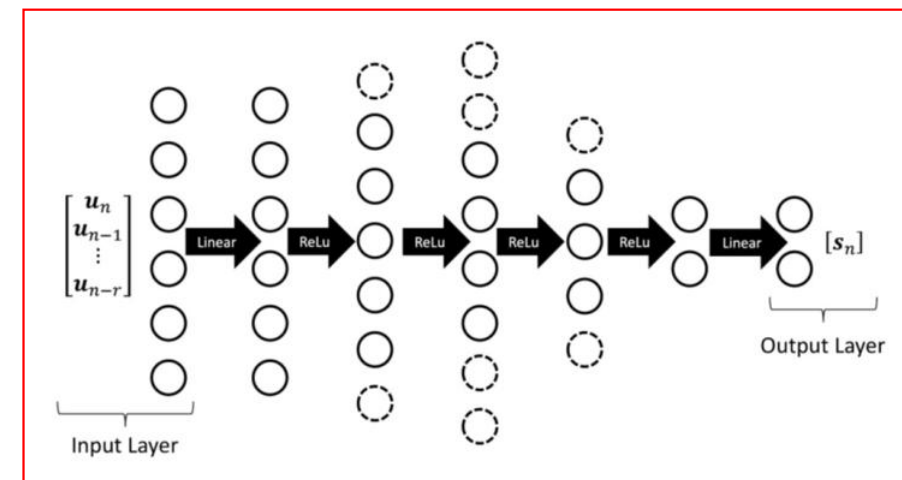
LO-NN corrected:

$$u_{n+1}^{NN} = u_n^{NN} + \Delta t_n [q^{LO}(u_n^{NN}; t_n) + s_n]$$



$$s_n = f(u_n^{NN}, u_{n-1}^{NN}, \dots, u_{n-r}^{NN}, \bar{u}^{HO})$$

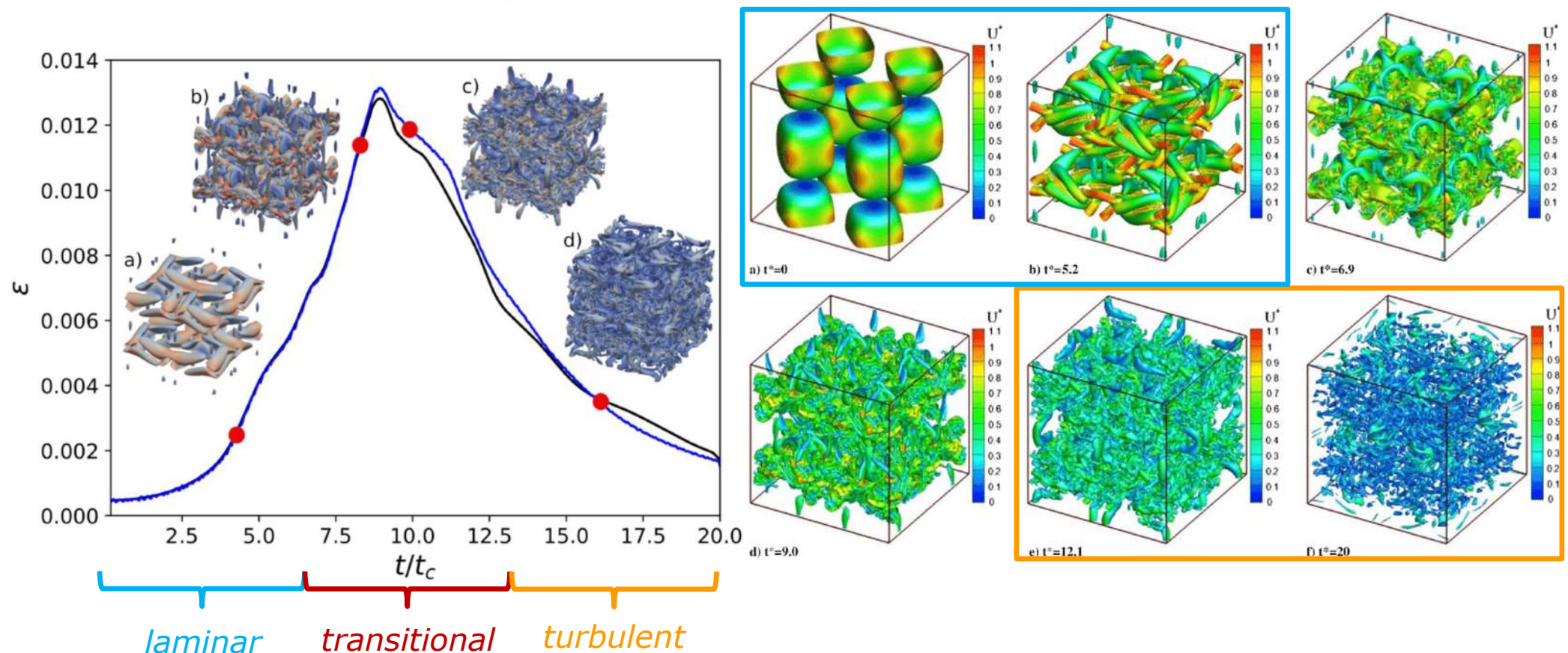
Trained to give HO solution



Machine Learning to accelerate CFD

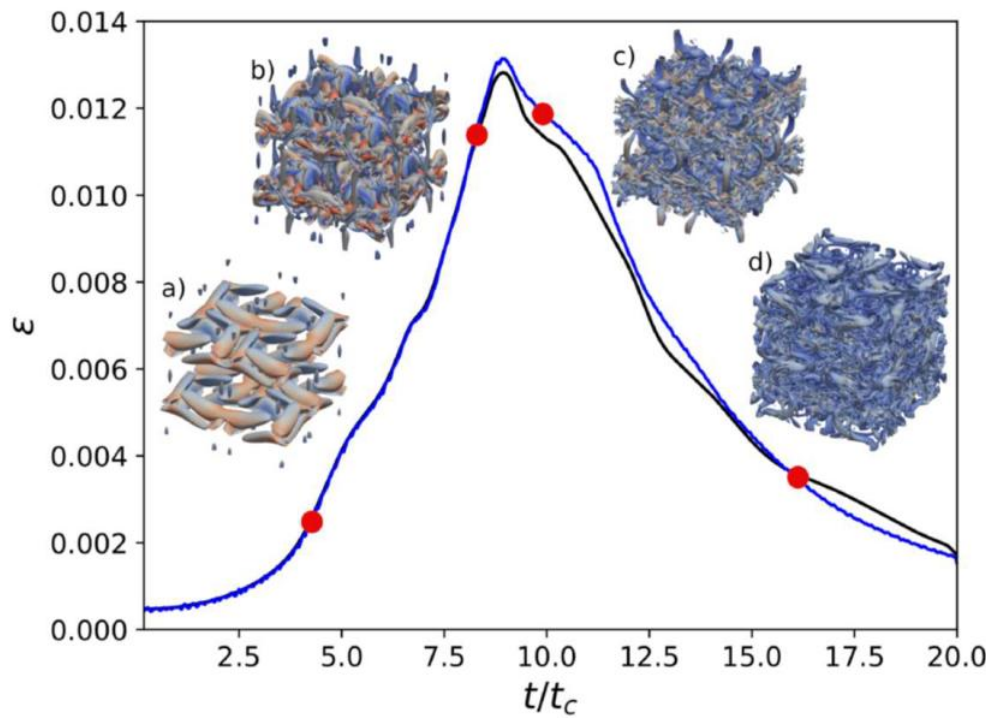
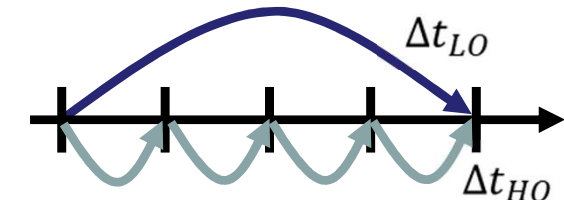
3D Navier-Stokes - LES

Taylor-Green – Reynolds 1600



Machine Learning to accelerate CFD

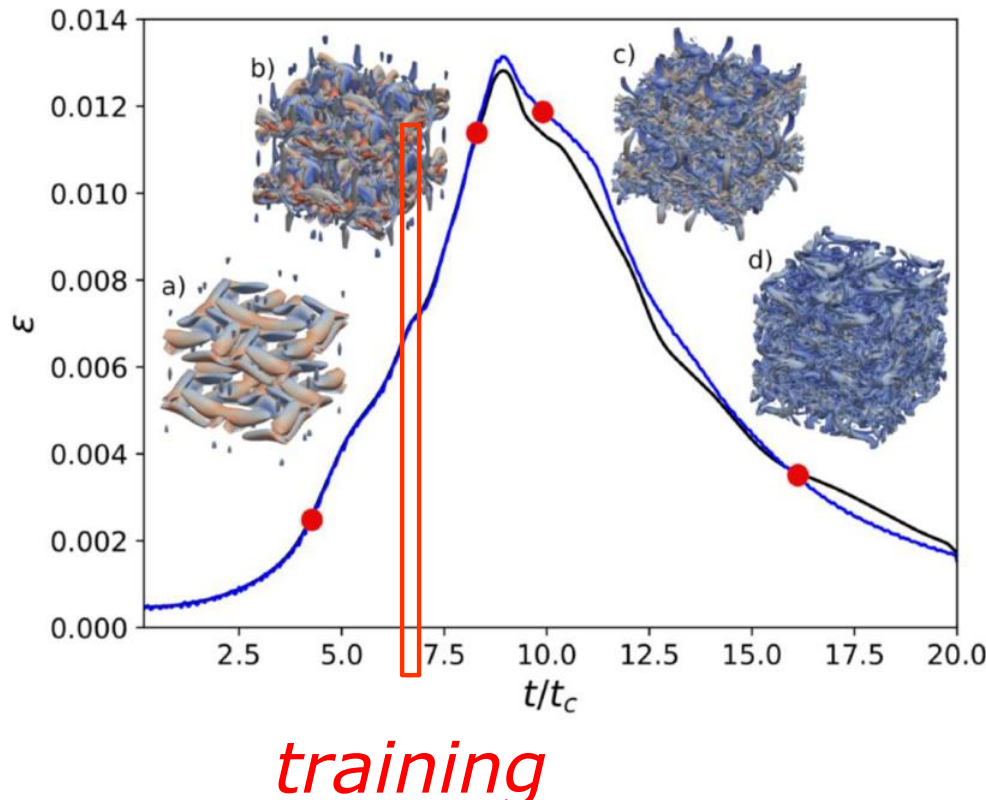
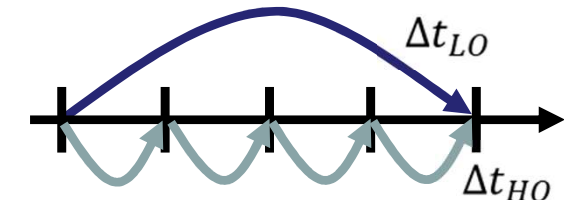
3D Navier-Stokes - LES
Taylor-Green – Reynolds 1600



$P8 \rightarrow P3$
 $\Delta t_{LO}/\Delta t_{HO} = 3$

Machine Learning to accelerate CFD

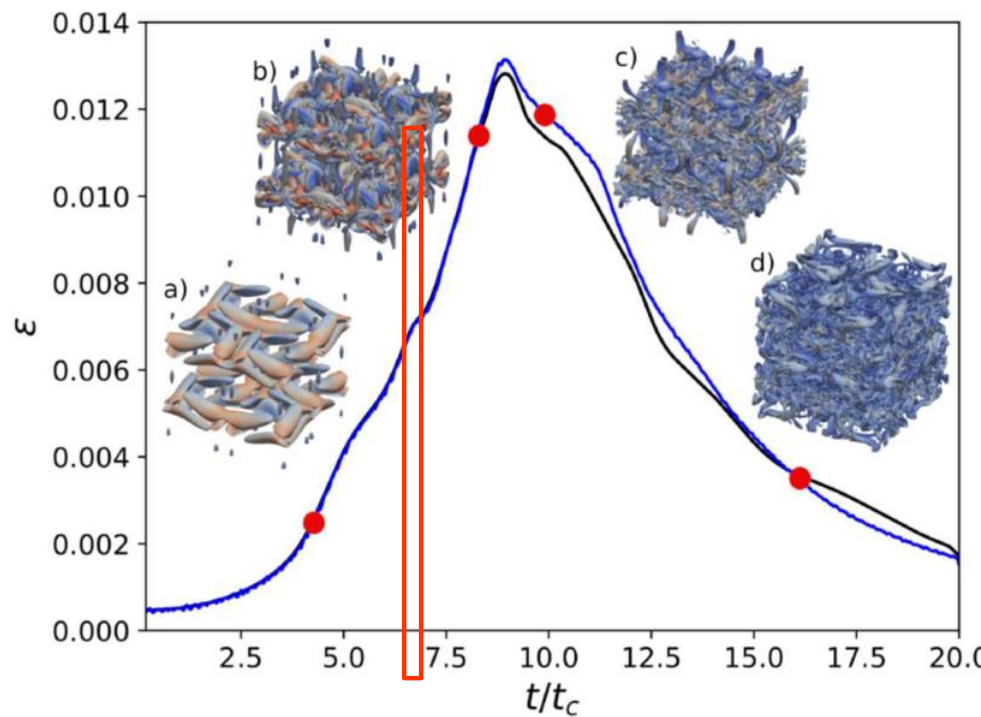
3D Navier-Stokes - LES
Taylor-Green – Reynolds 1600



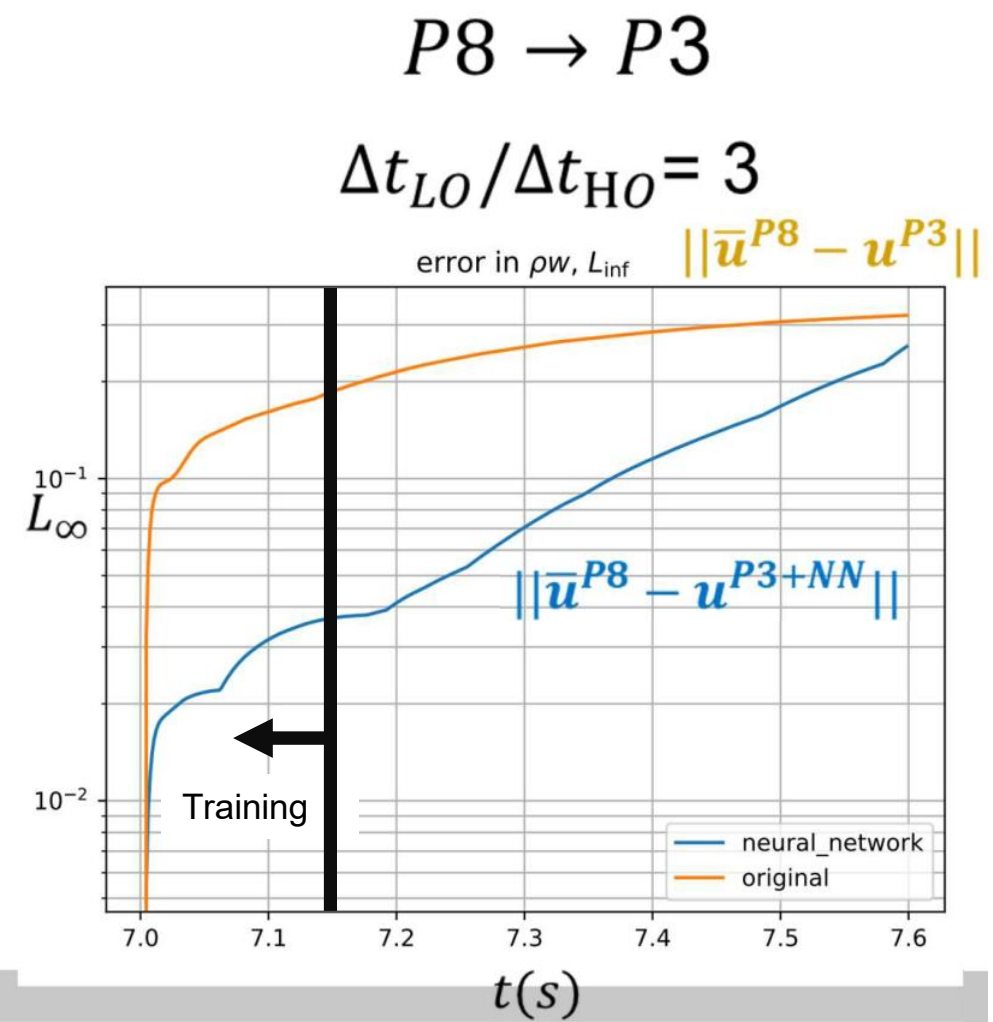
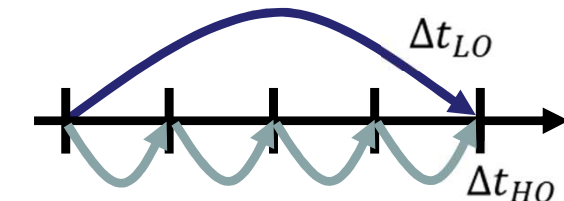
$$P8 \rightarrow P3$$
$$\Delta t_{LO} / \Delta t_{HO} = 3$$

Machine Learning to accelerate CFD

3D Navier-Stokes - LES
Taylor-Green – Reynolds 1600

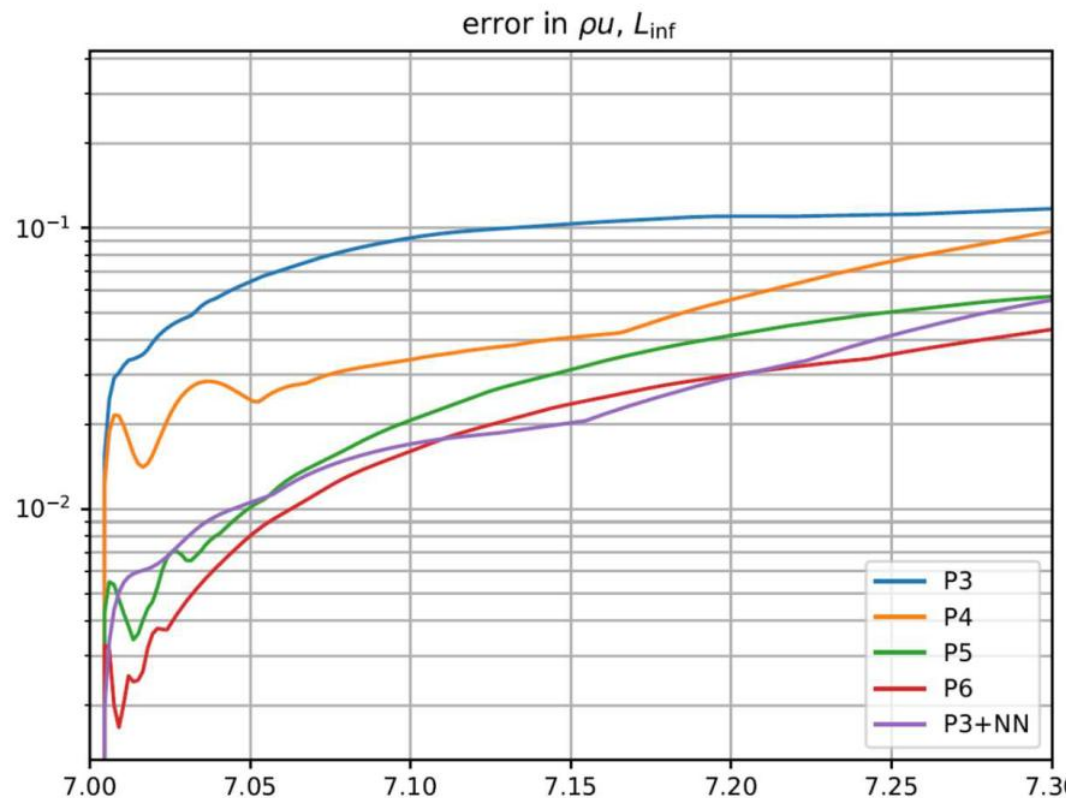
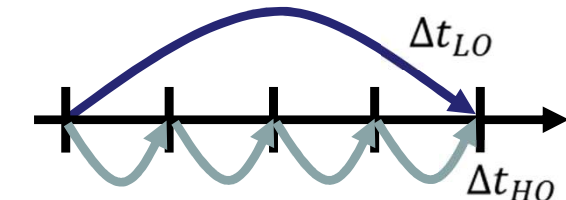


12 times faster



Machine Learning to accelerate CFD

3D Navier-Stokes - LES
Taylor-Green – Reynolds 1600



$P8 \rightarrow P3$

$\Delta t_{LO}/\Delta t_{HO} = 3$

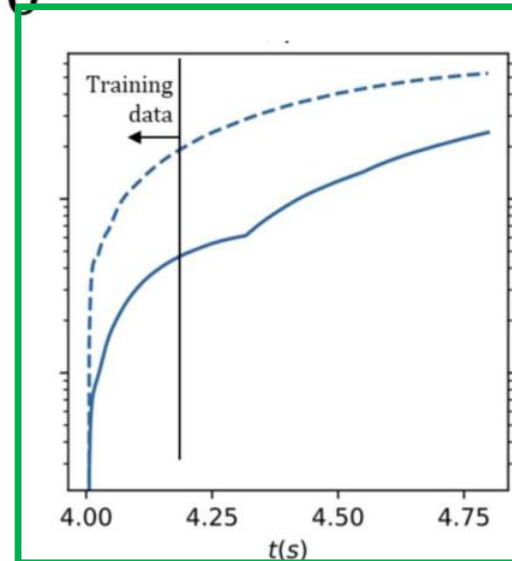
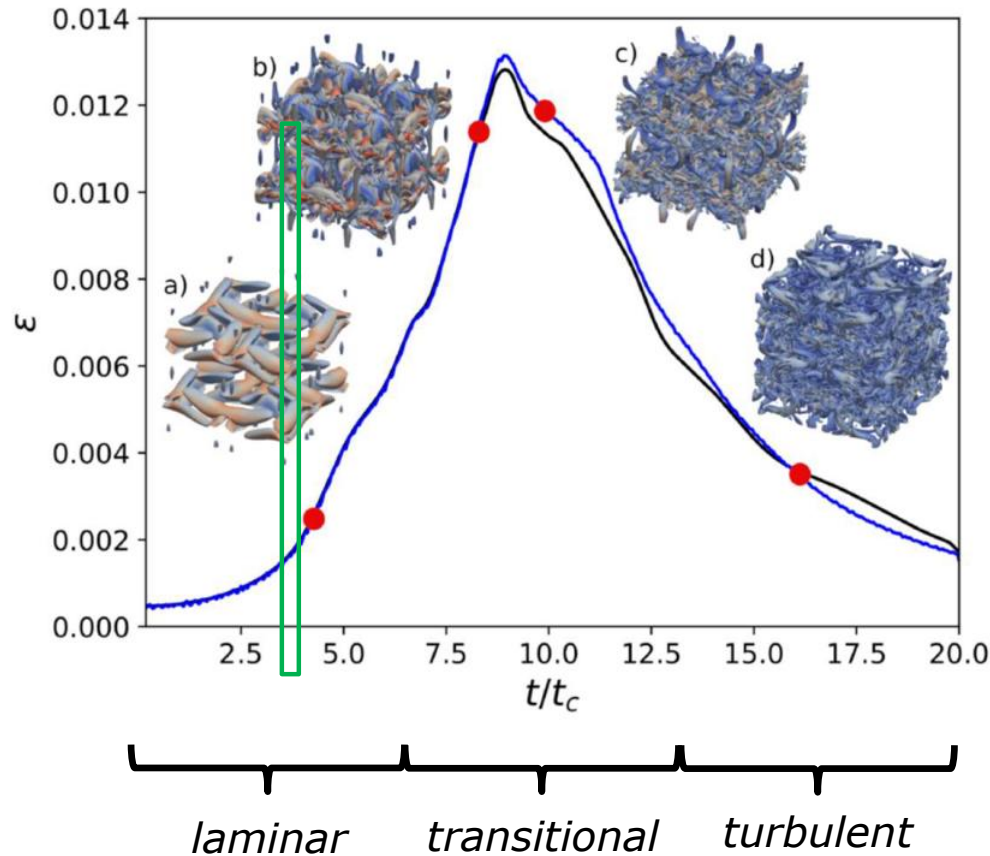
What is the real accuracy?

Probably P=6

P3+NN is 4-5 times faster
(compared to P6)

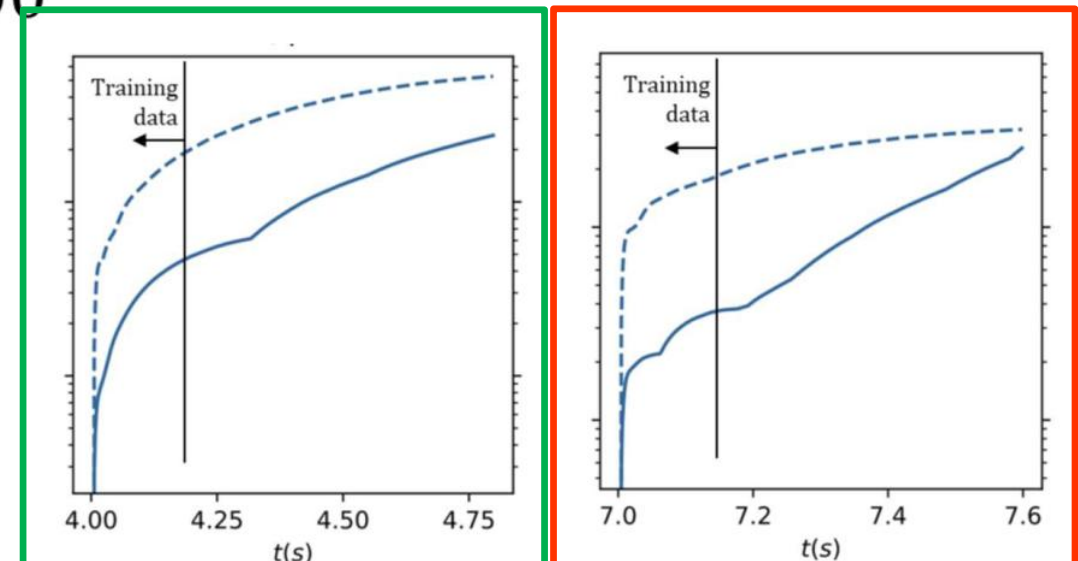
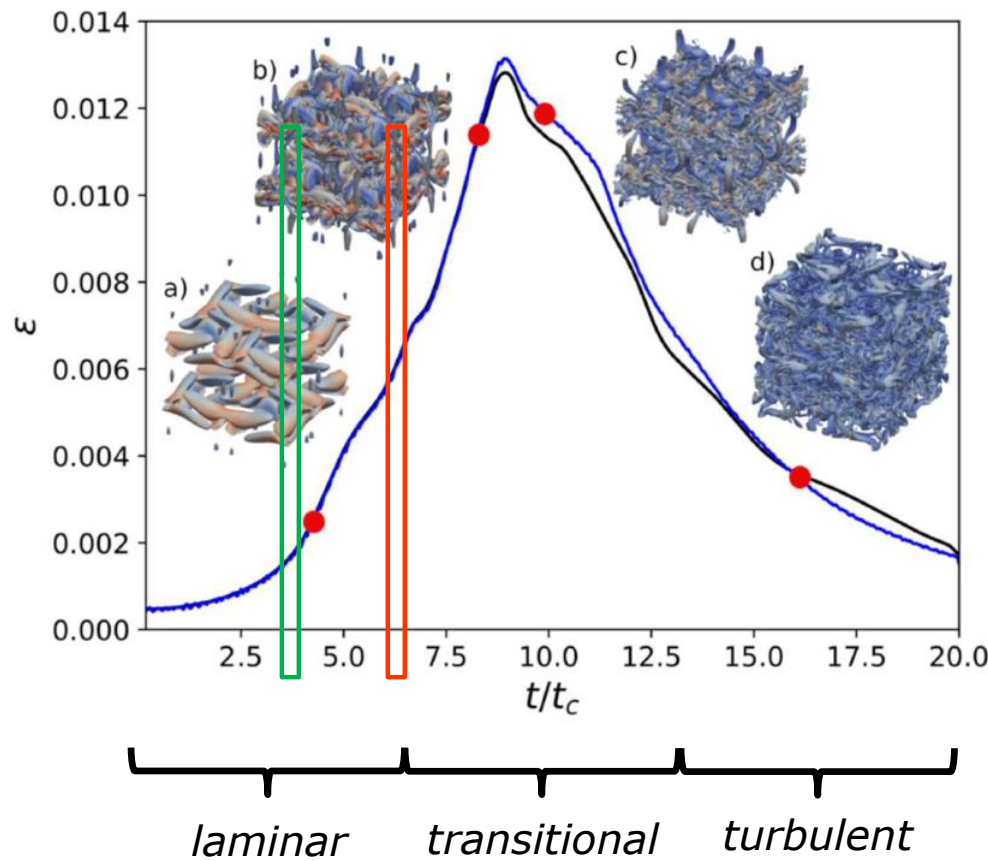
Machine Learning to accelerate CFD

3D Navier-Stokes - LES
Taylor-Green – Reynolds 1600



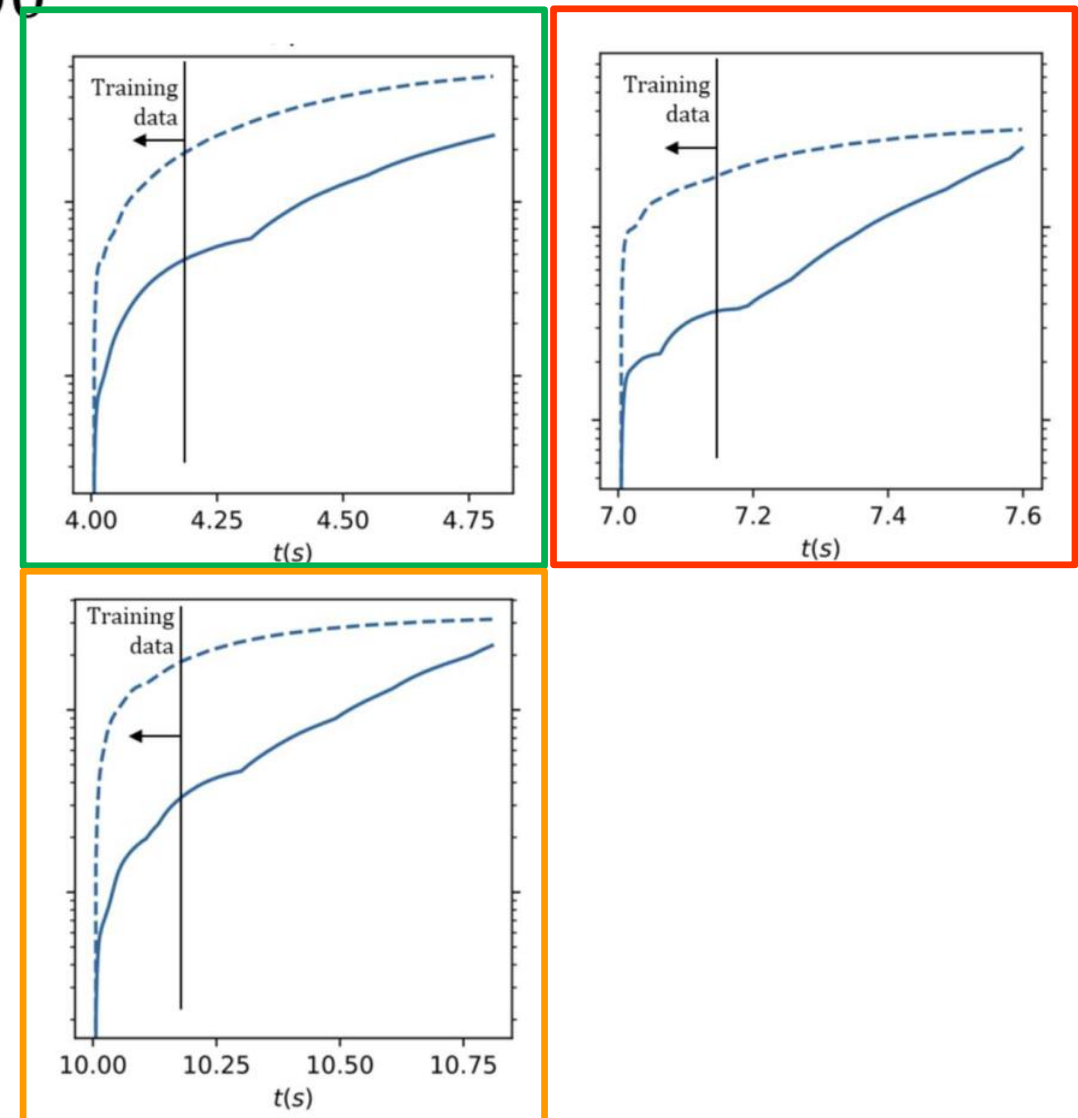
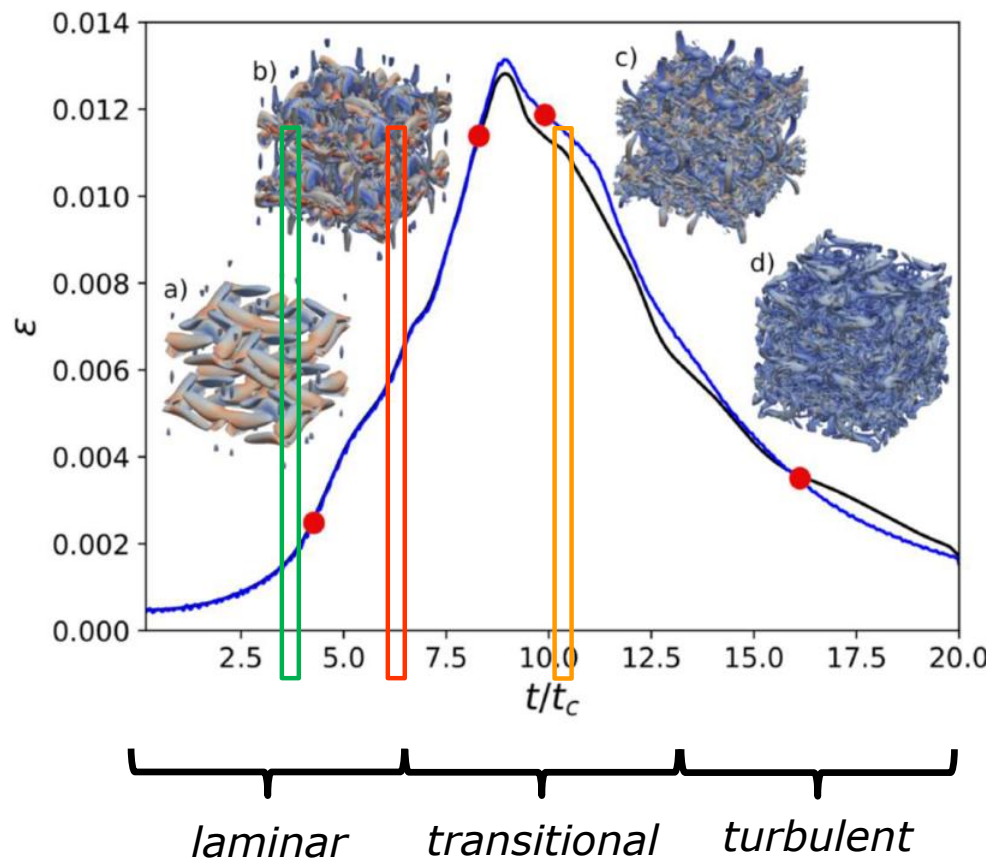
Machine Learning to accelerate CFD

3D Navier-Stokes - LES
Taylor-Green – Reynolds 1600



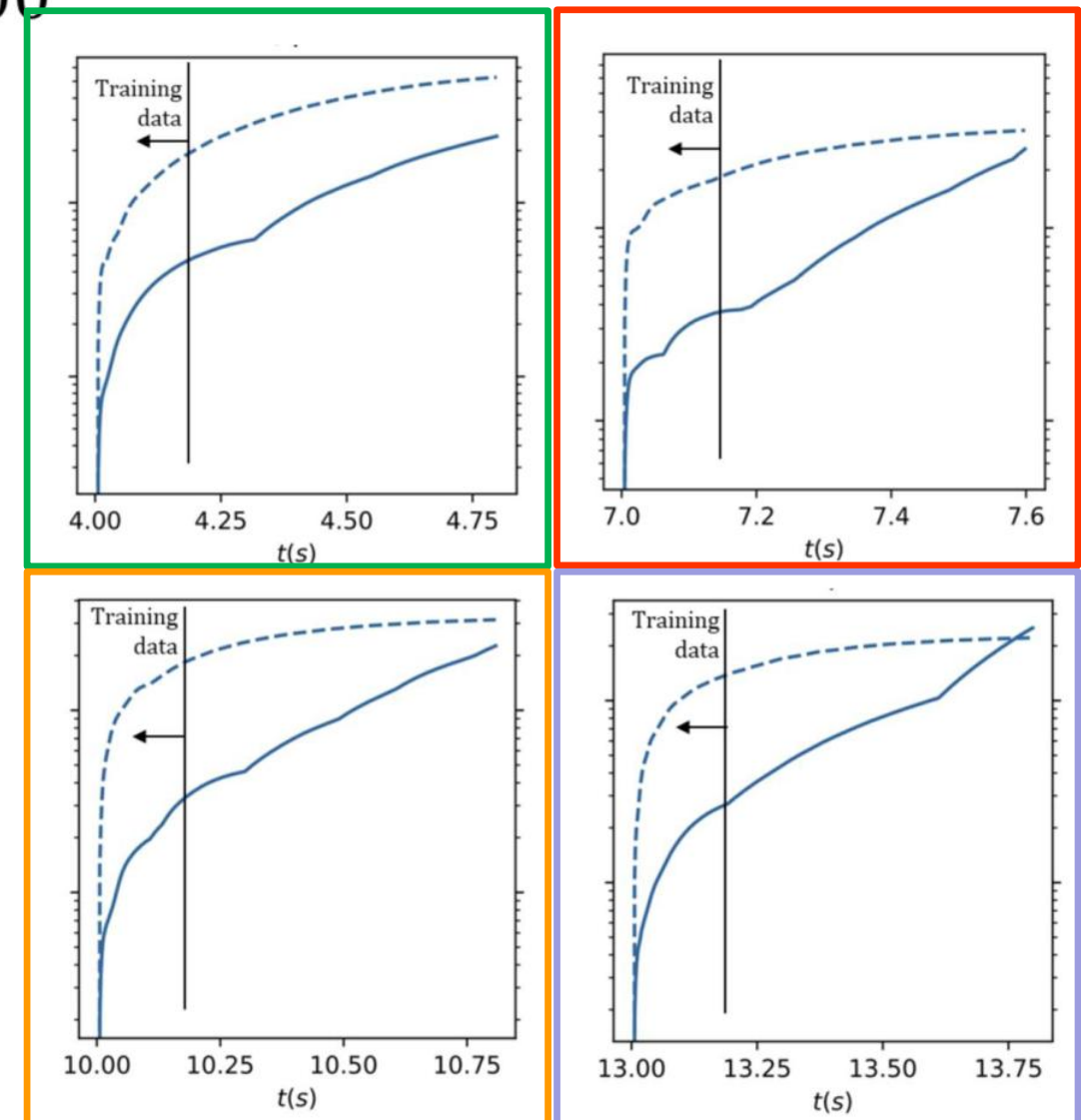
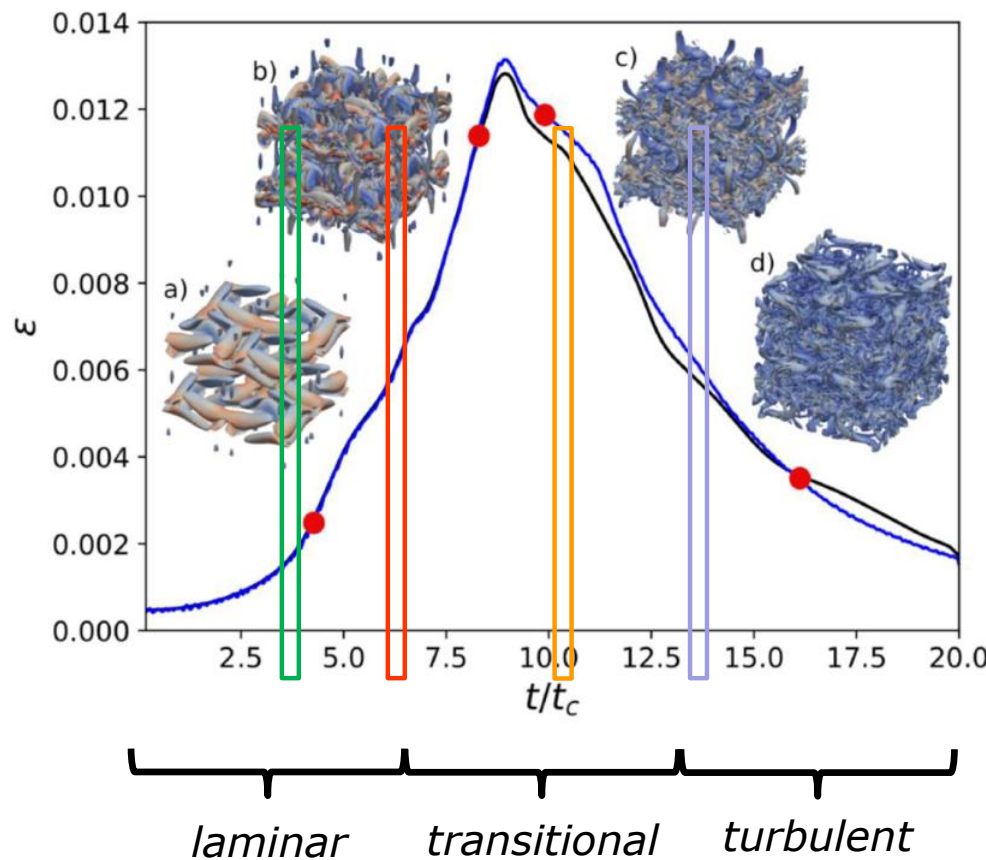
Machine Learning to accelerate CFD

3D Navier-Stokes - LES
Taylor-Green – Reynolds 1600



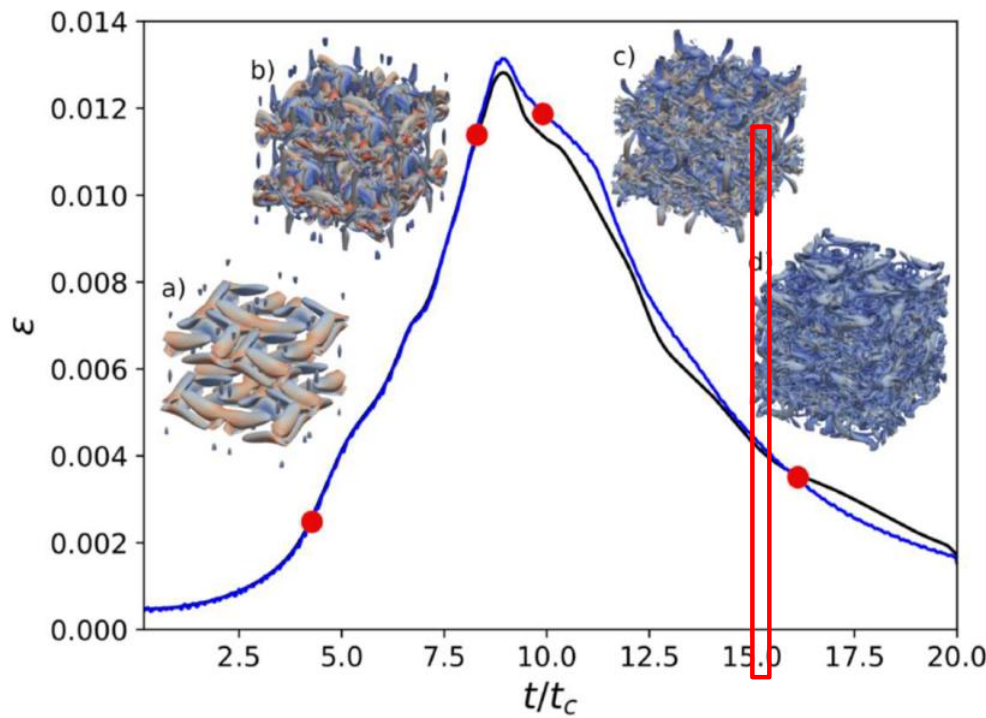
Machine Learning to accelerate CFD

3D Navier-Stokes - LES
Taylor-Green – Reynolds 1600

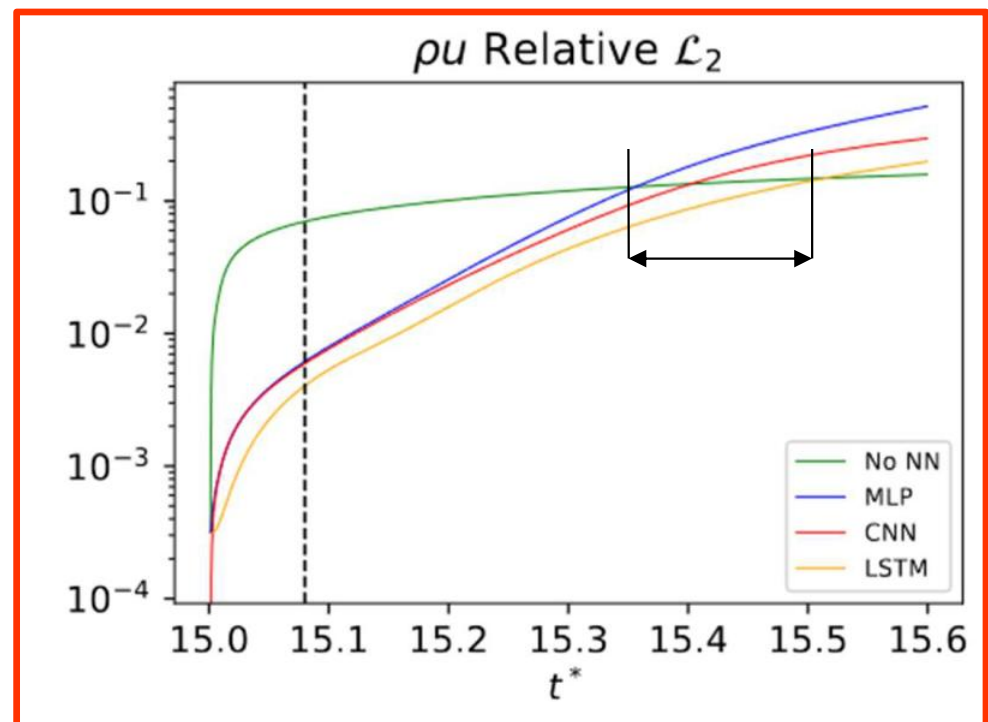
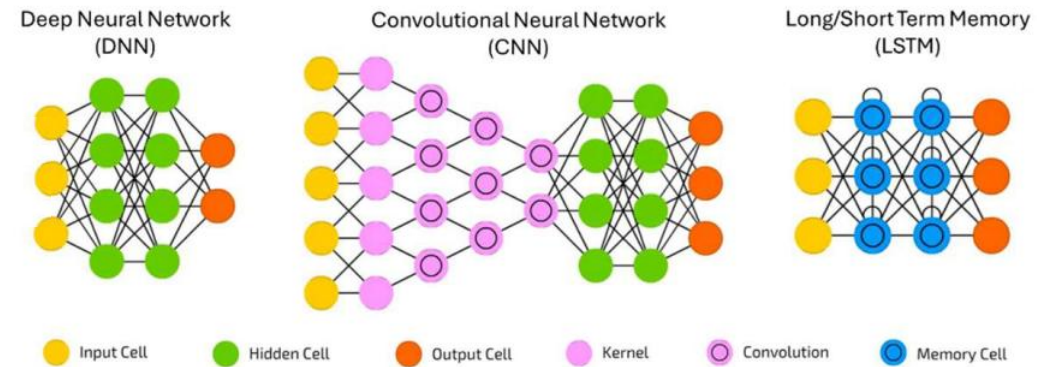


Machine Learning to accelerate CFD

3D Navier-Stokes - LES
Taylor-Green – Reynolds 1600



training

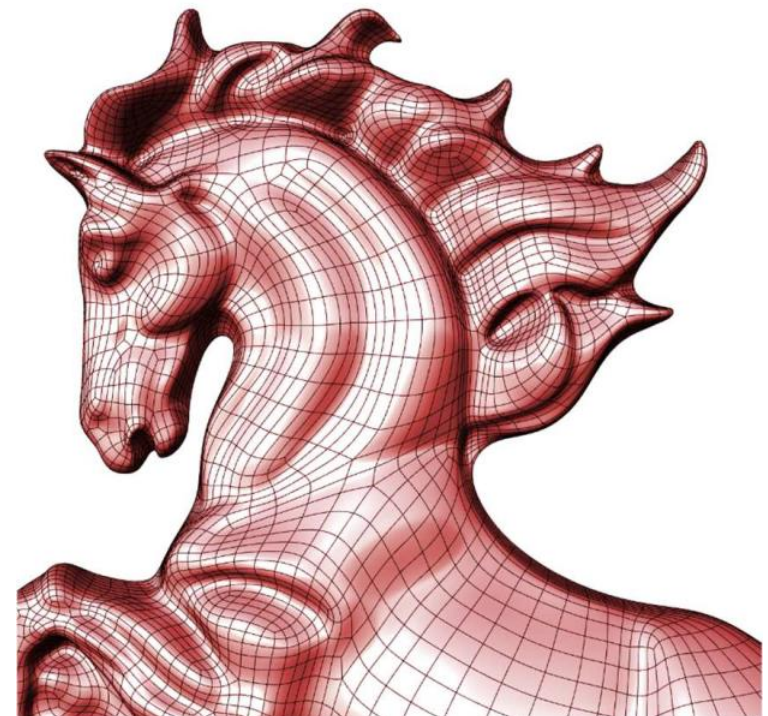


Summary

1- Introduction to DG & Horses3d

2- Multiphysics

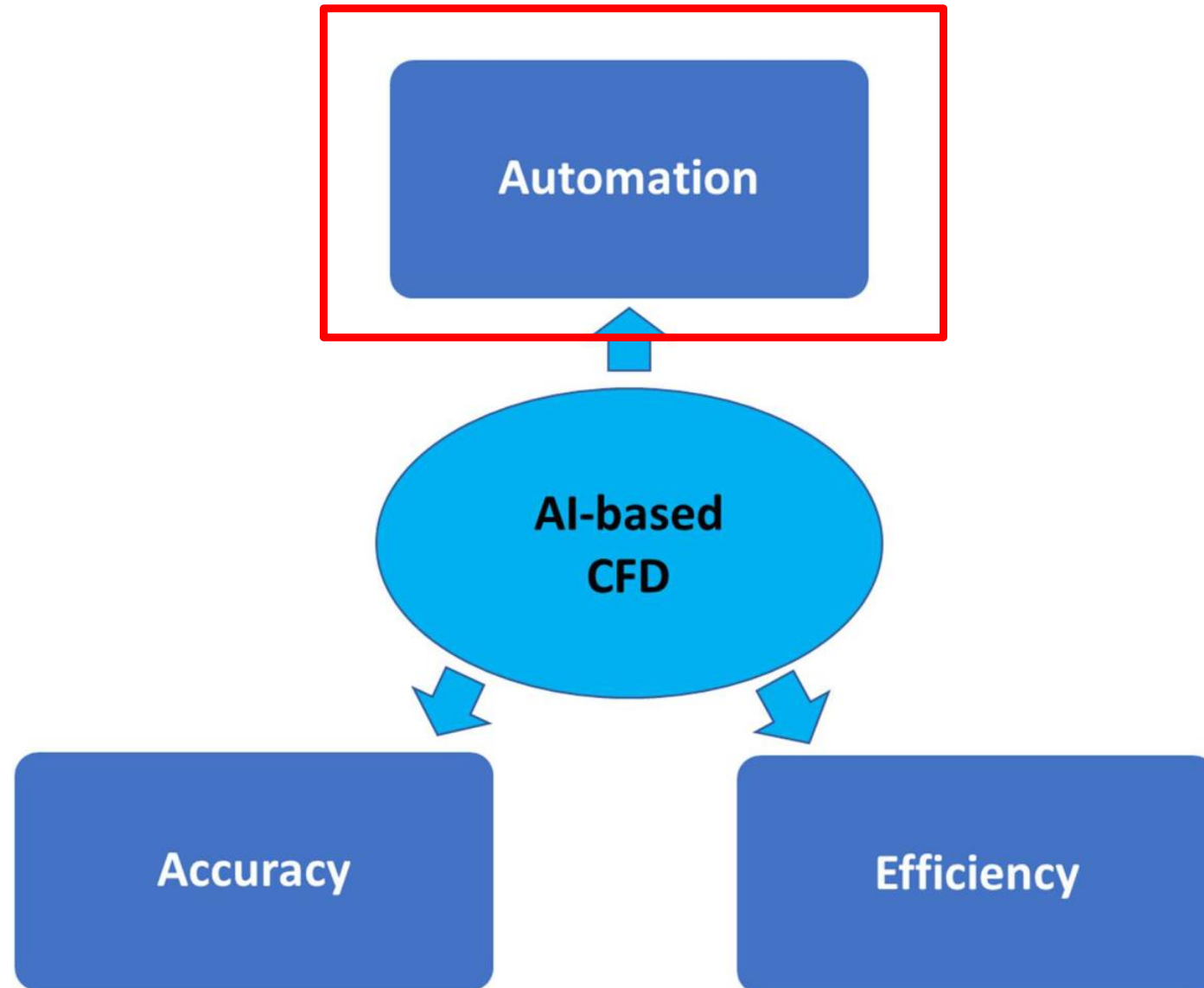
- Wind turbines
- Turbulence



3. Machine Learning + CFD

- Mesh adaption
- NN acceleration
- RL for automation

Towards AI-based Computational Fluid Dynamics





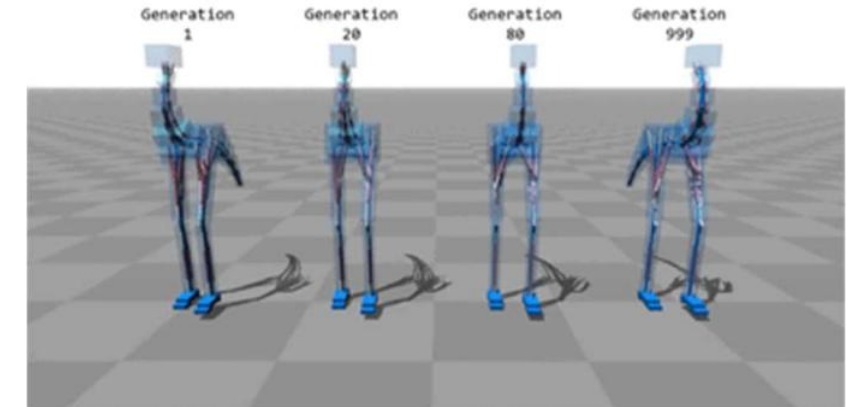
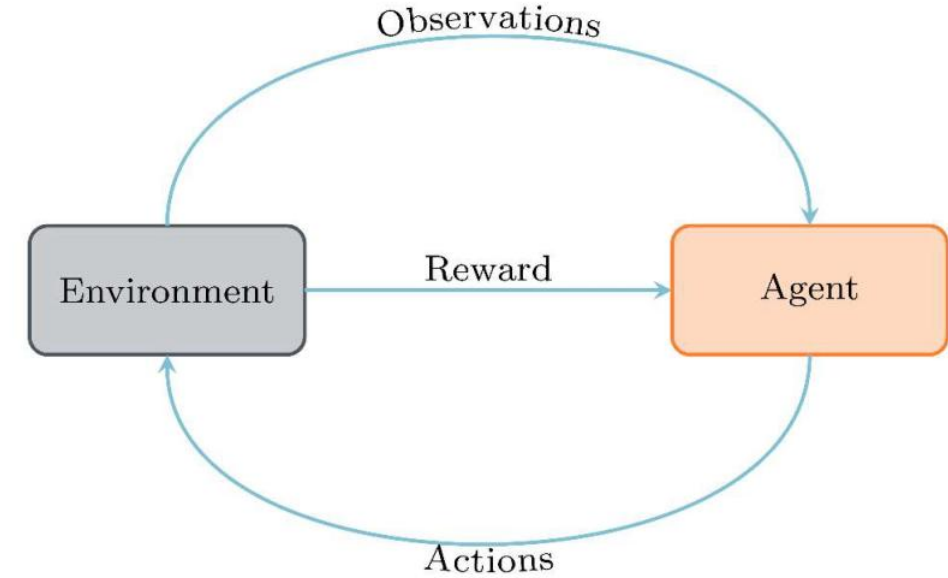
Machine Learning and Reinforcement Learning



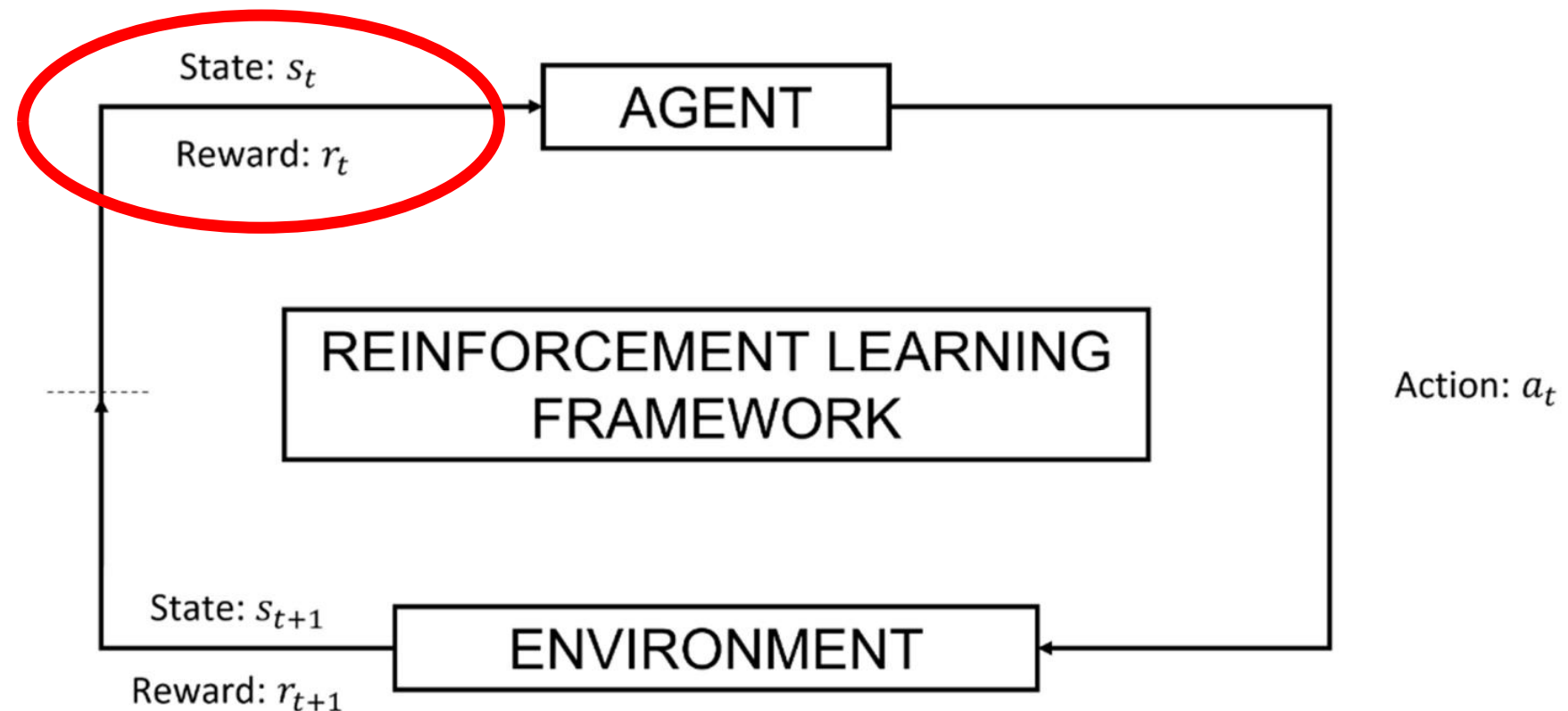
Go game



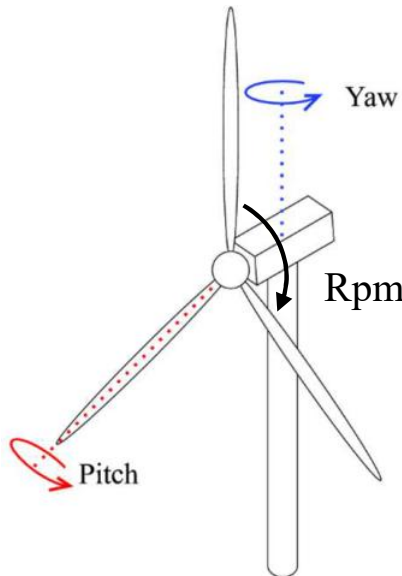
Chess game



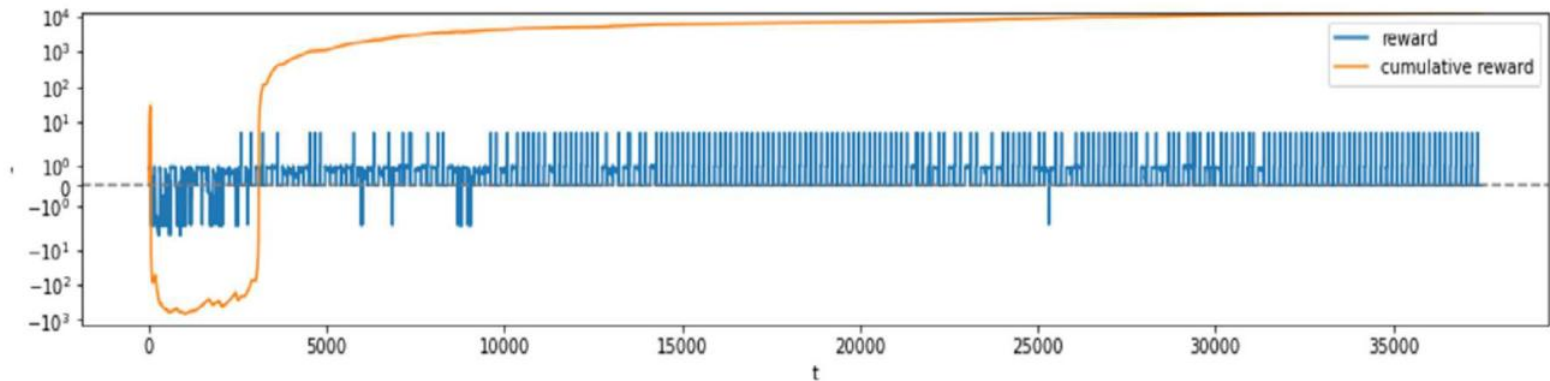
Defining the state, actions and rewards are the key aspects of RL



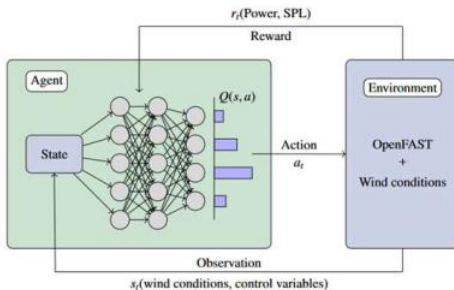
Deep reinforcement learning for wind turbine control



Training with simple winds



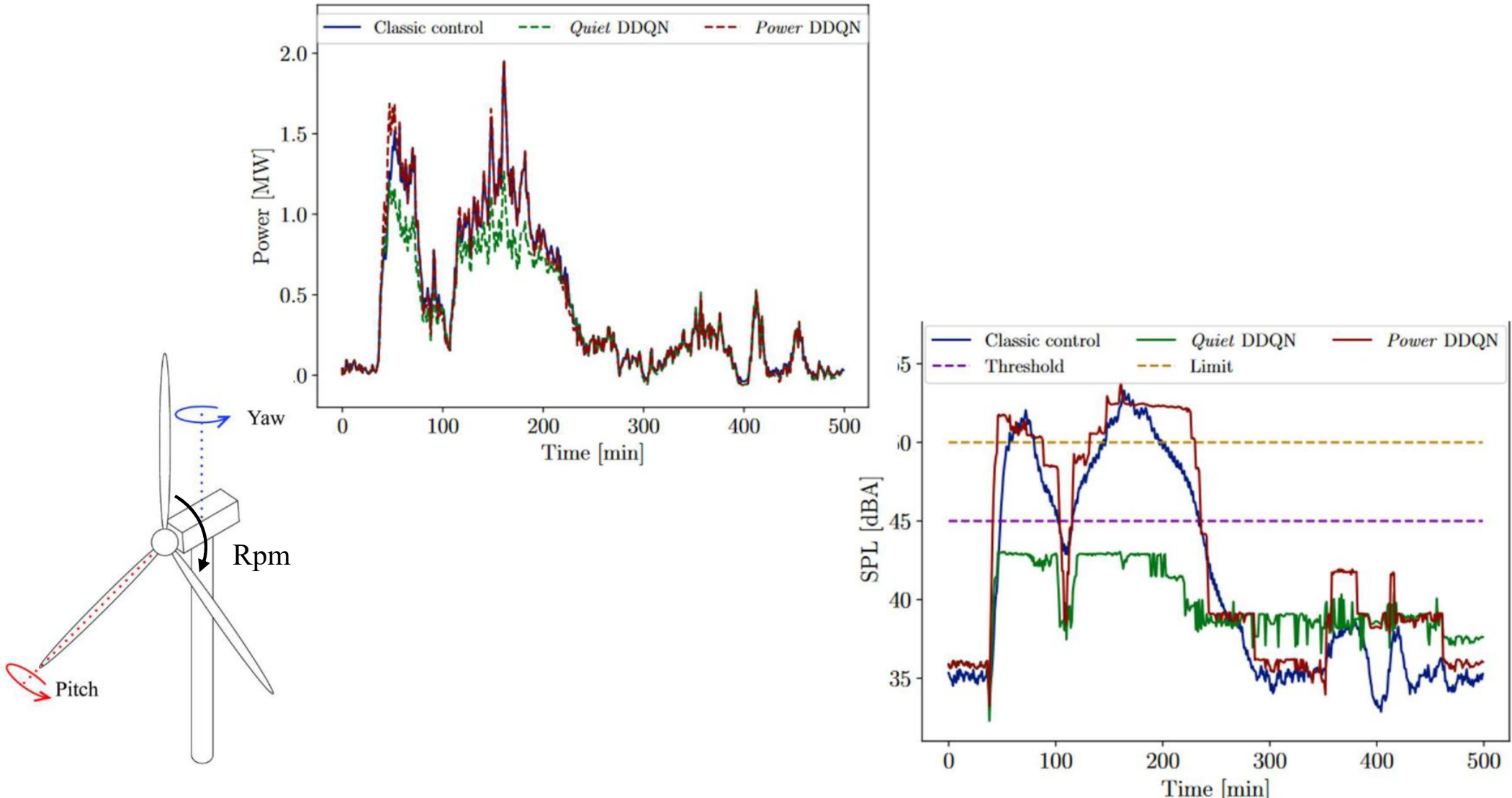
Validation with turbulent real winds



Metric	DDQN1	VI	PID	Uncontrolled
Control Capacity Factor (%)	91.31	87.50	57.60	12.77
Capacity Factor (%)	20.95	20.50	12.49	1.59
Yearly Production (MWh)	4162.95	4073.45	2481.97	316.12

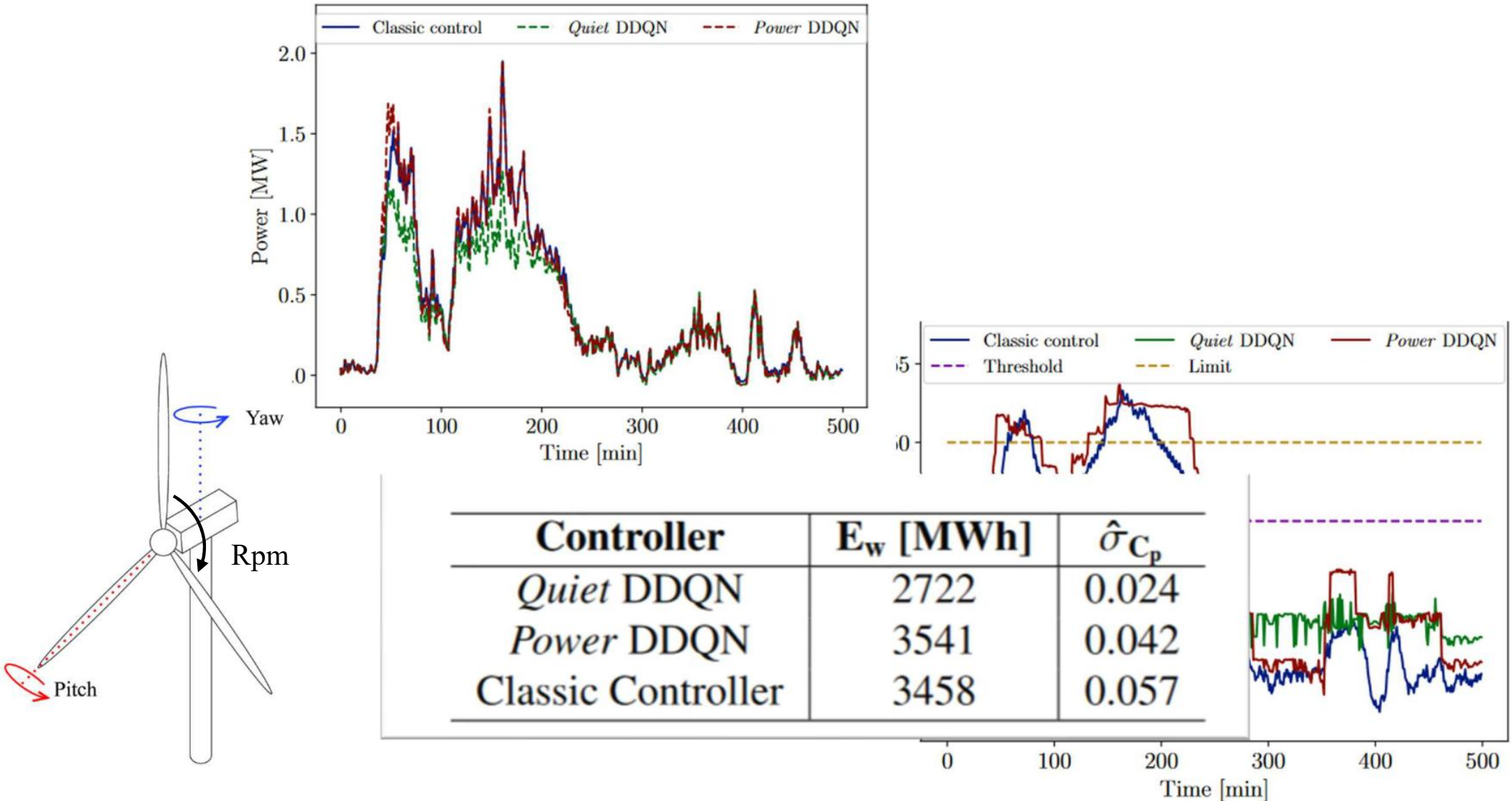
Deep reinforcement learning for wind turbine control

Adding Noise Constraints

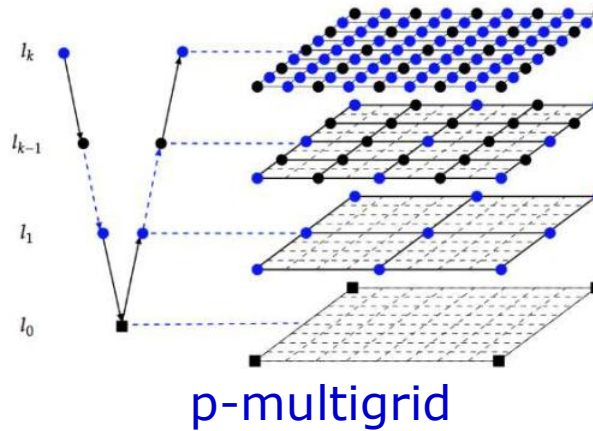


Deep reinforcement learning for wind turbine control

Adding Noise constraint



Reinforcement learning for p-multigrid



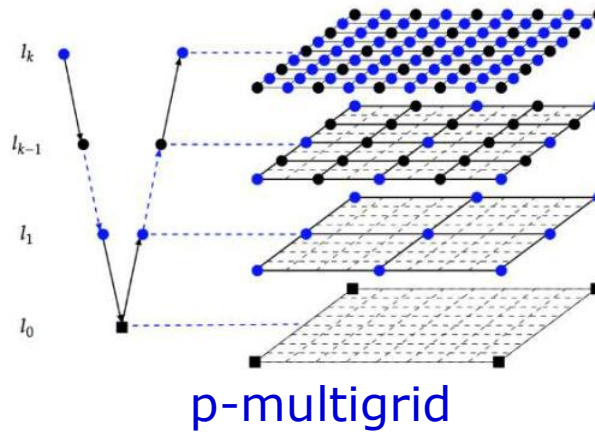
		Cases	0.1	0.2	0.3	0.4	0.5	0.6	0.7	0.8	0.9	1	
Advection-diffusion	P3	IC: Sine7	135	126	121	121	123	124	1186	U	U		
		IC: sine		121					1186	U	U		
		IC: exp		121					1186	U	U		
	P5	IC: Sine7	471						U	U	U		
		IC: sine		471					U	U	U		
		IC: exp		471					U	U	U		
	P7	IC: Sine7	1207						1205	U	U		
		IC: sine		1207					1205	U	U		
		IC: exp		1207					1205	U	U		
	P9	IC: Sine7	2466						U	U	U		
		IC: sine		2466					U	U	U		
		IC: exp		2466					U	U	U		
		P3 R10 IC: Sine7	229	146	144	142	140	138	136	1188	U	U	

$$u_t + au_x - \nu u_{xx} = S$$

Optimal parameters in p-multigrid multigrid?

- Sweeps
- Relaxation between levels

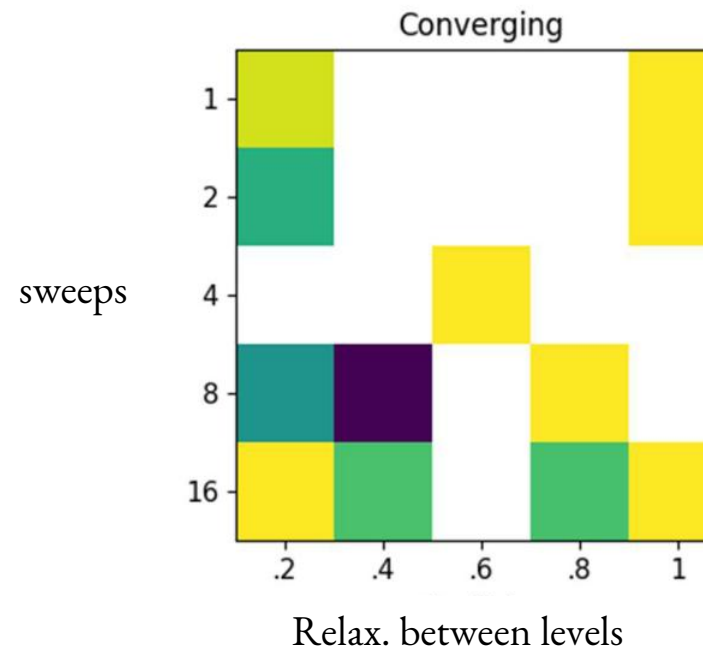
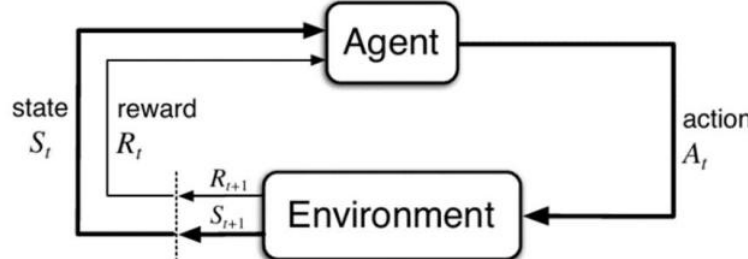
Reinforcement learning for p-multigrid



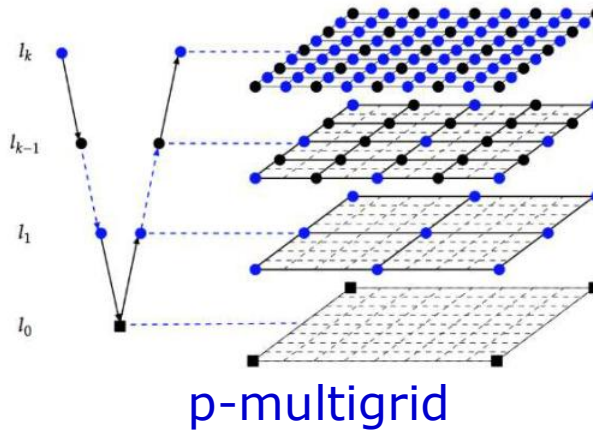
	Cases	0.1	0.2	0.3	0.4	0.5	0.6	0.7	0.8	0.9	1	
Advection-diffusion	P3	IC: Sine7 IC: sine IC: exp	135	126	121	121	123	124	1186	U	U	
	P5	IC: Sine7 IC: sine IC: exp	121	121	471	471	U	U	U	U	U	
	L0	IC: Sine7 IC: sine IC: exp	471	471	1207	1207	U	U	U	U	U	
	P7	IC: Sine7 IC: sine IC: exp	1207	1207	1207	1207	1205	1205	1205	U	U	
	P9	IC: Sine7 IC: sine IC: exp	2466	2466	2466	2466	U	U	U	U	U	
	P3	R10 IC: Sine7	229	146	144	142	140	138	136	1188	U	U

$$u_t + au_x - \nu u_{xx} = S$$

Reward: $f(\text{Relative drop in residual, time taken})$



Reinforcement learning for p-multigrid



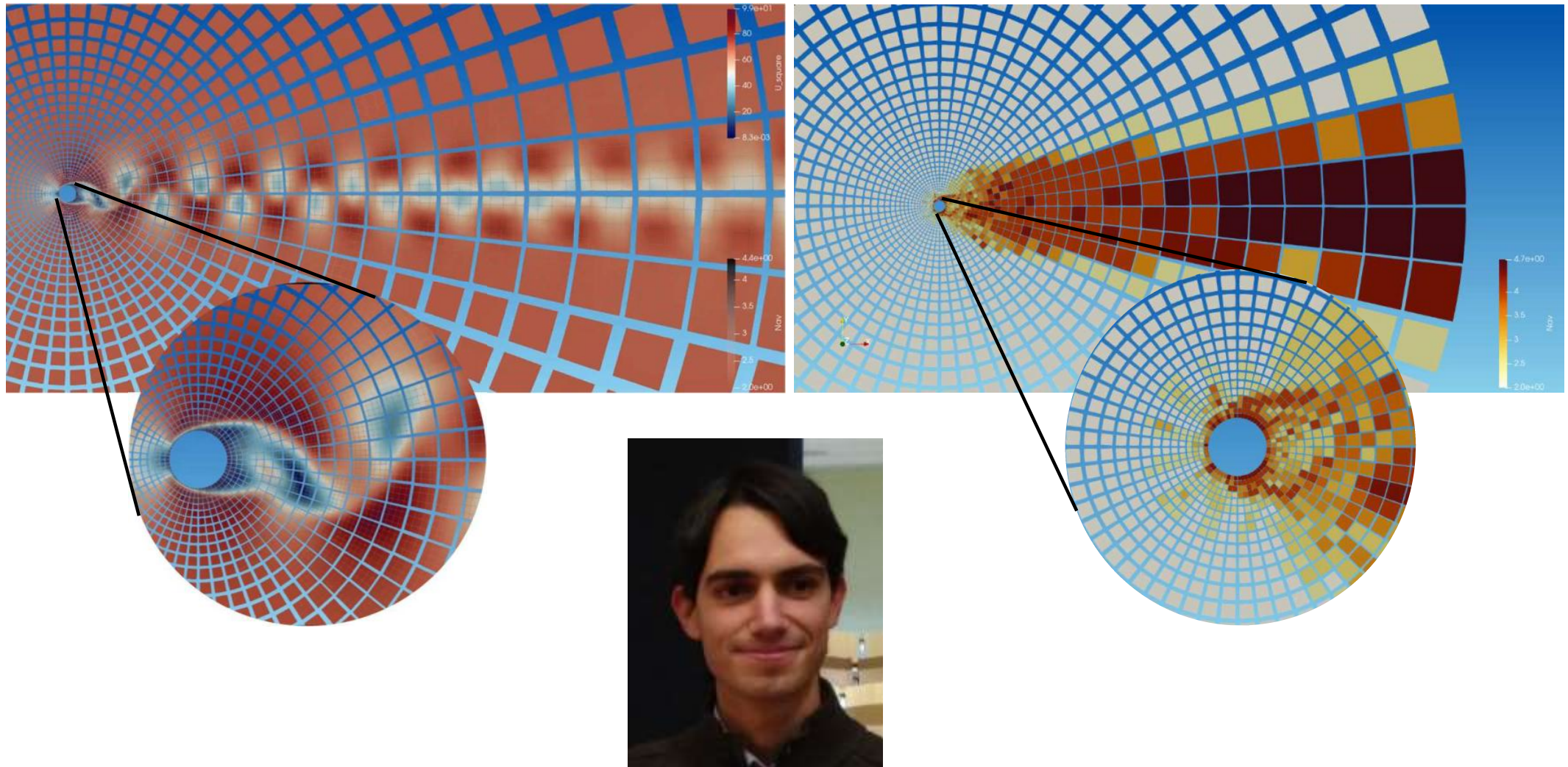
		Cases	0.1	0.2	0.3	0.4	0.5	0.6	0.7	0.8	0.9	1
Advection-diffusion	L0	P3	IC: Sine7	135	126	121	121	123	124	1186	U	U
		P5	IC: sine	121						1186	U	U
		P7	IC: exp	121						1186	U	U
		P9	IC: Sine7	471						U	U	U
		P3	IC: sine	471						U	U	U
	R0	P5	IC: exp	471						U	U	U
		P7	IC: Sine7	1207						1205	U	U
		P9	IC: sine	1207						1205	U	U
		P3	IC: exp	1207						1205	U	U
		R10	IC: Sine7	229	146	144	142	140	138	136	1188	U

$$u_t + au_x - \nu u_{xx} = S$$

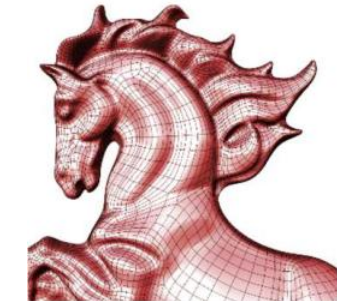
"Arbitrary"		MC		PPO		
runtime	iter	runtime	iter	runtime	iter	res
AD - Order 2						
a= 1., v = 0.01						
69.7168839	197	49.38292694	197	31.02763486	626	9.67E-09
a= 0.5., v = 0.01						
80.01094651	207	51.54315066	207	31.81400156	651	8.33E-09
a= 0.5., v = 0.5						
808.6031666	2178	480.8234568	2178	33.21327591	652	9.31E-09
a= 0.4, v = 0.6						
634.2691302	3166	582.4802358	3166	31.52360582	654	9.29E-09
a= 0.2, v = 0.8						
1476.47674	8063	1278.344407	7163	31.47797155	648	9.98E-09

Reinforcement learning for p-adaptation

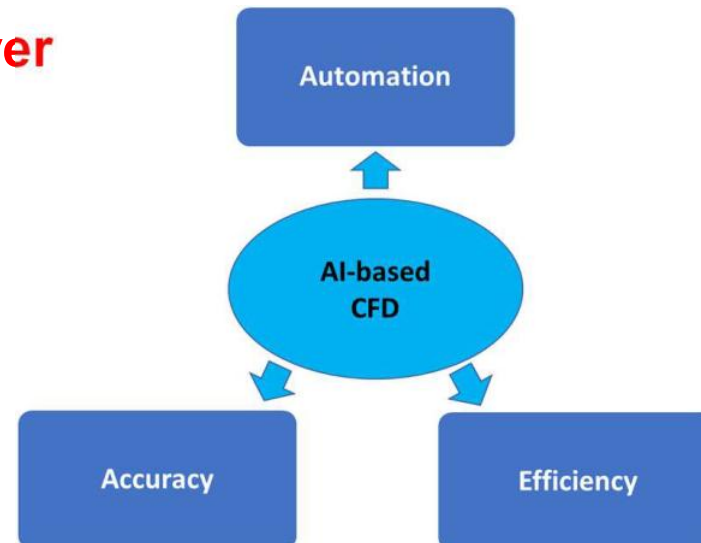
Cylinder $Re = 200$



Conclusions

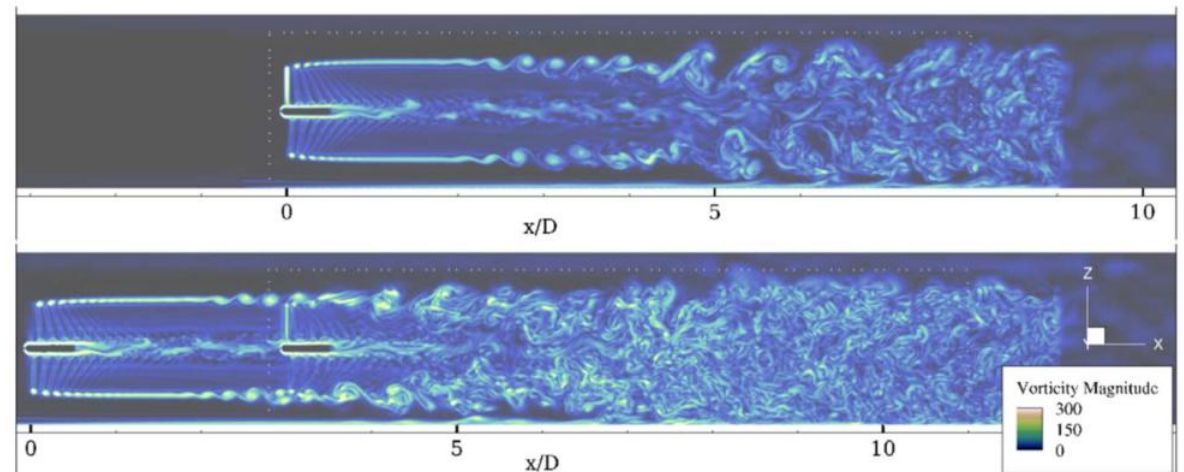
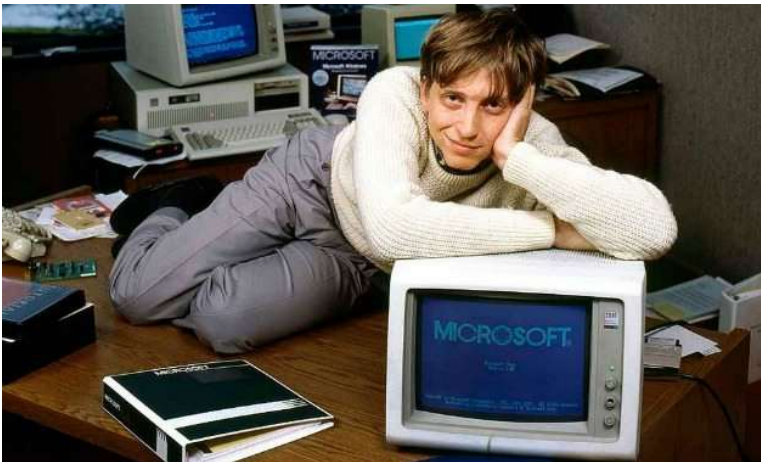


- **High order DG methods fairly well developed**
 - Incompressible flows & Compressible flows
- **Multiphysics:**
 - Wind turbines with various methods
 - Turbulence (iLES & explicit LES)
 - Aero-acoustics
 - Supersonic & Shocks
- **AI-based Solver**



Doc & PostDoc availables in the group

esteban.ferrer@upm.es

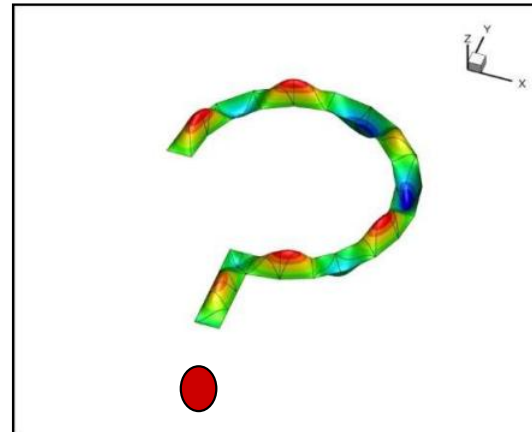


If you like computers (like B. Gates), fluids, wind turbines, etc.



Thank you very much

esteban.ferrer@upm.es



<http://sites.google.com/site/eferrerdg/publications>



Financiado por la Unión Europea
NextGenerationEU



We acknowledge the funding received by the Grant DeepCFD (Project No. PID2022-137899OB-I00) funded by MICIU/AEI/10.13039/501100011033 and by ERDF, EU.

We thank the support of Agencia Estatal de Investigación for the grant "Europa Excelencia" for the project EUR2022-134041 funded by MCIN/AEI/10.13039/501100011033) y the European Union NextGenerationEU/PRTR



This research has been cofunded by the European Union (ERC, Off-coustics, project number 101086075). Views and opinions expressed are, however, those of the author(s) only and do not necessarily reflect those of the European Union or the European Research Council. Neither the European Union nor the granting authority can be held responsible for them



POLITÉCNICA



Reinforcement Learning for Anisotropic p-Adaptation and Error Estimation in High-order Solvers

David Huergo Perea

UPM Collaborators:

M. de Frutos, E. Jané, O. Mariño, G. Rubio, E. Ferrer



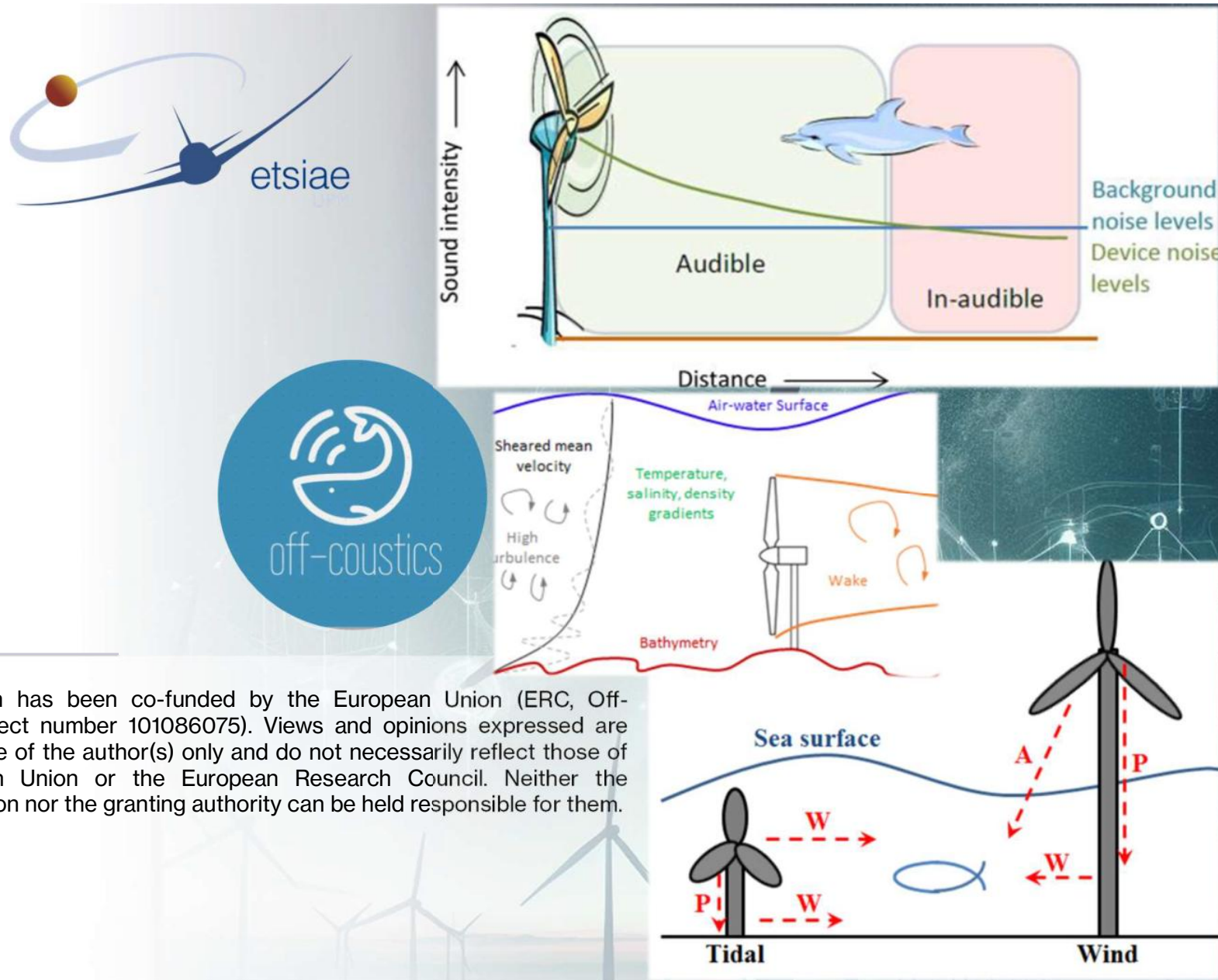


POLITÉCNICA

Funding



This research has been co-funded by the European Union (ERC, Off-coustics, project number 101086075). Views and opinions expressed are however those of the author(s) only and do not necessarily reflect those of the European Union or the European Research Council. Neither the European Union nor the granting authority can be held responsible for them.



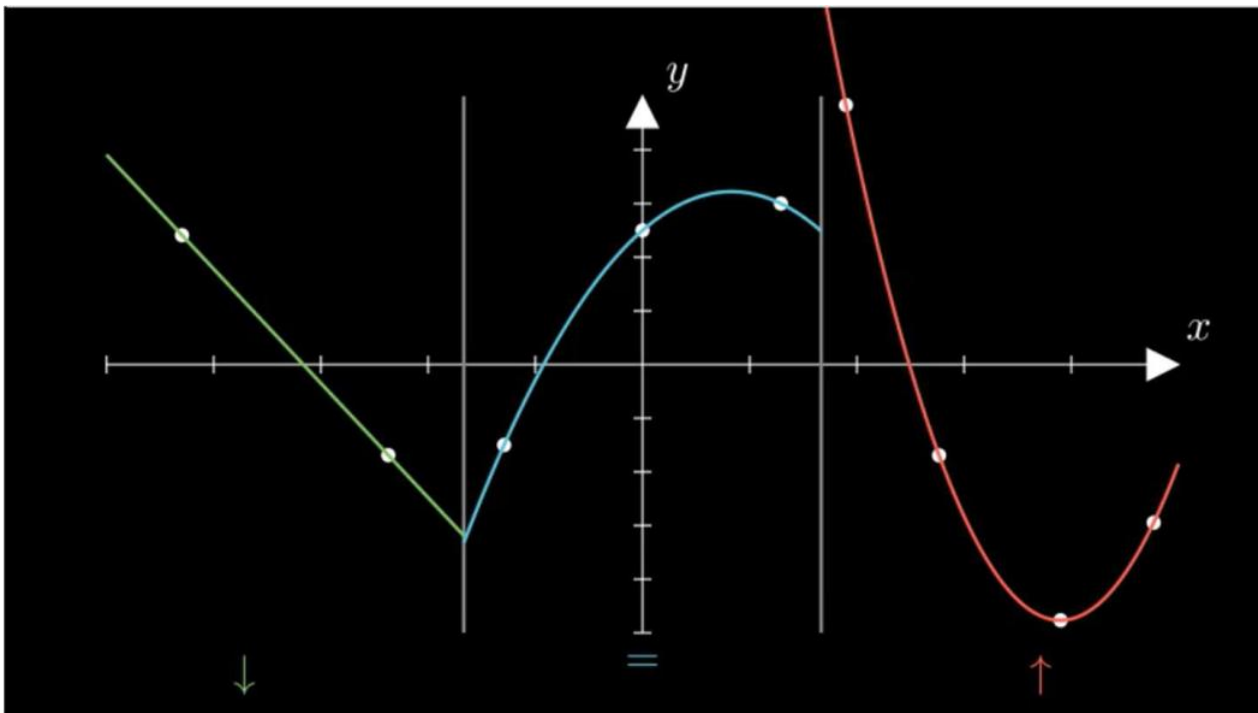
Contents

- p-Adaptation in DGSEM solvers
- Reinforcement Learning for p-adaptation
- Results
- Ongoing Work
- Conclusions

p-Adaptation in DGSEM solvers

1.1. p-Adaptation for DGSEM

Discontinuous Galerkin Spectral Element Method



- The solution is approximated in each element using **Lagrange polynomials** based on **Legendre-Gauss nodes**.
- p-Adaptation allows to select the **optimal polynomial in each element** of the mesh to obtain **accurate solutions** with a **reduced computational cost**.
- Manual p-adaptation requires to know beforehand the behaviour of the solution.

1.2. p-Adaptation with Truncation Error

DGSEM simulation

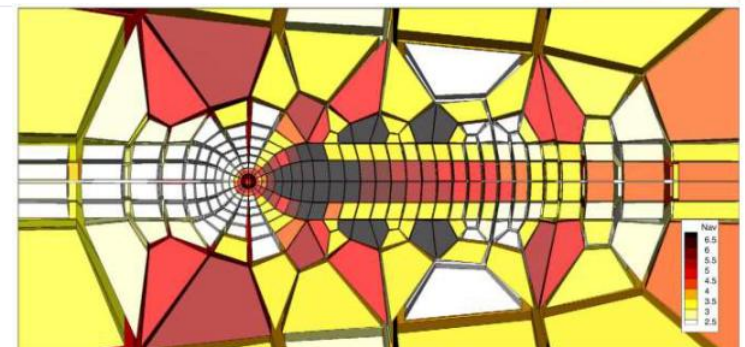
Example of a p-adapted mesh, based on the **Truncation Error**, for the flow around a sphere at Reynolds 200.

The contours indicate the average polynomial order ($N_{av} = (N_1 + N_2 + N_3)/3$). [1, 2]

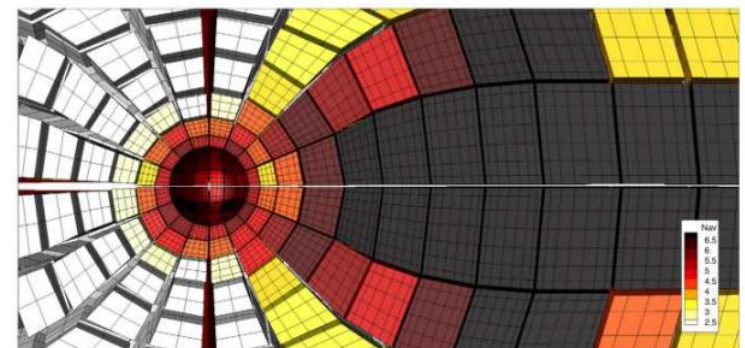
Simulated using HORSES3D

<https://github.com/loganoz/horses3d>

[3] E. Ferrer, G. Rubio, W. Laskowski, O.A. Mariño, S. Colombo, A. Mateo-Gabín, H. Marbona, F. Manrique de Lara, D. Huergo, J. Manzanero, A.M. Rueda-Ramírez, D.A. Kopriva and E. Valero, HORSES3D: A high-order discontinuous Galerkin solver for flow simulations and multi-physics applications, Computer Physics Communications 287 (2023): 108700.



(a) Average polynomial order (N_{av}).

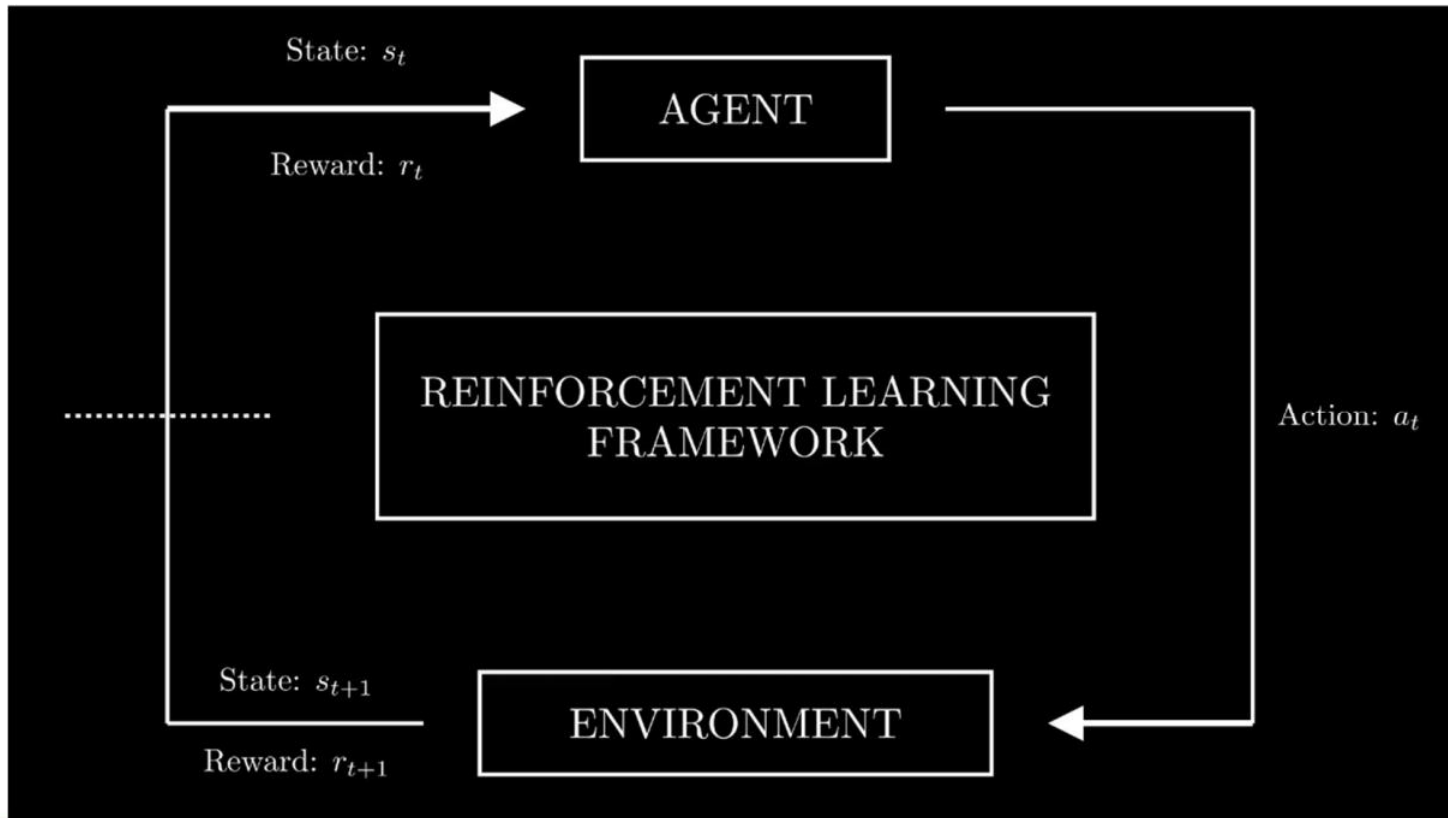


[1] A. M. Rueda-Ramírez, J. Manzanero, E. Ferrer, G. Rubio, E. Valero, A p-multigrid strategy with anisotropic p-adaptation based on truncation errors for high-order discontinuous Galerkin methods, Journal of Computational Physics 378 (2019).

[2] A. M. Rueda-Ramirez, G. Ntoukas, G. Rubio, E. Valero, E. Ferrer, Truncation Error-Based Anisotropic p-Adaptation for Unsteady Flows for High-Order Discontinuous Galerkin Methods, International Journal of Computational Fluid Dynamics, 37(6), 430–450 (2024).

Reinforcement Learning for p-adaptation

2.1. The RL framework

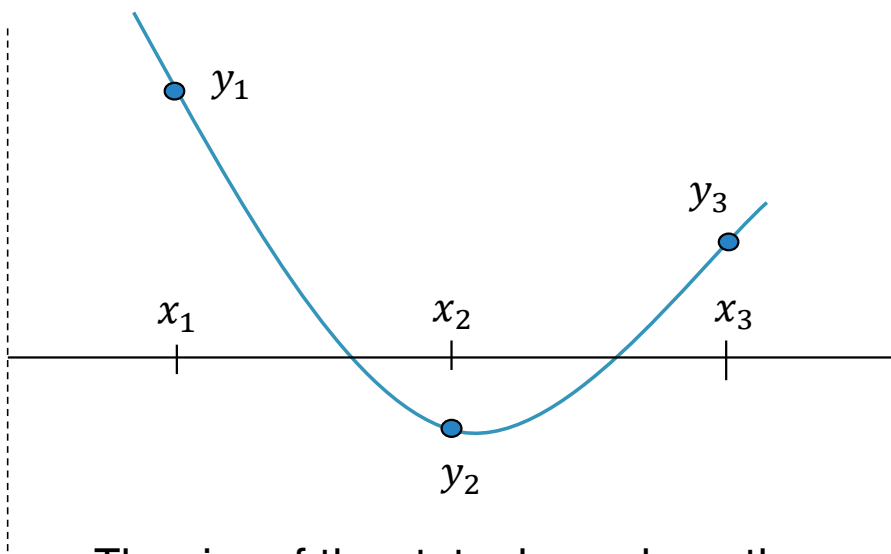


- **Agent:** Decides the action.
- **Environment:** Current problem (our DGSEM solver).
- **Action:** Increment or decrement the polynomial order p .
- **State:** To be defined.
- **Reward:** To be defined.

2.2. State and Reward

State

$$s = [y_1, y_2, \dots, y_n]$$



Reward

Two main objectives:

- **Minimum polynomial order:** Computational cost is reduced.
- **High accuracy:** High order required if strong gradients are present.

$$\text{reward} = \left(\frac{p_{max}}{p} \right)^\alpha e^{-\frac{rmse^2}{2\sigma^2}}$$

- $rmse$: Between the solution and the analytical function in 14 points.
- σ = 0.05: Standard deviation.
- p_{max} = 6: Maximum order allowed.
- α = 0.9: Control parameter.

2.3. Training

Drawbacks

Expensive training when coupled with a CFD solver

Reward function based on **analytical solution**

Solution

Training based on **polynomial functions** in a single element

Advantages

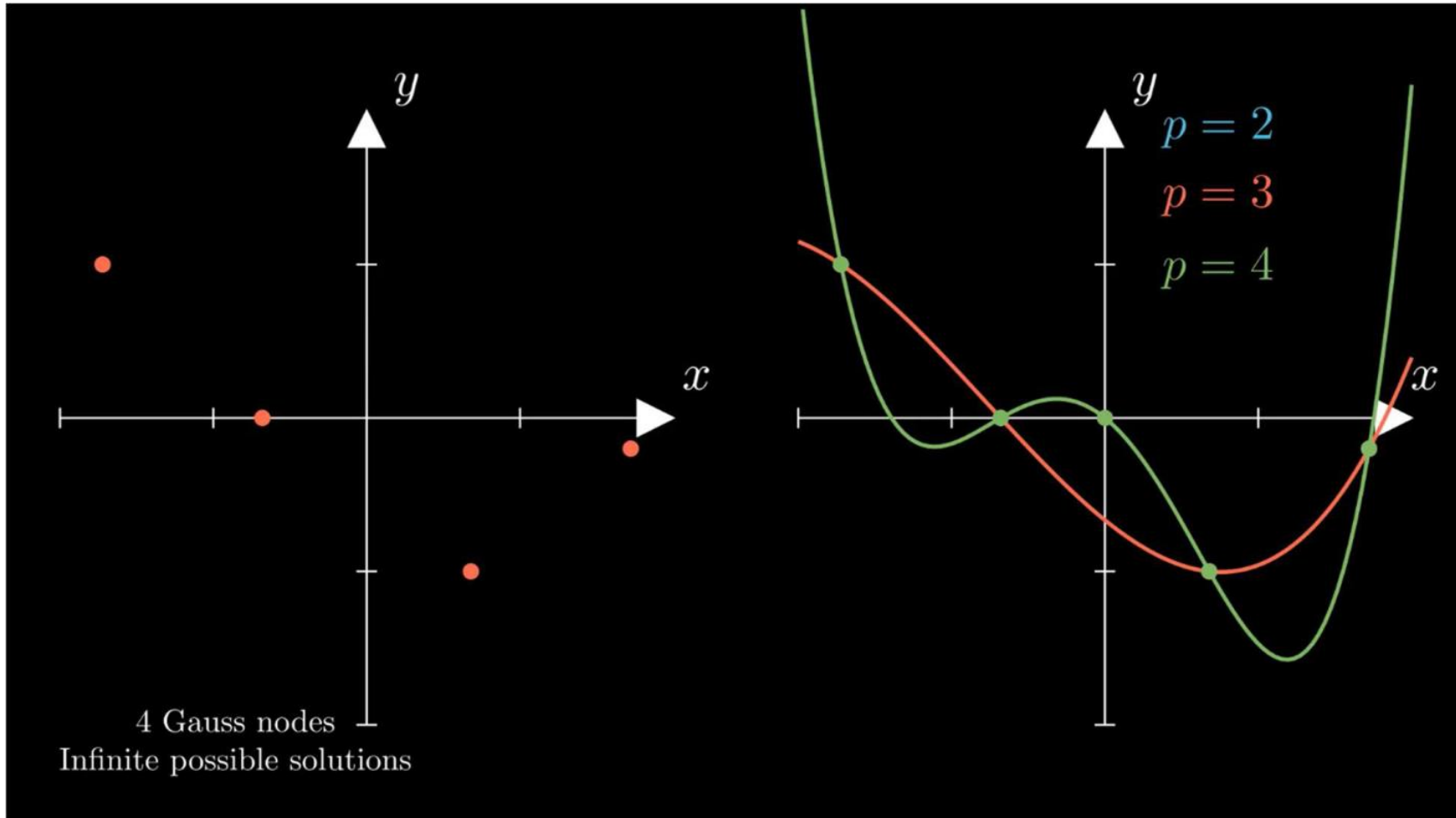
CFD not required during the training

Analytical solution known during the training

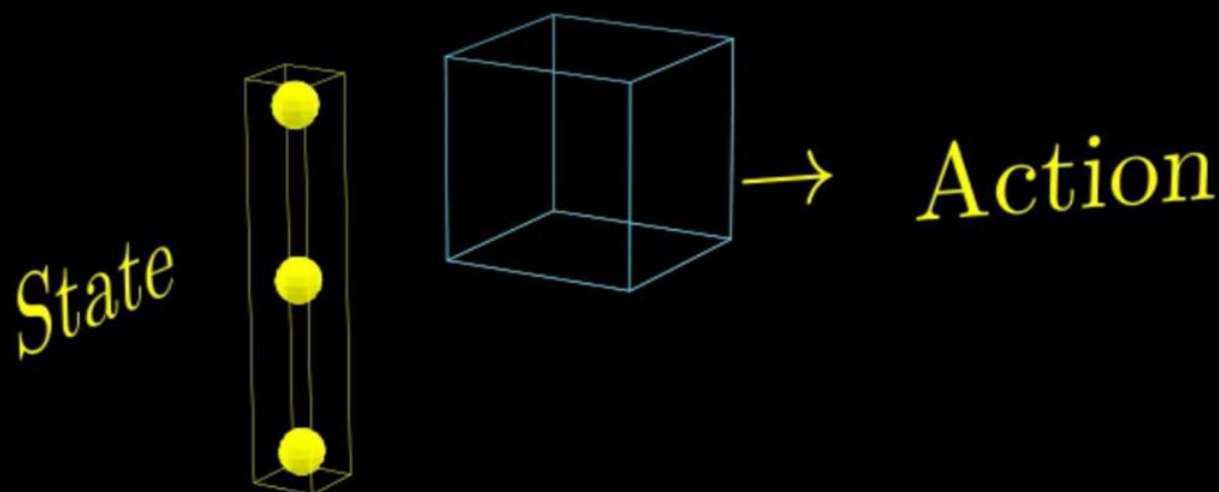
The resulting agent:

- Has to be **trained only once**.
- **Can be potentially applied to any PDE** solved with a DGSEM solver.
- **Can be used in an arbitrary mesh**: the agent chooses the optimum polynomial order individually for each element.

2.3. Training



2.4. Extrapolation for 3D cases



2.5. Error Estimation

Bellman Optimality Equation

$$V^*(s) = \max_a \sum_{s',r} p(s',r | s,a) [r + \gamma V^*(s')]$$

- **V-values**
- **Reward**
- **Discount factor**
- **Probability transition function**



$$\widehat{rmse} = \sqrt{-2\sigma^2 \log \left(\frac{V^*(s) - \bar{r} - \gamma \bar{r}'}{\gamma^2 V_{\max,p}} \right)}$$

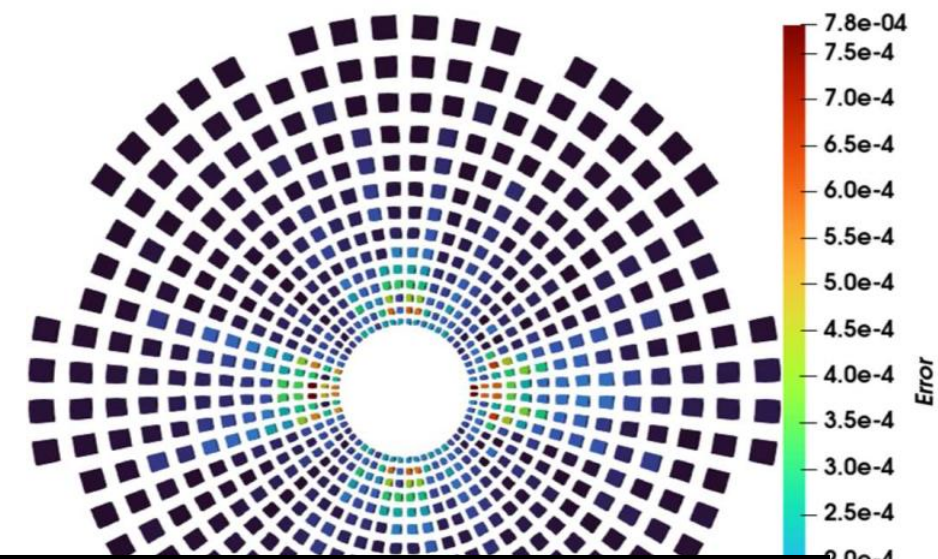
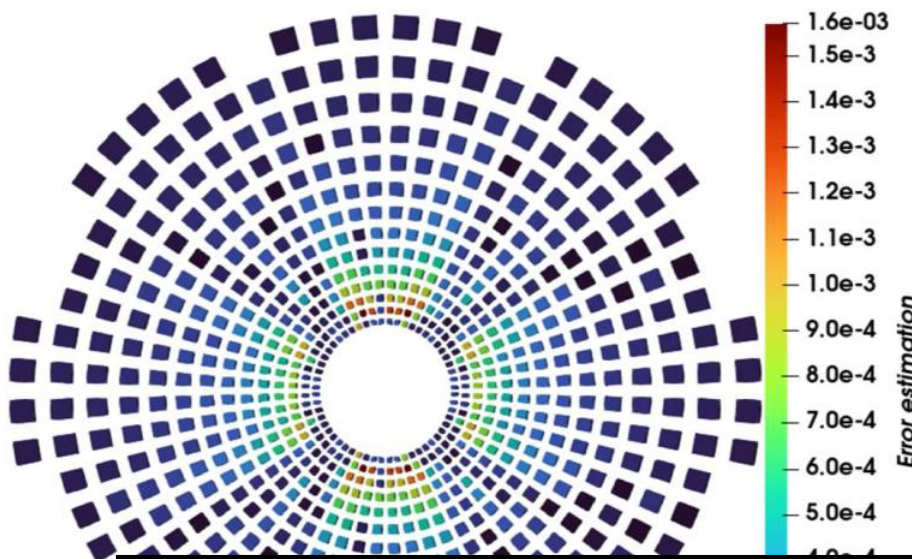
The error estimation:

- Provides the **spatial error that the RL agent believes to be real** inside each element.
- **Is learned during the training** and can be applied without additional knowledge of the problem to be solved.
- **Is more accurate if coupled with p-adaptation.**

Results

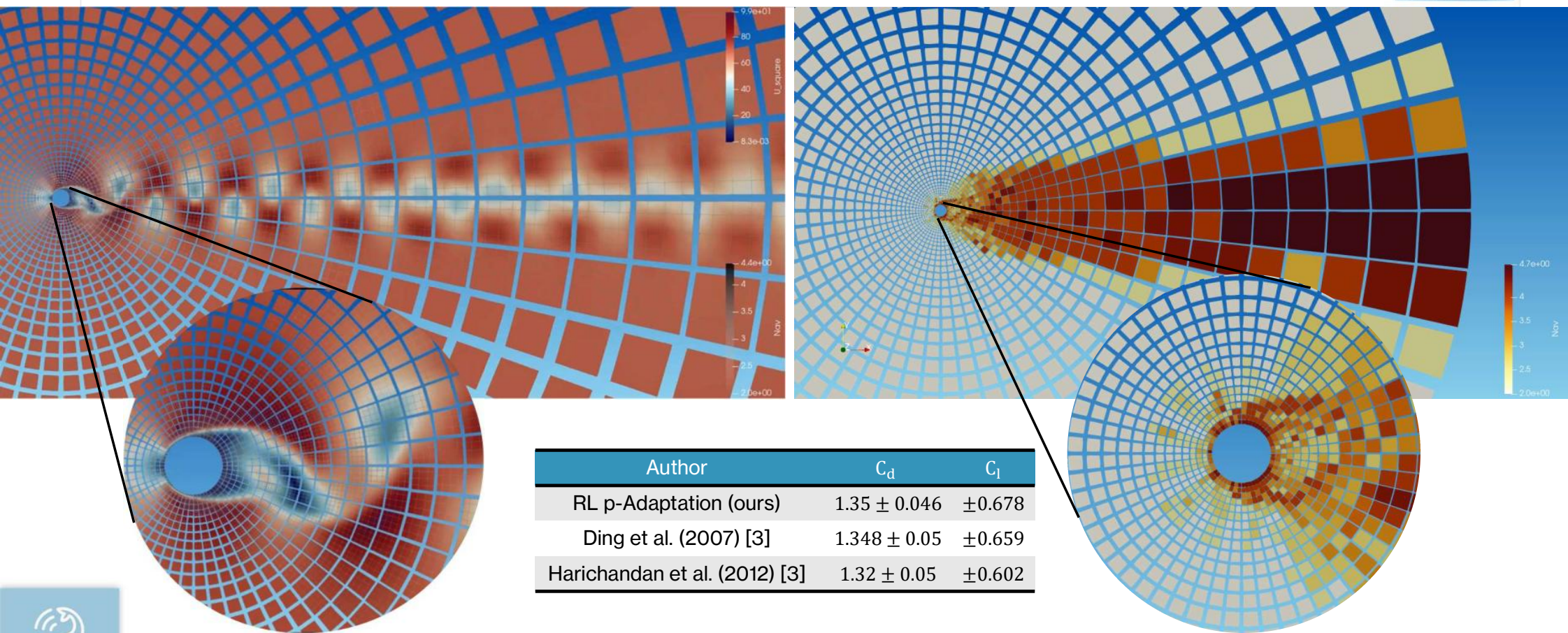


3.1. Euler Flow around a cylinder



Polynomial order	DOFs	Computational cost (s)	Real Error	Error Estimation	
$p = 2$	58968	252	$8.1 \cdot 10^{-3}$	$2.1 \cdot 10^{-3}$	$1.0\text{e-}4$
$p = 3$	139776	431	$6.7 \cdot 10^{-4}$	$2.8 \cdot 10^{-4}$	$5.0\text{e-}5$
$p = 4$	273000	737	$6.5 \cdot 10^{-5}$	$3.0 \cdot 10^{-5}$	$1.0\text{e-}6$
$p = 5$	471744	1181	0.0 (reference)	0.0 (reference)	
p – adapted	27708	197	$7.8 \cdot 10^{-4}$	$1.6 \cdot 10^{-3}$	

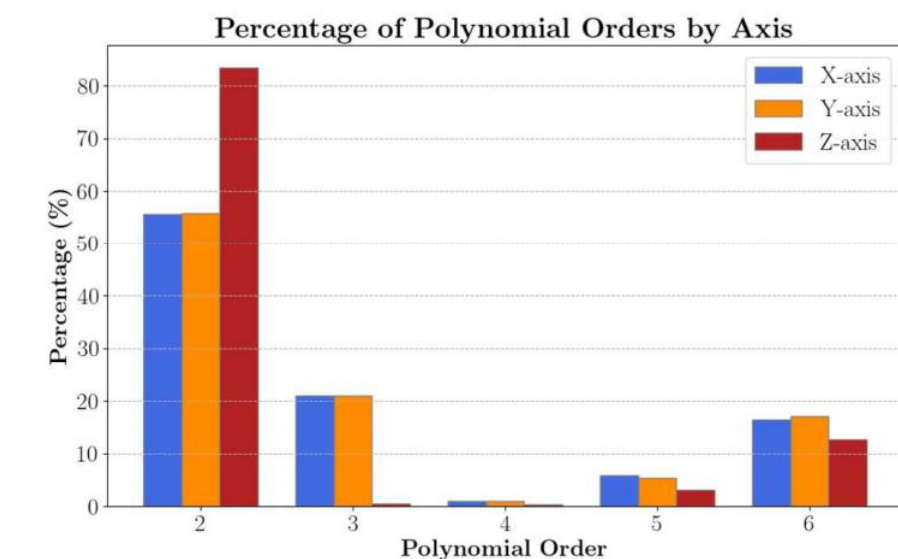
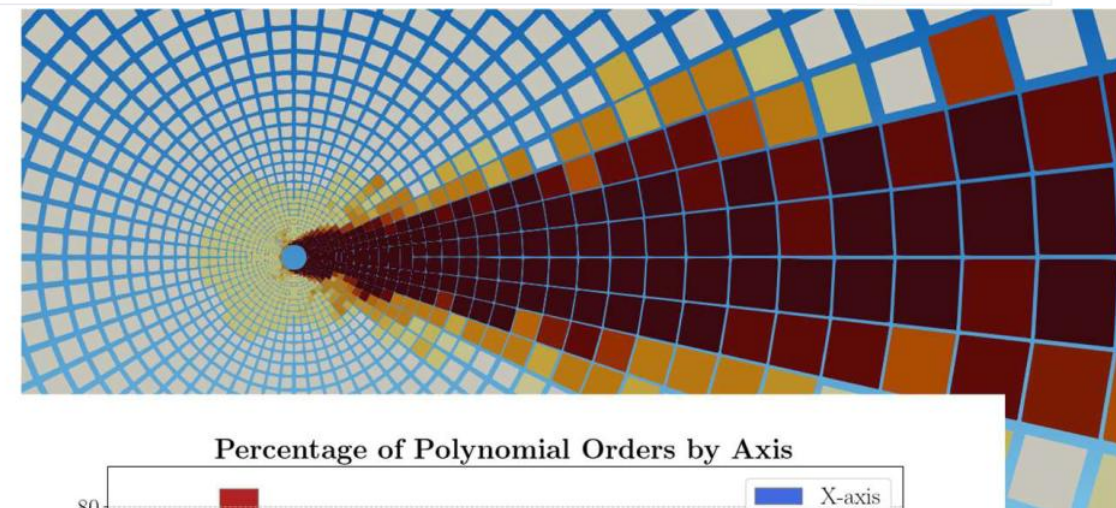
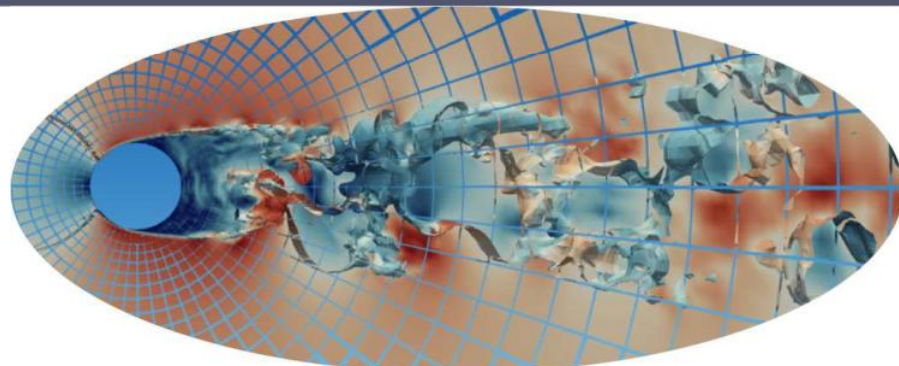
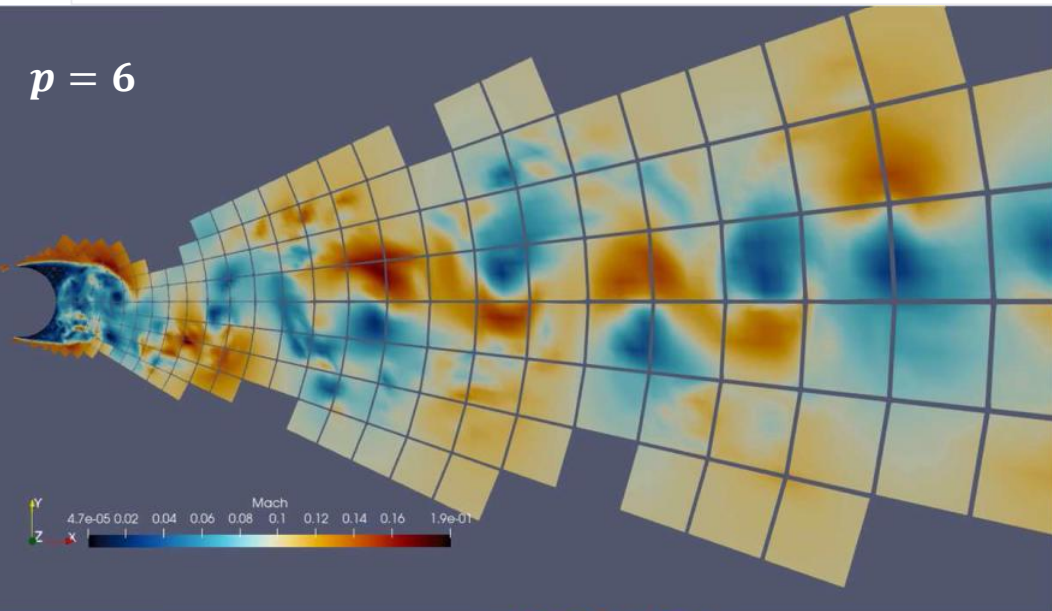
3.2. Cylinder $Re = 200$



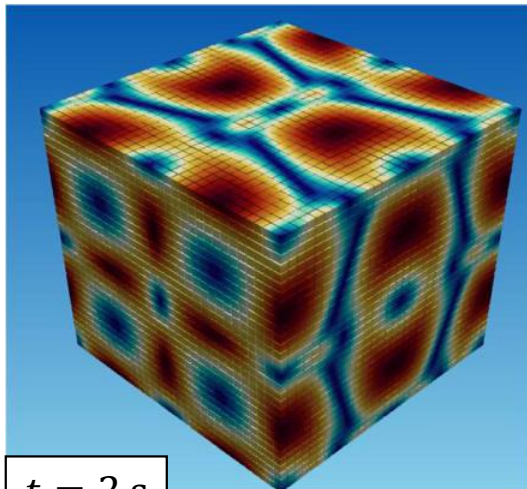
[3] AB Harichandan and A Roy. Numerical investigation of flow past single and tandem cylindrical bodies in the vicinity of a plane wall. Journal of Fluids and Structures, 33:19–43, 2012.

3.3. Cylinder $Re = 3900$

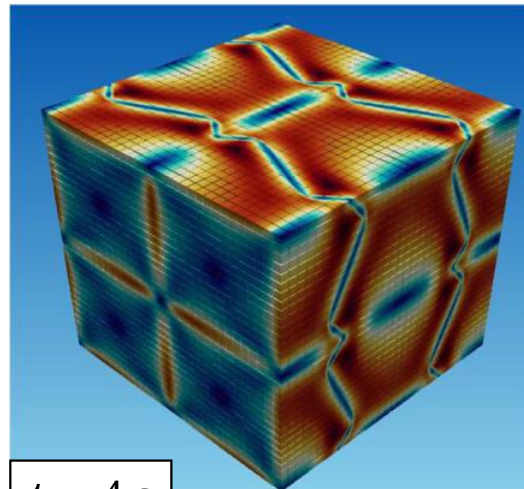
$p = 6$



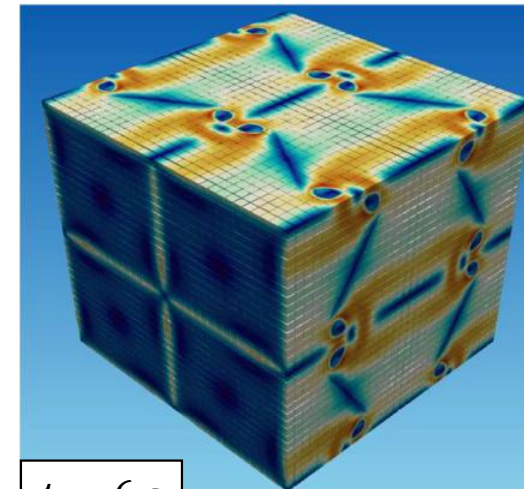
3.4. Taylor Green Vortex



$t = 2$ s

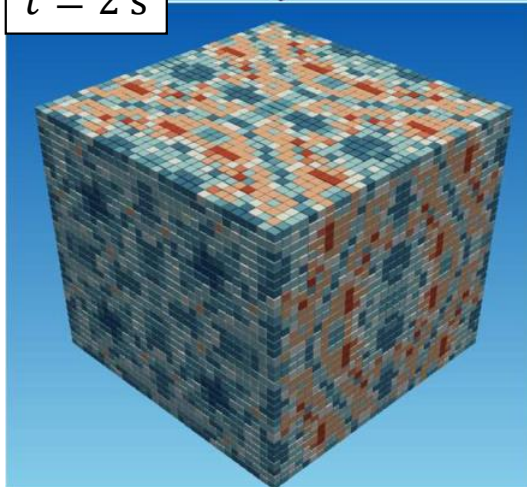


$t = 4$ s

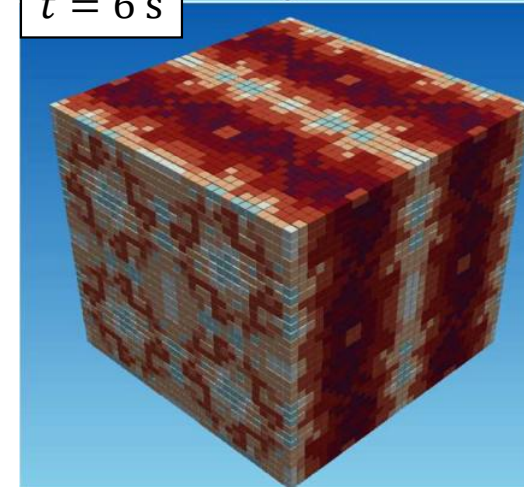
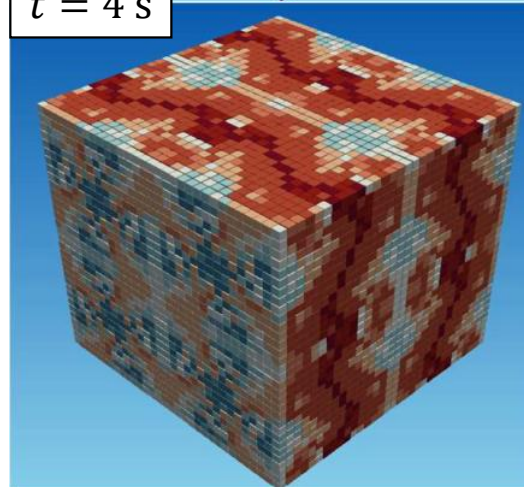


$t = 6$ s

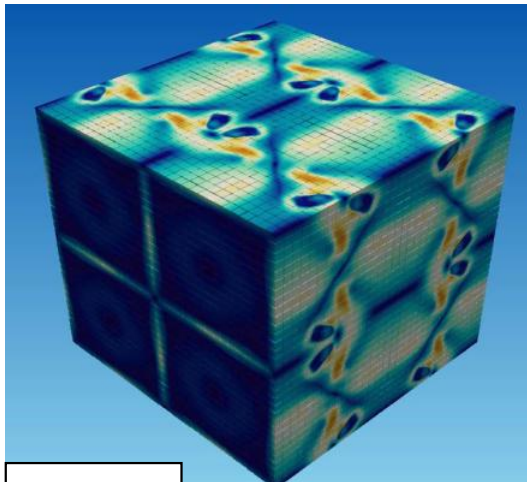
Velocity
magnitude



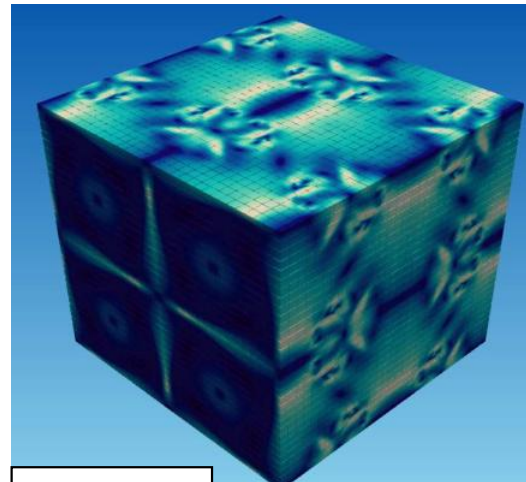
p_{av}



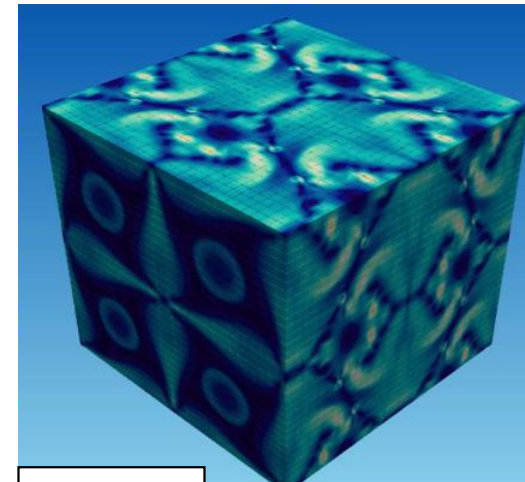
3.4. Taylor Green Vortex



$t = 8$ s

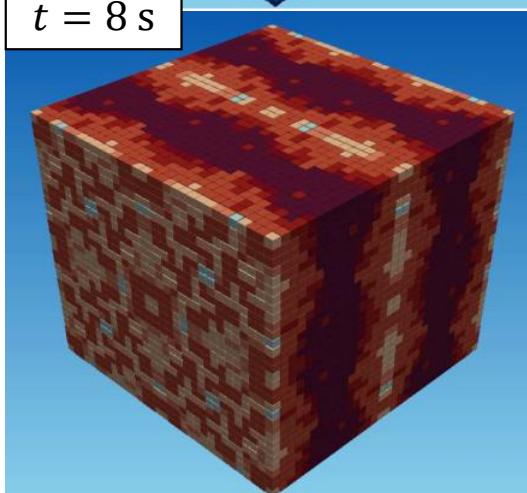


$t = 10$ s

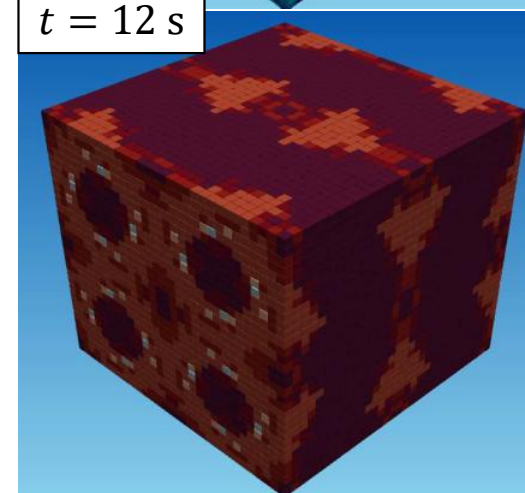
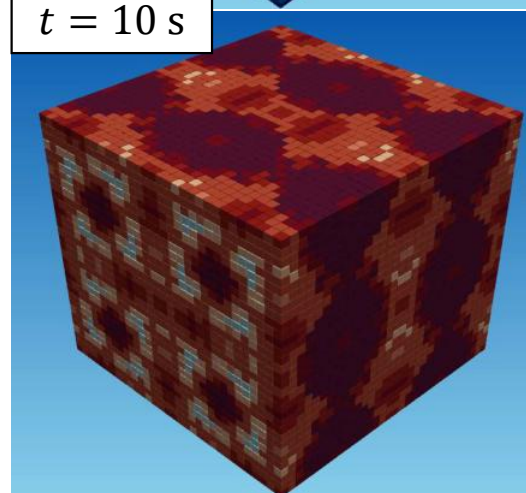


$t = 12$ s

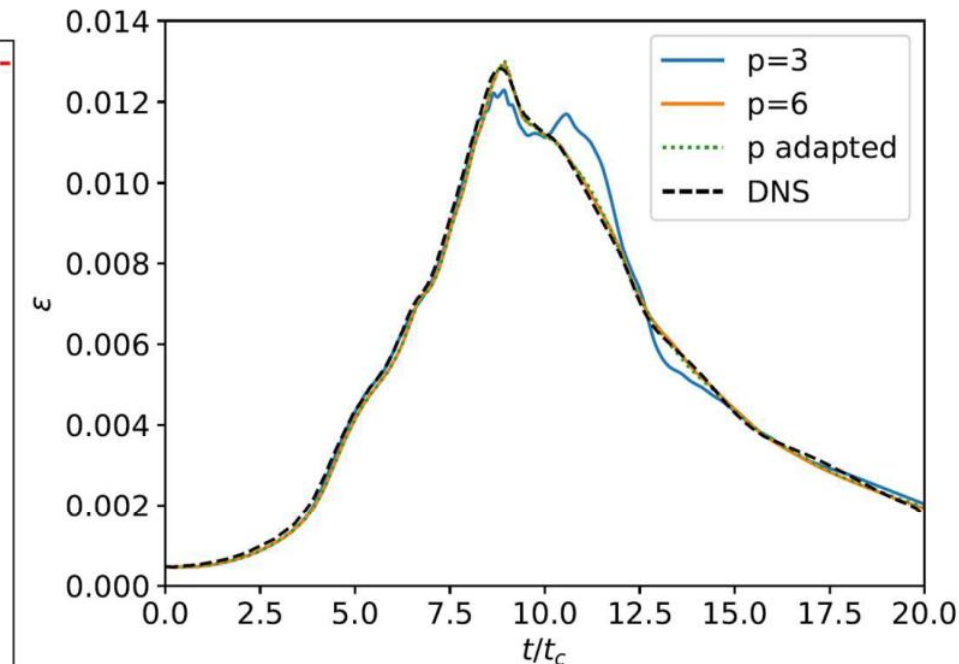
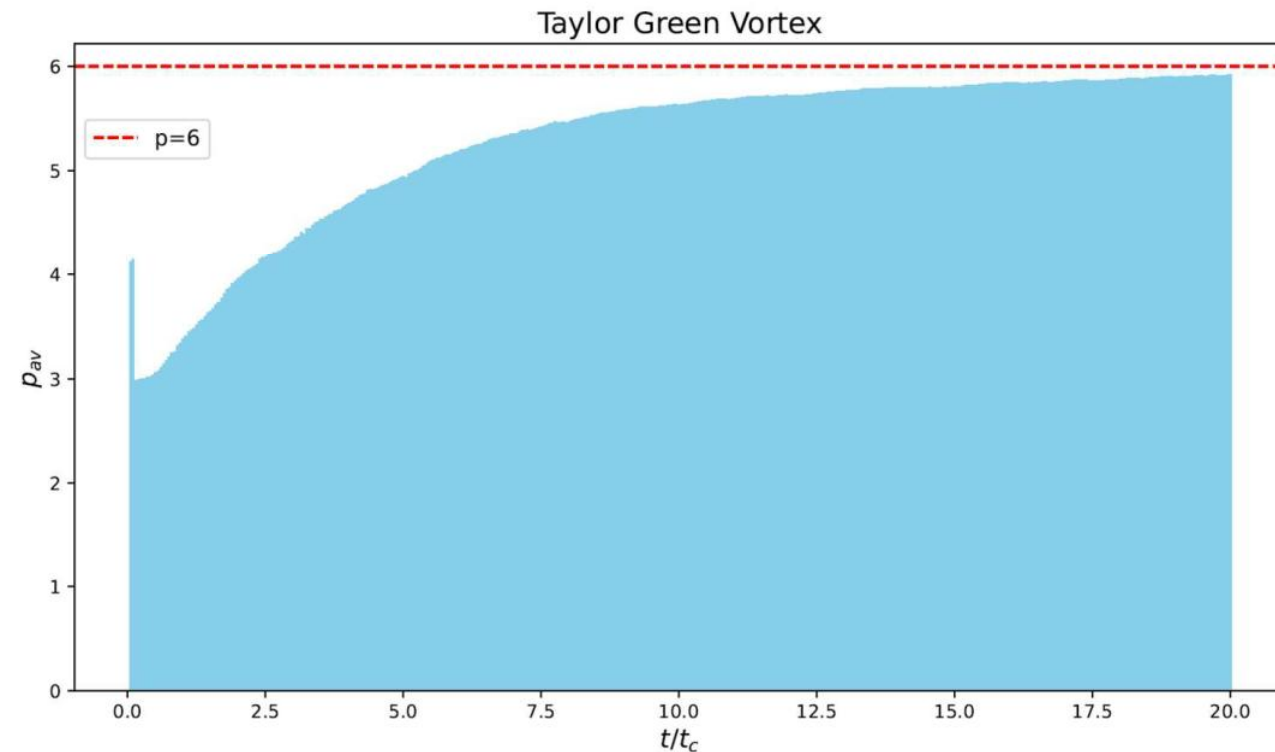
**Velocity
magnitude**



p_{av}

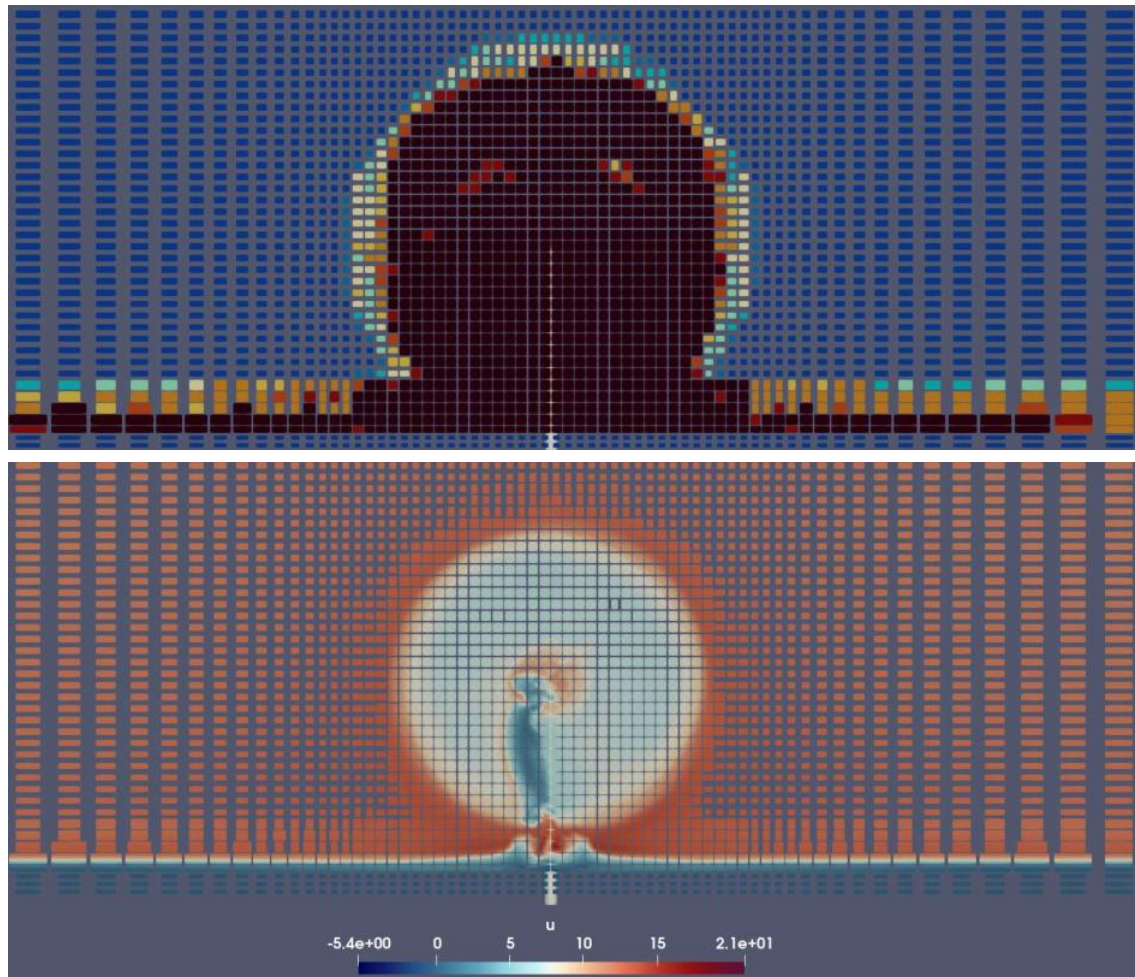
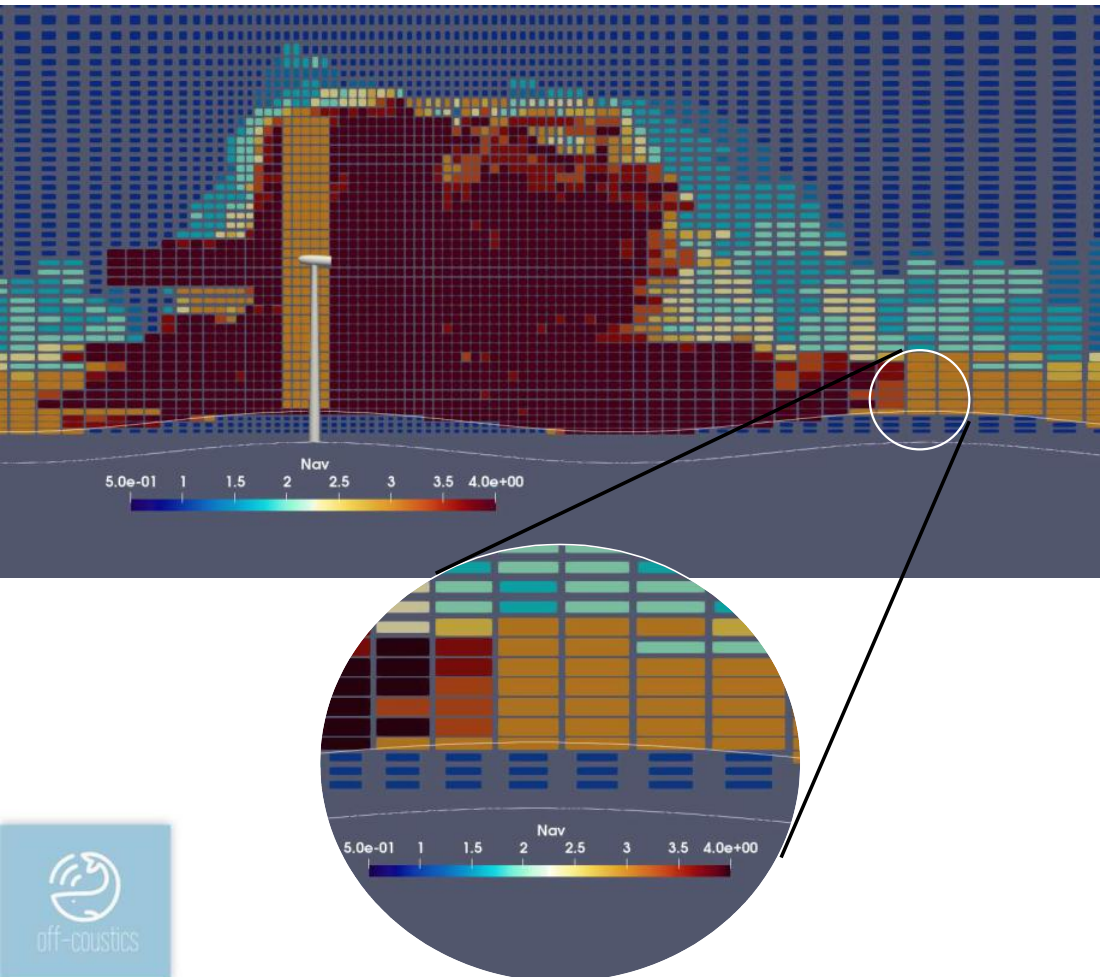


3.4. Taylor Green Vortex

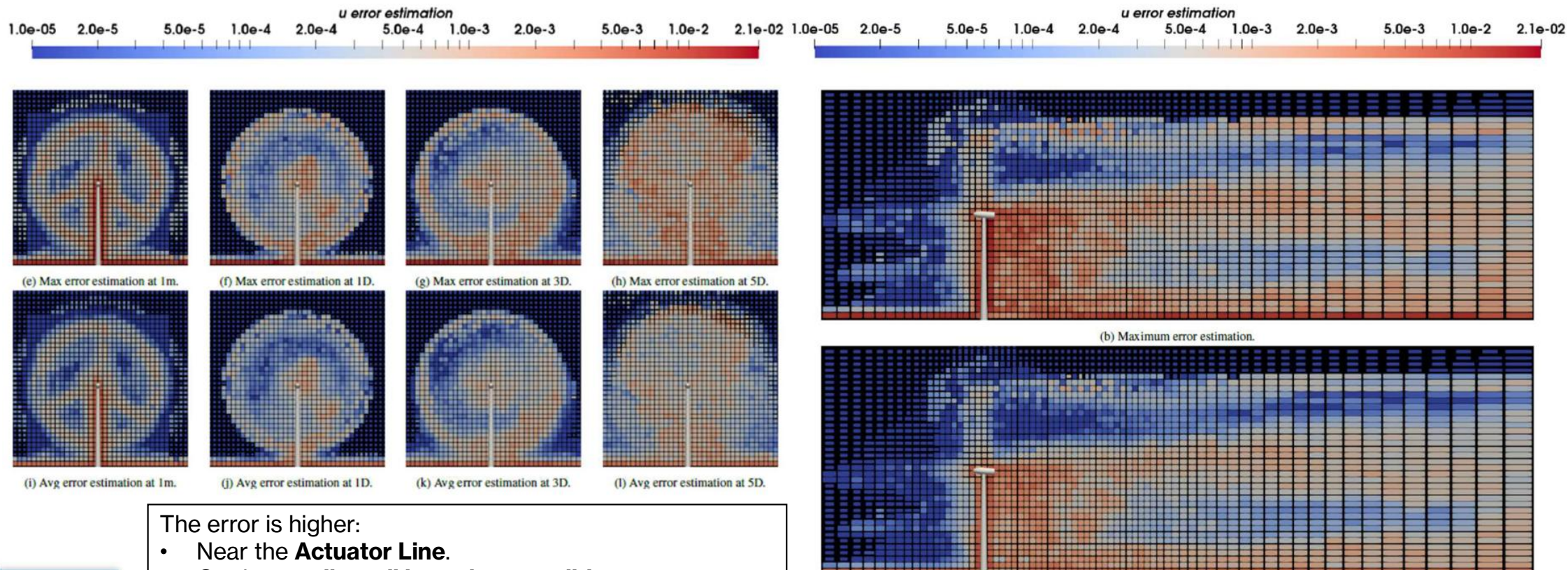


	$p = 6$	p_{adapted}
Computational cost (h)	102	41

3.5. Offshore Wind Turbine DTU 10MW



3.5. Offshore Wind Turbine DTU 10MW



The error is higher:

- Near the **Actuator Line**.
- On the **no-slip wall boundary condition**.
- Inside the **Immersed Boundaries (tower and nacelle)**.
- Inside the **wake**.

Ongoing Work

4. Ongoing work

- RL p-adaptation for moving **Immersed Boundaries**.
- RL p-adaptation for **acoustics**.
- **Comparison** with different state-of-the-art p-adaptation algorithms.
- Dynamic **load balancing** to improve MPI parallelization for evolving meshes.



Results in Engineering
Volume 21, March 2024, 101693

Full Length Article
A reinforcement learning strategy for p-adaptation in high order solvers

David Huergo  , Gonzalo Rubio   , Esteban Ferrer  

Show more 

Add to Mendeley  Share  Cite 

<https://doi.org/10.1016/j.rineng.2023.101693> 

Under a Creative Commons license 



SCAN ME



Reinforcement learning for anisotropic p-adaptation and error estimation in high-order solvers

David Huergo
david.huergo.perea@upm.es

Martín de Frutos

Eduardo Jané

Oscar A. Marino

Gonzalo Rubio

Esteban Ferrer

ETSIAE-UPM-School of Aeronautics, Universidad Politécnica de Madrid, Plaza Cardenal Cisneros 3, E-28040 Madrid, Spain Center for Computational Simulation, Universidad Politécnica de Madrid, Campus de Montegancedo, Boadilla del Monte, 28660 Madrid, Spain

Conclusions

5. Conclusions

- RL for **p-adaptation** leads to a general approach to **improve the accuracy** and **reduce the computational time** of CFD simulations.
- The proposed methodology can be potentially applied for **any PDE and computational mesh**.
- The RL agent **has to be trained only once for 1D** cases, but provides an **accurate adaptation in 3D turbulent simulations**.
- The proposed methodology provides a cheap **estimation of the spatial error in each element** of the computational mesh.

Reinforcement Learning can be applied to **minimize manual intervention**, to **improve the accuracy** of numerical simulations and to **speed-up** a CFD code.



POLITÉCNICA



Thank you!

Funding



This research has been co-funded by the European Union (ERC, Off-coustics, project number 101086075). Views and opinions expressed are however those of the author(s) only and do not necessarily reflect those of the European Union or the European Research Council. Neither the European Union nor the granting authority can be held responsible for them.